UNIVERSITY OF MOLISE

DEPARTMENT OF BIOSCIENCES AND TERRITORY

PhD in Biology and Applied Sciences

Curriculum Biology

XXXV cycle

Effects of bovine Lactoferrin on iron dysregulation and oxidative stress induced by HIV-1 Tat and SARS-CoV-2 Spike viral proteins

SSD BIO/11

Coordinator

Prof. **Filippo Santucci De Magistris**

Supervisor

Prof. **Giovanni Musci**

Co-Supervisor

Prof. **Antimo Cutone**

PhD Student

Giusi Ianiro

167209

Giusi Ianiro

ACADEMIC YEAR 2021-2022

Effects of bovine Lactoferrin on iron dysregulation and oxidative stress induced by HIV-1 Tat and SARS-CoV-2 Spike viral proteins

Reviewers

Prof.ssa Maria Rosaria Fullone. Department of Biochemical Sciences, Sapienza University of Rome.

Prof.ssa Tiziana Persichini. Department of Science, University of Roma Tre.

Examination committee

Prof.ssa Eleonora Sgambati. Department of Biosciences and Territory, University of Molise.

Prof. Marco Colasanti. Department of Science, University of Roma Tre.

Prof.ssa Catia Longhi. Department of Public Health and Infectious Diseases, Sapienza University of Rome.

INDEX

1. INTRODUCTION

1.1. Iron

Iron is by far the most abundant transition metal on Earth. Iron can have more than one ionic form and therefore oxidation state. For this reason, it participates in numerous biochemical reactions that cannot be catalyzed by any other inorganic or organic compound. In general, this transition metal acts as cofactor in different enzymes and electron transport complexes, as well as in proteins involved in oxygen transport, such as hemoglobin and myoglobin. Nutritional or genetically derived deficiencies of the metal are associated with a variety of pathologic conditions, including pernicious anemia. Generally, iron is assumed through a balanced diet or as nutritional supplement. However, iron homeostasis requires the levels of the metal be maintained in a definite functional range: lower concentrations may result in the impairment of metabolic processes whereas higher concentrations may result in toxicity. It should be recalled that toxicity of iron is strictly linked to the free fraction rather than to the total quantity. In fact, the free form is highly reactive in solution due to the strong propensity toward oxidation, with consequent overproduction of reactive oxygen species (ROS). Excess intracellular ROS disrupt the redox cell balance, thus increasing oxidative stress, which, in turn, promotes the modification of cellular biomolecules (proteins, lipids, nucleic acids), and the malfunctioning of mitochondrial respiration, protein folding, DNA repair processes, inflammation, autophagy, apoptosis, ultimately leading to tissue damage and organ failure. For that reason, all organisms have evolved tightly controlled networks to keep iron in its unreactive forms and at the same time ensure that a proper balance between metal uptake, chelation, distribution and storage is achieved. Generally, iron is sequestered in organometallic complexes and sorted out when and where needed, and its propensity to promote the generation of harmful ROS is thus minimized.

Iron can switch between different oxidation states, with divalent ferrous (Fe^{2+}) and trivalent ferric (Fe^{3+}) being the most common forms. Evolutionary success of this element relies on its unique redox potential, ranging from 1000 to −550 mV depending on the ligand chemistry (other transition elements show a much narrower range), which makes its chemical reactivity very easy to be adapted to specific biological needs. Aerobic life makes Fe^{3+} thermodynamically favored over Fe^{2+}, but this leads to serious problems of metal solubility: for ferric hydroxides, the equilibrium concentration of hydrated Fe^{3+} cannot exceed 10^{-17} M at pH 7. Despite its primary role in oxygen transport in multicellular organisms, iron has been evolutionary selected for numerous essential biochemical processes throughout the entire living scale, from prokaryotes to higher eukaryotic organisms. Iron usually bound to heme or non-heme proteins participates to different metabolic processes, including cellular respiration and electron transport (cytochromes), oxygen metabolism (peroxidases and

catalases), DNA synthesis (ribonucleotide reductase), gene regulation, drug metabolism, and steroid synthesis (Pantopoulos et al., 2012). Iron levels in the human body are controlled only by absorption, since no excretion pathway is present. For these reasons, the acquisition and transport of iron constitutes a formidable challenge for cells and organisms due to its low solubility and high toxicity. To overcome these issues, higher organisms have evolved extracellular carrier proteins to acquire, transport and manage iron.

1.2. Iron metabolism

In humans, total body iron amounts to approximately 3–4 g, two-thirds of which is incorporated, as heme, in the hemoglobin present in erythroid precursors and mature erythrocytes (Nemeth and Ganz 2021). Under physiological conditions, around $4x10^{11}$ senescent erythrocytes, containing a total of 20 mg of iron, are engulfed by macrophages each day. Thus, to preserve homeostasis, 20 mg of iron is required daily for production of hemoglobin for new erythrocytes (Fig. 1).

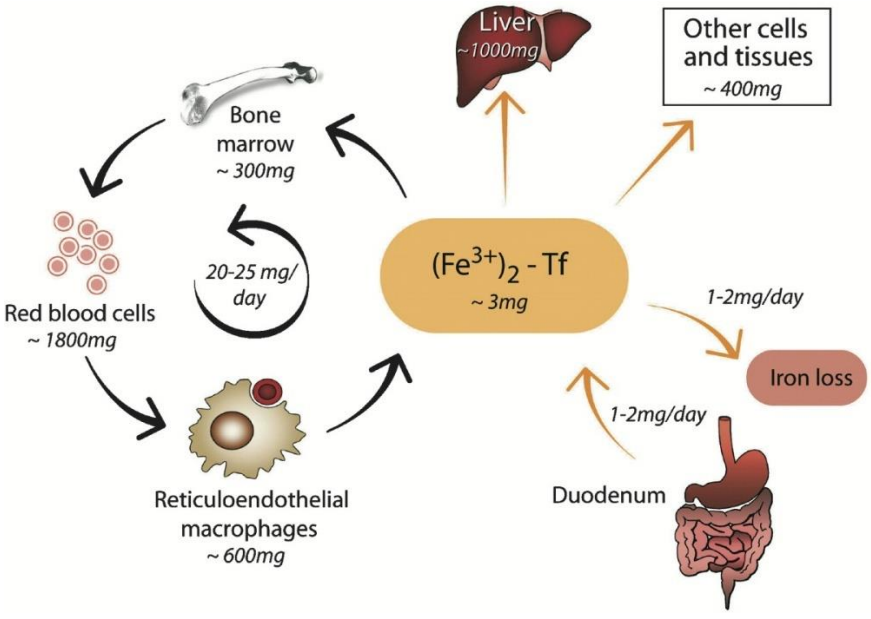

Figure 1. Systemic iron homeostasis. Iron is absorbed from the diet through the enterocytes and released into the bloodstream where it is bound to transferrin. Approximately 20-25mg of iron is used for erythrocyte biosynthesis. Reticuloendothelial macrophages recycle iron from senescent or damaged erythrocytes thus rendering it available for biological processes. Minor amounts of iron are used by the tissues. Iron loss, about 1-2 mg, is not directly regulated and occurs through scaling of duodenal enterocytes or hemorrhage. Abbreviation: Tf, Transferrin (Hentze et al., 2004).

Dietary iron assumption is necessary in all stages of human life, from fetal to neonatal development, childhood and adulthood. Bioavailability of iron sources depends on iron-relative solubility, the age

and relative developed gut, as well the state of health of the consumers. From the diet, the average daily iron intake is around 15 mg for children aged 2–11 years, 20 mg for men and 18 mg for women, depending on diet habits. However, due to the low solubility, only about 10% of dietary iron is actually absorbed by the intestinal mucosa (Nemeth and Ganz 2021) (Fig. 1).

In the first months of life, iron is taken up as a micronutrient from breast milk meeting the daily requirement (0.3 mg/L) (Prel and Koletzko 2016). After weaning, the main bioavailability sources are heme iron, mainly from hemoglobin and myoglobin, and non heme iron, deriving from vegetal and animal foods. Although historically meant to be non-easily absorbed, heme iron is a key source for metal intake (Carpenter and Mahoney 1992). Heme, released from myoglobin and hemoglobin by proteolytic activity in the stomach and small intestine, is stabilized by hemoglobin degradation products, dietary components and alkaline pH of small intestine, thus avoiding aggregation (Anderson et al., 2005). Differently from inorganic iron, which is more prone to be sequestered by some food components, such as humic substances (tannins, phytate) and chelators (deferoxamine), intact heme is easily absorbed by intestinal enterocytes (Anderson et al., 2005). The different bioavailability regarding iron sources explains the high predisposition to iron deficiency of vegetarian people with respect to meat consumers. Despite importance of heme iron as dietary source, the mechanism by which it is absorbed by enterocytes is still poorly characterized. The passive diffusion theory was abandoned when studies found higher absorption rate for heme than Vitamin B12, a macromolecule with similar structure, size, and ionic charge (Roberts et al., 1993). To date, a principal heme uptake pathway involves the Heme Carrier Protein 1 (HCP1), a proton-coupled folate transporter (PCFT/HCP1) (Shayeghi et al., 2005), capable to transfer heme directly into the cell cytoplasm. Here, heme is catabolized to free iron and biliverdin by heme oxygenase or it crosses the basolateral membrane by means of the heme exporter FLVCR1, thus reaching the blood. Further analyses are needed, however, studies suggest that heme-iron intake by enterocytes is facilitated by a vesicular transport system, presumably binding first to the brush-border membrane of enterocytes, and then undergoing internalization into the cytoplasm, finally appearing within enclosed vesicles, where iron is detached from heme and released into cytoplasm probably by Divalent Metal Transporter 1 (DMT1) (Hooda et al., 2014). DMT-1 is well known for its fundamental role in inorganic iron absorption at intestinal level. Four DMT-1 isoforms, generated by alternative splicing and translational regulation, are regulated by iron request in different cell types. The isoform DMT1A-I is expressed on the apical side of enterocytes and can cotransport Fe^{2+} and H^{+}, but also uncoupled substrate (Fig. 2). In all other cell types, DMT1 A-II, B-I and B-II isoforms promote the release of endocytosed Fe^{2+} into the cytoplasm (Hubert and Hentze 2002). Since dietary iron is mostly found in the ferric state, it must be reduced by duodenal cytochrome b, making it accessible to DMT1A-I.

DMT1 is an integral membrane protein containing 12 transmembrane domains, with both N- and C-terminus located in the cytoplasm (Wang et al., 2011).

Once inside the cell, ferrous iron is either used for cellular functions or captured by poly(rC)-binding protein (PCBP) chaperones, which escort the metal to the storage/utilization routes or to the basolateral membrane to be exported into blood. As free iron would organize into toxic aggregates, it is sequestered in the main cell iron storage protein, namely Ferritin (Ftn), as well as stored in hemosiderins in macrophages and hepatocytes. Ftn is a spherical heteropolymer of 24 Heavy (H) and Light (L) subunits. As PCBP1 can only interact with the exterior of the Ftn shell, it is likely to transfer its bound iron to sites located in the Ftn pores that funnel iron to the interior (Leidgens et al., 2013). The Ftn ferroxidase center is able to oxidize and conserve up to 4500 iron atoms as ferric ions (Sargent et al., 2005). Ferritin stores ferric iron in a mineralized, non-toxic state. However, ferritin-bound iron cannot be directly utilized by the cell. Consequently, iron must be released from ferritin to be bioavailable, through lysosomal (Kidane et al., 2006; Zhang et al., 2010), or proteasomal (Voss et al., 2006) degradation of ferritin. Nuclear receptor coactivator 4 (NCOA4) was identified as the cell cargo responsible for mediating Ftn autophagy (Dowdle et al., 2014). Depending on iron tissue requirements, the ability to cross the basolateral membrane and the consequent release into the plasma is guaranteed by the coupled Ferroportin (Fpn)/multicopper ferroxidase (MCFs) system (Fig. 2). Fpn, the only known iron exporter in mammals, provides a ferrous iron gate not only for enterocytes, but also for the main cell types involved in iron homeostasis. Fpn is a member of the Major Facilitator Superfamily (MFS) of transporters, consisting of N- and C-lobe each composed of 6 transmembrane helix bundles with both N- and C-termini located into the cytoplasm, similarly to DMT1 (Billesbolle et al., 2020). Structural characterization of the ortholog *Bdellovibrio bacteriovorus* Fpn with 24% identity and 40% similarity with human Fpn provided the first support of the alternate access mechanism model for iron export (Bonaccorsi et al., 2015; Taniguchi et al., 2015). Resolution of the structure of human Fpn by cryo-EM confirmed the predicted 12TM organization typical of MFS and identified metal- and hepcidin-binding sites (discussed in more detail below). Fpn switching from open inward conformation to open outward conformation ensures cytosolic iron passage through a central cavity. Once exported from the cell, ferrous iron is oxidized by Fpn-coupled MCFs, such as Hephaestin (Heph), Ceruloplasmin (Cp) or Zyklopen (Zp), depending on the cell type (Bonaccorsi et al., 2018). Heph is the sole MCF in enterocytes, tethered to the cell membrane through a single C-terminal transmembrane domain, but it is also moderately expressed in multiple other tissues, such as the central nervous system (Vulpe et al., 1999; Jiang et al., 2015) and the kidney (Jiang et al., 2016). Cp, first discovered as soluble plasma protein, is produced by hepatocytes, macrophages and immune cells, induced by inflammation or iron loading (Bonaccorsi et al., 2018). It is an

inflammatory, acute-phase plasma protein with numerous functions, ranging from copper transport to biological amines oxidation, to antioxidant activity exerted through several different mechanisms (Bonaccorsi et al., 2018). In addition, alternative splicing processes give rise to a membrane-anchored glycosylphosphatidylinositol (GPI)-linked Cp. This latter form, mainly expressed in astrocytes (Jeong and David 2003), hepatocytes, macrophages and retinal epithelial cells (Mostad and Prohaska 2011; Marques et al., 2012), is particularly important in facilitating iron release from the liver and CNS. Lastly, Zp was recently identified in placenta, but it is also expressed in mammary gland, kidney, brain, and testis (Chen et al., 2010). Like Heph, Zp contains a single C-terminal transmembrane domain, anchoring it to the cell membrane.

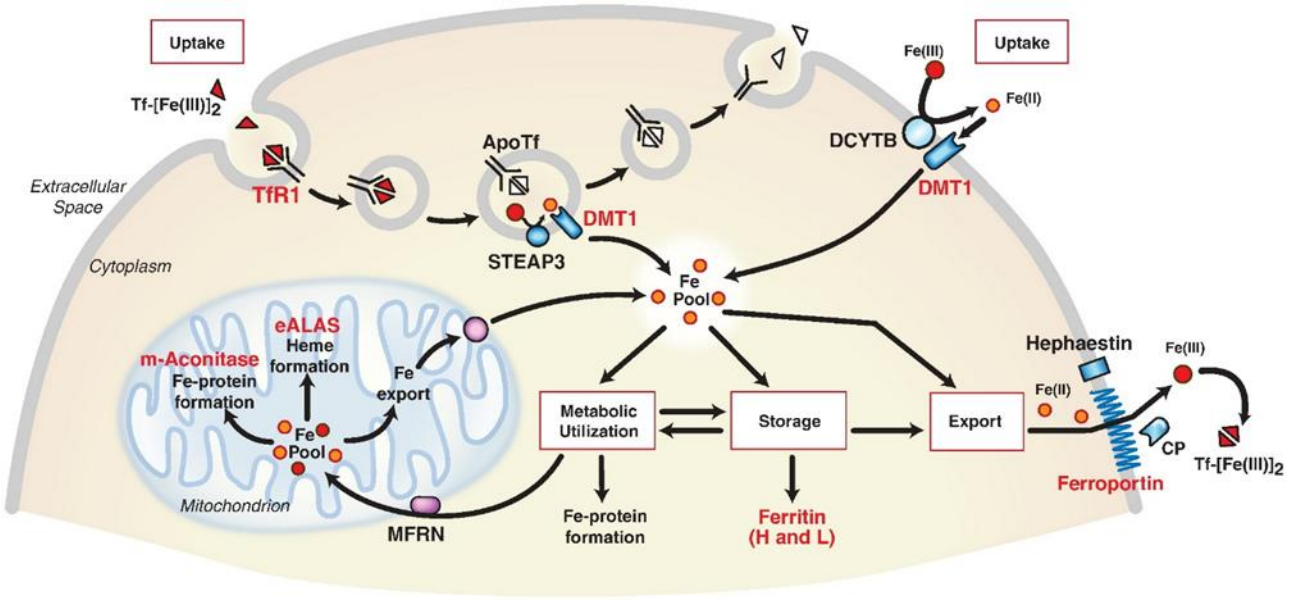

Figure 2. **Iron metabolism.** DMT1 located in the apical membrane of enterocytes allows Fe^{2+}, previously reduced by DCYTB, to enter the cell. Iron in turn can be: **i**) used for biological processes such as heme biosynthesis as well formation of Fe-S clusters; **ii**) stored in Ftn; **iii**) become part of the cytosolic iron pool **iv**) being exported via Fpn. The export of iron from the cell is coupled to oxidation by Heph in enterocytes and Cp in macrophages. Saturated Tf binds to TfR1 on the surface, where the Tf-TfR1 complex is endocytosed. Acidification of the endosome ensures the release of iron from Tf and following STEAP3-mediated oxidation, it is released by DMT1 into the cytoplasm. Abbreviations: DMT1, Divalent Metal Transporter 1; DCYTB, Duodenal Cytochrome b; MFRN, Mitoferrin; eALAS, erythroid Aminolevulinic acid synthase; Cp, Ceruloplasmin; Tf, Transferrin; TfR1, Transferrin Receptor 1 (Anderson et al., 2012).

After MCF-mediated oxidation, iron is ready to be bound by serum Transferrin (sTf) which delivers it to cell targets. This occurs by the well-known iron internalization mechanism mediated by sTf /Transferrin Receptor 1 (TfR1) complex formation. At the extracellular pH of 7.4, Tf can bind one or two ferric ions, and two iron-bearing Tf molecules can bind the dimeric TfR1 as iron-free Tf is not recognized by TfR1 at this pH (Cheng et al., 2004). The binding between these two proteins induces

clathrin-mediated endocytosis, where lowering of pH triggers iron release from Tf. Iron is then converted to Fe^{2+} by metalloreductase STEAP3 and transported by DMT1A/B-II to the cytoplasm. Meanwhile Tf and TfR1 are recycled to the cell surface, where Tf is released from TfR1 at the neutral pH of the extracellular environment. Of note, TfR1 is also able to uptake serum heavy-chain ferritin (H-Ftn) as an additional iron source (Anderson and Frazer 2017; Li et al., 2010). From a structural point of view, TfR1 is a homodimeric type II transmembrane protein composed by two identical glycosylated subunits with an approximate mass of 95 kDa, each linked by two disulfide bonds (Al-Refaei et al., 2020). Each monomer is folded in a small cytoplasmic domain, a single-pass transmembrane region and a complex extracellular domain (Al-Refaei et al., 2020). Crystallographic studies of the ectodomain region have revealed that it possesses a butterfly-like shape with three subdomains: protease-like, apical, and helical (Lawrence et al., 1999). In particular, the ectodomain is used as binding site by sTf, which binds to the basal portion composed of protease-like and helical domains (Cheng et al., 2004; Montemiglio et al., 2019) whereas the apical domain is an attractive viral particles target (Giannetti et al., 2003). After being taken up by TfR1-mediated endocytosis, iron employed for cellular functions mainly reaches mitochondria, where numerous metabolic processes take place. Significant iron demand is necessary for biosynthesis of heme for hemoglobin in reticulocytes/erythrocytes and other heme-containing proteins in all cells, as well as Fe-S cluster assembly of enzymes involved in oxidative phosphorylation (Fig. 2). In addition, excess metal is incorporated into the homologous of cytosolic Ftn, named Mitochondrial ferritin (Katsarou et al., 2020).

When the amount of iron exceeds the binding capacity of the proteins which make use of it, or is inappropriately shielded, its correlated toxicity is more visible in those organs with low regeneration rates, such as Central Nervous System (CNS). In the brain, the higher demand of iron for myelin sheath formation, neurotransmitter metabolism and mitochondrial electron transport is guaranteed by finely regulated iron flow. It is well known that the brain is protected by a special structure called Blood–Brain Barrier (BBB), which can prevent the entry of pathogen and other macromolecular compounds into CNS. The BBB is characterized by formation of tight junctions between endothelial cells, which form a selective barrier for the transport of ions and molecules from the blood to the parenchyma of the brain, and vice versa (Abbott 2002). A proper balance of iron uptake at the BBB is of pivotal importance since too much or too little iron can result in various neurological diseases (Duck and Connor 2016). Therefore, iron transporters and receptors play a crucial role in the maintenance of brain iron homeostasis; their dysregulation is usually associated with many neurological diseases and they are the major targets of current research (Ward et al., 2014). Once iron has passed through the endothelial cells of BBB, it is picked up by astrocytes that make it available

to other cells (Duck et al., 2017; McCarthy and Kosman 2013; Simpson et al., 2015). In astrocytes, microglia and neuronal cells the main iron uptake system is the Tf/TfR1 complex, while the coupled system of Fpn/Cp is highly conserved for iron release (Duck and Connor 2016). Very interestingly, astrocytes act as regulatory cells of metal homeostasis, being a sort of iron reservoir that can act as neuronal protectors by reducing the pool of iron in the synaptic cleft (Jeong and David 2003). Therefore, the natural barrier and astrocytes play a fundamental role in finely regulating brain iron homeostasis. However, from local to systemic iron homeostasis, numerous cellular and systemic regulatory mechanism are needed. Thus, it is not surprising that each type of brain cells, such as neurons, oligodendrocytes and astrocytes, possesses distinct iron metabolism. For that reason, even more than other tissues, brain requires a fine and tight iron homeostasis in order to maintain normal physiological functions and avoid neurotoxicity.

1.2.1. Regulation of iron metabolism

The daily iron requirement comes not only from new food intake, but also from iron recycling by macrophages and mobilization from the main reserve source, the liver (Nemeth and Ganz 2021). Currently, a route of iron excretion has not yet been found, hence homeostasis is regulated in a coordinated manner by the absorption, use, recycling, storage and export of the metal. The post transcriptional modulation is an iron-dependent mechanism involving the binding of iron regulatory proteins (IRPs) to stem loop iron-responsive element (IRE) located at the untranslated regions (UTRs) of iron proteins mRNA. During iron deficiency, IRPs bind to 3' UTR of DMT1 and TfR1 mRNAs. This event stabilizes and increases the mRNA half-life, thus promoting protein expression and maximizing iron supply. On the other hand, the binding to 5'UTR of Fpn and Ftn blocks translation, reducing export and storage. During iron overload, IRP2 is degraded while Fe-S cluster formation in IRP1 favors aconitase activity and hinders IRE binding. Upon this condition, both Fpn and Ftn can be expressed whereas TfR1 and DMT1 mRNA are readily degraded, thus limiting cellular iron uptake and promoting export and storage. Interestingly, in erythroid cells, the intake of large amount of iron can bypass the negative IRP regulation for TfR1, indicating a tissue dependent modulation (Gao et al., 2019).

At systemic level, the pivotal regulator of iron metabolism is the peptide hormone hepcidin, produced as pre-pro-hepcidin of 84 amino acids by hepatocytes and in smaller quantities by macrophages and adipocytes. Following two proteolytic events, the 25 amino acids mature form is produced, folding in a hairpin structure stabilized by 4 disulfide bridges (Rochette et al., 2015). The main role played by hepcidin is to reduce iron levels in the blood by down-regulating Fpn. Ultimately, the hormone

reduces the absorption of intestinal iron and its recycling from the reserve organs, making it unavailable (Palaneeswari et al., 2013). The mechanism is similar to receptor internalization and its subsequent ligand-mediated degradation (Nemeth et al., 2004). The interaction between hepcidin and Fpn induces a conformational change followed by the ubiquitination of the transporter leading to its degradation by proteasome/lysosome (Ross et al., 2012; Qiao et al., 2012). Another mechanism involves the Fpn reversible occlusion mediated by hepcidin, dependent on the hormonal dose (Aschemeyer et al., 2018). The study by Billesbolle et al. 2020, aimed at clarifying the hepcidin-Fpn interaction, employed a combination of cryo-electron microscopy, molecular simulations, and biochemical approaches. The results showed that the hormone was able to bind Fpn in an outward-open conformation, thus occluding the iron efflux pathway. Interestingly, hepcidin binding affinity to Fpn is 80-folds higher in presence of the metal ligand, suggesting that iron-loaded Fpn is the favorite target (Billesbolle et al., 2020).

Hepcidin production is influenced by systemic iron status, inflammation, erythropoiesis, hypoxia (Nemeth and Ganz 2021). The main organ sensitive to systemic iron overload is the liver, where sinusoidal epithelial cells secrete bone morphogenetic protein (BMP)-6, which interacts with BMP receptors (types I and II) and hemojuvelin complex (BMPRs/HJV). The interaction between BMP-6 and BMPRs/HJV induces phosphorylation of the SMAD factor which, by translocating into the nucleus, increases the expression of hepcidin (Canali et al., 2017). Activation of the BMP-SMAD pathway could be mediated by the hemochromatosis protein (HFE) that acts as a sensor for the Tf-TfR complex. The proposed mechanism involves the interaction between HFE and TfR, thus activating the pathway that reduces the systemic iron content (Hare 2017). As inflammation is concerned, hepcidin induction is typically mediated by pro-inflammatory cytokines, with special regard to interleukin (IL)-6 as well as IL-1β e IL-22 (Lee et al., 2006). The transduction pathways involve IL-6 binding to its receptor constituting a hexameric complex that in turn activates Janus Kinase 2 (JAK2) by promoting STAT3 phosphorylation, dimerization and translocation into the cell nucleus (Ganz and Nemeth 2015), where it activates hepcidin expression (Baker et al., 2007). Overall, inflammatory stimuli result in iron sequestration into enterocytes, reticuloendothelial system and hepatocytes, therefore restricting metal availability to other tissues.

1.2.2. Iron homeostasis and inflammation

The alteration of iron metabolism is closely associated with pathologies. Iron deficiency/overload can be caused by insufficient amounts of iron from the diet, blood loss, hemolysis, but also by gene mutations and blood transfusions. Iron deficiency is the leading cause of anemia affecting three billion people worldwide (Cappellini et al., 2020). Since iron is used for 2/3 in the process of erythropoiesis, its deficiency is reflected in a reduced production of red blood cells. Iron deficiency is more frequent in children and women, causing poor development of growth and cognitive functions, inattention, asthenia, headache, premature birth. Persistent anemia is associated with complications mainly affecting the cardiovascular system such as angina and heart attack and in children high risk of infections and slowed growth (Andrews 1999). The systemic disorder characterized by reduced serum iron content is the well-known anemia of chronic inflammation (AI) (Fig. 3), a syndrome primarily associated to systemic inflammation and disorder of iron distribution, usually characterized by low transferrin saturation and high serum ferritin. At the base of this pathology there may be other problems such as tumors or microorganism and virus infections (Nemeth et al., 2003), including Human Immuno-Deficiency Virus (HIV) and the recent Severe Acute Respiratory Syndrome Coronavirus (SARS-CoV-2) (Araújo-Pereira et al., 2022; Bergamaschi et al., 2021). Usually, inflammation is a systemic defense response against viral and microbial infections. However, its protraction can result in a harmful process for the host, leading to tissue damage and organ failure. The inflammatory process influences hepcidin synthesis which increases predominantly for the JAK2-STAT3 activation mediated by IL-6. In enterocytes and macrophages, the hepcidin-mediated Fpn down regulation is usually accompanied by the coordinated decrease in TfR1 and DMT1 expression (Rosa et al., 2017), whereas hepatocytes take up most of the systemic iron by increasing TfR1 expression (Malik et al., 2011) thus reducing systemic iron load. Such regulation reflects the different functions performed by these cell types: intestinal iron absorption is inhibited and although iron is stored, it is not available for cellular processes, whereas iron retention in reticuloendothelial cells results in iron-restricted erythropoiesis. Globally, cellular iron accumulation and systemic metal deficiency are observed.

On the other side, iron overload occurs as a result of an excessive iron content in the bloodstream that exceeds the binding capacity of sTf or erythropoiesis needs. Hemochromatosis is the prevalent monoallelic disease in white population, collecting disorders associated with hepcidin reduction or a reduction in Fpn/Hepcidin binding. There are two main groups, hepcidin deficiency and hepcidin resistance characterized by several genetic mutations which affect the Fpn/Hepcidin regulatory axis. In hepcidin deficiency group, the mutations concern genes coding for HFE1, HFE2, Transferrin Receptor-2(TfR2) and hepcidin (HAMP) sabotaging hormone upregulation. The absence of hepcidin

leads to uncontrolled intestinal absorption of iron (a rates up to 8-10 mg / day). Once it reaches the bloodstream it exceeds the sTf binding capacity and causes the accumulation of toxic free iron thus leading to iron deposition in liver, heart, and a subgroup of endocrine tissues. In hepcidin resistance group, Fpn mutation renders the exporter insensitive to peptide hormone regulatory action causing uncontrolled release of iron from macrophages and duodenal enterocytes into the plasma (Drakesmith et al., 2005) (Fig. 3).

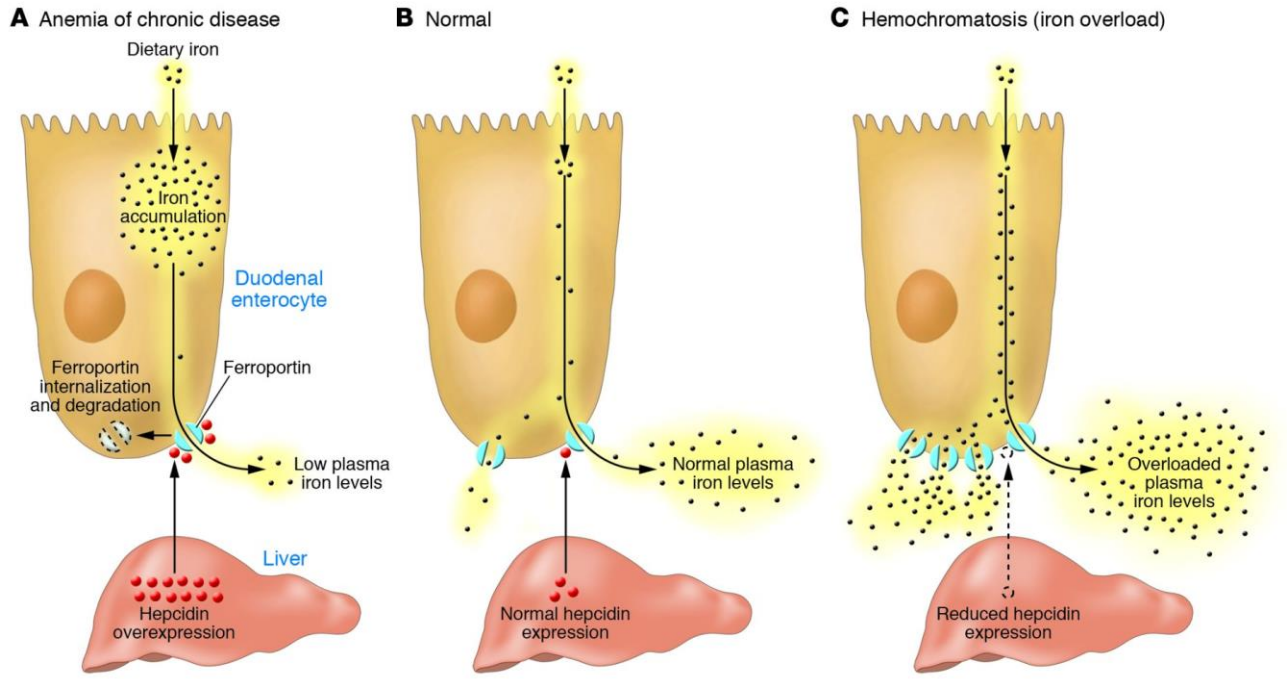

Figure 3. A) Following inflammatory stimuli, hepcidin is produced by the liver. High levels of hepcidin in the bloodstream lead to degradation of Fpn resulting in iron accumulation in macrophages, low iron levels and thus saturation of Tf in plasma and reduced erythropoiesis. (**B**) Normal levels of hepcidin regulate the amount of iron in plasma. (**C**) Haemochromatosis is caused by insufficient hepcidin levels resulting in increased plasma iron, high Tf saturation and excess iron accumulation in the liver (De Domenico et al., 2007).

Notably, hepcidin indirect role in iron-mediated oxidative stress is typical of pathological conditions from neuroinflammation (Xu et al., 2020; Probst et al., 2021) to viral infections (Bayraktar et al., 2022), thus highlighting the wide implication of iron homeostasis alteration. Overall, in various pathological conditions, the inflammatory process, dysregulation of iron metabolism and oxidative stress are closely interrelated.

1.3. Iron homeostasis during viral infections

The viral infection is a pathological condition beginning with penetration of viral particles into the host, which defends itself by implementing cellular and systemic responses. The first defense line to prevent invasion and diffusion is the host innate immune system, which takes place before a specific adaptive immune response is set up. Tissue inflammation is typical of excessive leucocyte population recruitment at the site of infection, whereas systemic inflammation consists of excessive activation of circulating leucocytes. Not many viruses cause disease and activate acute inflammation. Some of the most dangerous include Rabies, Ebola viruses, Influenza Viruses, Human Immunodeficiency Virus (HIV), Coronavirus Acute Respiratory Syndrome (SARS-CoV), Middle East Respiratory Syndrome (MERS)-CoV and the most recent SARS-CoV-2 (Casanova and Abel 2021). Iron, as an overseer of the immune response, promotes the differentiation of immune cells and affects cell-mediated response and cytokines activity. Host susceptibility to viral infections is influenced by iron availability, fundamental for viral replication and multiplicity. To limit accessible iron, the body intervenes with effector weapons such as immune cells, liver derived acute-phase proteins and pro- and anti-inflammatory cytokines. In particular, IL-6 actively promotes iron traffic veering from the bloodstream to the endothelial reticulum system reserve. As iron localization is concerned, in vitro studies have shown that the cellular response leads to reduction of Fpn levels in infected enterocytes (Frioni et al., 2014) and in inflamed macrophages, in parallel with a reduction of both TfR1 and Cp as well as an increase of Ftn (Cutone et al., 2014; Cutone et al., 2017). The reduction in circulating iron has been so far attributed to host defense mechanism to limit the metal to extracellular pathogens (Cairo et al., 2006). However, high availability of iron is requested as a nutrient for viral survival (Drakesmith and Prentice 2008) and intracellular infectious agents, including viruses, multiply extensively in iron loaded sites, thus this concept should be deeply reconsidered. Efficient viral spread is correlated with increased host metabolism, as the enzymes involved in viral genome duplication and viral proteins synthesis require iron to carry out their activities. Therefore, the expansion of viral populations must be accompanied by an increase in iron bioavailability (Drakesmith and Prentice 2008). Usually, progression of the infection is promoted by cellular iron overload, as demonstrated for human immunodeficiency virus (HIV) (Schmidt 2020) as well as for SARS-CoV-2 (Habib et al., 2021) where it contributes to pathogenesis. An exception is the hepatitis C virus (HCV), in which iron excess damages viral particles (Armitage et al., 2014). In addition, the Tf/TfR1 system plays a key role in viral entry into host cells. TfR1 apical domain is a cell gate for different viruses, ranging from canine parvovirus (CPV) to feline panleukopenia virus (FPV) (Parker et al., 2001). Although numerous studies have been carried out, the relationship between iron homeostasis and viral infection is still not well understood and further investigations are needed. The promotion of viral infectivity,

transmissibility, disease severity and the development of immunity against infection is also mediated by structural and non-structural viral proteins. Infected cells can release viral proteins that act at a distance on other target cells. Many studies have attributed a key role to viral proteins, describing them as virulence factors and neurotoxins (Bansal et al., 2000; Saadi et al., 2021). For instance, since HIV-1 does not infect neuronal cells, viral proteins are the causative agents of the neuronal death observed in infected patients (Marino et al., 2020). In addition, with regard to SARS-CoV-2, researchers have shown that virus-specific virulence factors can have a major impact on viral spread and blockade of the host cell defense response (Weiss and Leibowitz 2011). Therefore, current therapies require a targeted approach to counteract the adverse effect of such viral proteins. For this reason, two prominent viral proteins, Tat of HIV-1and Spike of SARS-CoV-2, will be investigated in the present research study.

1.3.1. HIV-1 and the role of Tat protein

HIV-1 is the infectious agent responsible for acquired immunodeficiency syndrome (AIDS). Despite the development of antiretroviral therapies (ART) which considerably increase the survival of people, HIV infections are the leading cause of mortality worldwide.

HIV is an enveloped retrovirus currently grouped into two subtypes, HIV-type 1(HIV-1) and HIV-type 2 (HIV-2). The first is the most widespread in the world, while the second is mainly located in Africa. During the infection, the body responds with systemic inflammation (Appay and Sauce 2008) by altering cellular and systemic iron homeostasis, leading to lower hemoglobin (Hb) levels associated with worse outcomes of HIV infection (Chauhan et al., 2011). Despite ART, about 50% of patients show signs of HIV associated neurocognitive disorders (HAND), such as behavioral abnormalities, memory and learning deficits as well as psychomotor disorders (Rojas-Celis et al., 2019). Indeed, infected patients show altered brain iron metabolism, resulting in mitochondrial damage (Darbinian et al., 2020).

At the mechanistic level, the viral envelope trimeric complex, composed of the heterodimer proteins gp120 and gp41, recognizes the host glycoprotein CD4 expressed on T-lymphocytes, monocytes/macrophages, eosinophils, dendritic cells and microglial cells of the Central Nervous System (CNS), allowing viral capsid entry. Following membrane fusion, viral RNA released into the cytosol is converted into DNA and integrated into the cellular genome (Fig. 4). At this point, latent infection can set in, with the main permanent reservoirs represented by the macrophages and CD4+ T lymphocytes (Alexaki et al., 2008). This is the main strategy that allows the persistence of the virus even in the presence of ART and immune response.

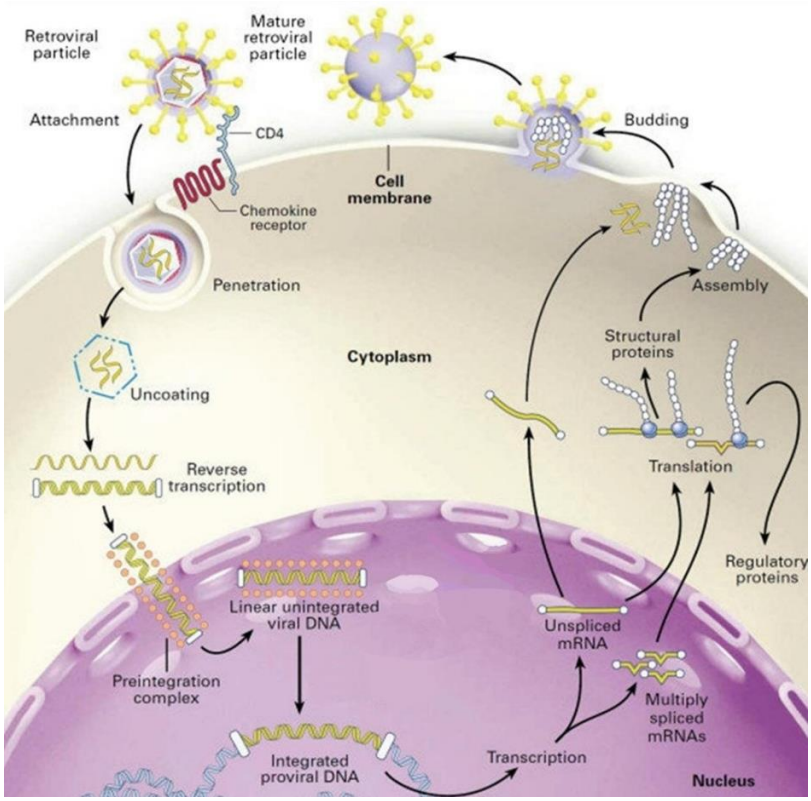

Figure 4. The crucial stages of the HIV-1 life cycle. The virus binds to the host cell's CD4 receptor and is internalized. The RNA genome is retro-transcribed into a double-stranded DNA molecule. As part of the pre-integration complex, the linear DNA enters the nucleus. Here, the linear viral DNA is the precursor to the integrated proviral DNA, which is a stable structure that remains indefinitely in the genome of the host cell and serves as a template for viral transcription. The viral transcripts are exported into the cytoplasm, where translation, assembly and processing of the retroviral particle take place. The cycle is concluded when the infectious retroviral particles are released from the cell (Modified from Pasternak et al., 2013).

The "Trojan Horse" model is the main mechanism proposed for HIV-1 brain infection, in which virus-carrying cells, such as T lymphocytes and monocytes, primarily cross the BBB and invade the CNS (Gras and Kaul 2010). Here, microglia and perivascular macrophages support HIV replication, while neuronal cells are not infected and astrocytes behavior is controversial. As shown in some pioneer studies, astrocytes rarely undergo HIV infection, indeed they were thought to play a secondary role in neuropathogenesis (Nuovo et al., 1994; Takahashi et al., 1996). In contrast, Churchill et al. 2009 highlighted much higher frequency of infected astrocytes in patients suffering from HIV-associated dementia (Churchill et al., 2009.). Recently, it was concluded that up to 20 percent of astrocytes are carriers of viral DNA (Sénécal et al., 2021). Therefore, being astrocytes a latent HIV-DNA reservoir, their dysfunction could greatly contribute to neuropathogenesis. In HAND, there is a shift in the balance between neuroprotection and neurotoxicity. Neuronal damage becomes prominent along with the production of proinflammatory cytokines and neurotoxic viral proteins from infected cells. During HIV infection, the release by activated microglia of proinflammatory cytokine factors, including

Tumor Necrosis Factor-α (TNF-α), IL-1β, IL-6, IL-8 (Alvarez-Carbonell et al., 2019), can shift astrocytes activity to a reactive state, thus promoting further proinflammatory cytokines production (Hyvärinen et al., 2019). As shown by Chang et al. 2015, high iron levels in CD4+ T cells are associated with increased HIV infection and replication. In addition, HIV-positive patients have an increase in serum iron regardless of ART. Besides depression of the immune system, HIV causes metabolic dysfunctions, including oxidative stress, due to the continuous immune activation associated with increased viral replication **(**Salman and Berrula 2012). This demonstrates the connection between inflammation, alteration of iron metabolism and HIV infection, suggesting iron metabolism-related systems as possible therapeutic targets. The ART is the standard therapy for HIV-1 infection that significantly reduces viral load and prolongs life expectancy, but the treatment does not suppress the expression of HIV-1 non-structural proteins. The neurotoxic effects have been reported to be mainly linked to the chronic basal expression of different viral proteins, such as gp120, Nef (Negative factor) and Tat (Transactivator of transcription) (Jadhav and Nema 2021). Tat is known to be toxic to neurons, and it can be secreted from HIV-infected cells, including astrocytes (Chauhan et al., 2003). This chronic low-level production of Tat has been proposed to contribute to neuronal damage over prolonged periods of time (Dickens et al., 2017). Specifically, the viral protein Tat is a cationic polypeptide whose length varies from 86 to 101 amino acids (Bagashev et al., 2013) produced immediately after host infection and acting as a transcriptional activator, promoting transcription initiation and elongation phase. Tat strongly activates viral gene expression from the long terminal repeat (LTR) through the recognition of short-stem loop structure known as Trans-Activation Response region (TAR) (Fig. 5).

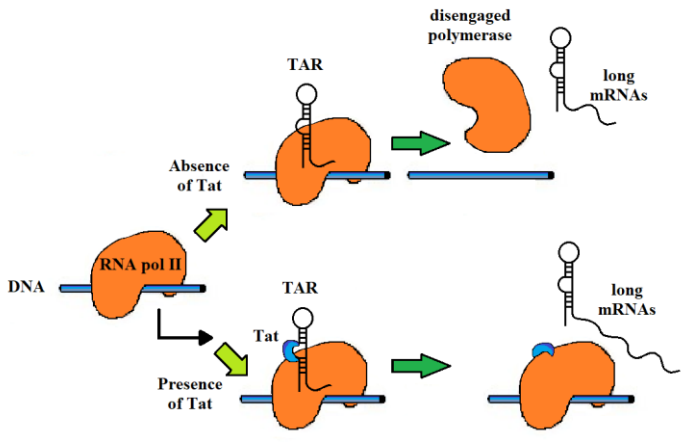

Figure 5. **Schematic representation on the function of the Tat-TAR interaction in transcription elongation**. In the absence of Tat (top), transcription complexes assemble on DNA and release short viral transcripts. In the presence of Tat (bottom), the transcription complexes are stabilized by the binding of Tat to TAR, promoting the production of long mature mRNAs. Abbreviations: Tat, Transactivator of transcription; TAR, Trans-Activation Response (Modified from Greenbaum 1996).

In addition, Tat is found in the serum of infected individuals (Barillari and Ensoli 2002) as well in cerebrospinal fluid (CSF), consistent with a release of neurotoxins from infected cells (Mediouni et al., 2012). The viral protein binds to and enter the cell through receptors for integrins or chemokines. Upon entrance, Tat can act as a multifunctional protein which regulates gene expression and different pathways to promote viral spreading. Depending on cell types it can promote chemokine expression, or act as neurotoxin in SNC. Being able to passively cross the BBB (Banks et al., 2005), Tat increases membrane permeability by reducing the expression of tight junction (András et al., 2011) and adhesin (Mishra and Singh 2013) proteins, thus facilitating the entry of the infected monocytes into the CNS (Bethel-Brown et al., 2011). Here, Tat can enter cells, including neurons, and modulate gene expression according to cell type to promote viral spread, neuroinflammation and neuronal loss (Dhillon et al., 2007; Asensio and Campbell 2001). Numerous cellular processes are modulated, such as DNA damage repair, apoptosis (Selliah and Finkel 2001), increased production of cytokines, chemokines and receptors (Ott et al., 1998; Secchiero et al., 1999; Gavioli et al., 2004). In addition, Tat protein, together with IFN-γ and TNF-α, promotes the generation of ROS and the activation of NF-kB signaling (Williams et al., 2009). In neuronal cells, Tat increases lipid peroxidation, ROS, nitric oxide (NO) as well peroxynitrite (ONOO-) formation by the activation of inducible nitric oxide synthase (Kim et al., 2015) promoting neurodegenerative disease. Recent studies have shown that constitutively Tat expression in astrocytes induces oxidative stress (Fig. 6). This state triggers a compensatory cellular response which implement the activation of erythroid Nuclear factor 2-related factor 2 (Nrf2), its subsequent nuclear translocation and the promotion of antioxidant response element (ARE) genes expression, including Glutathione Peroxidase 4 (GPX4), Glutamate-Cysteine Ligase (GCL) and a subunit of System Xc^--cystine/glutammate antiporter (SLC7A11) (Mastrantonio et al., 2019). This latter is a membrane antiport that guarantees the entry of cystine as a precursor of glutathione and the export of glutamate. Tat-mediated System Xc^- overexpression and, consequently, higher release of glutamate in the extracellular space induces a reduction of neuronal viability. Although astrocytes normally guarantee a protective antioxidant response for themselves and for neuronal cells, in this stress condition, the response translates into neurotoxicity (Gupta et al., 2010).

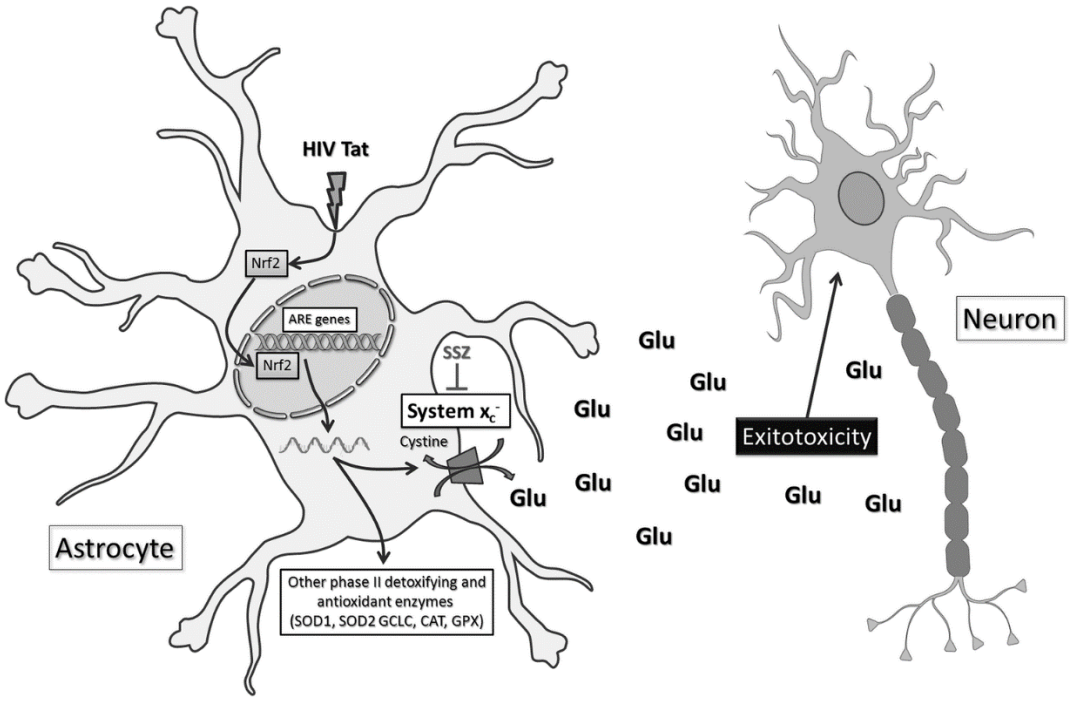

Figure 6. Model for the effects of Tat on Nrf2 translocation, ARE gene upregulation, Xc activation and glutamate release during HAND. In astrocytes, Tat activates the cellular response mediated by the nuclear translocation of Nrf2, which promotes the expression of antioxidant genes such as SOD1, SOD2, GCLC, CAT, GPX, including a subunit of the Xc-cystine/glutamate antiport system. The import of cystine is crucial for glutathione production and the reduction of oxidative stress; whereas the high release of the neurotransmitter glutamate into the extracellular space may promote neurotoxicity. Abbreviations: ARE, antioxidant response element; CAT, catalase; GCLC, γ-glutamyl-cysteine ligase; Glu, glutamate; GPX, glutathione peroxidase; Nrf2, erythroid nuclear factor 2-related factor 2; SOD, superoxide dismutase (Modify from Mastrantonio et al., 2019).

Glutamate is an excitatory neurotransmitter important for learning, memory and synaptic plasticity, yet a too high content constantly stimulates receptors, including the N-methyl-D-aspartate (NMDA) receptor. The situation is exacerbated by the further action of Tat, which prevents neurotransmitter reuptake by astrocytes (Zhou et al., 2004) and phosphorylates the NMDA receptor (Haughey et al., 2001; Song et al., 2003). Overall, Tat-induced neuronal degeneration is attributed to the dysregulation of calcium homeostasis, ROS induction, activation of caspase and excitatory amino acid receptor (Nath et al., 1996; Kruman et al., 1998; Haughey et al., 2001). However, HAND has many facets and involves numerous cellular processes yet to be discovered and clarified.

1.3.2. SARS-CoV-2 and the role of Spike glycoprotein

Coronaviruses (CoVs) are a family of single-stranded RNA viruses characterized by a positive envelope grouped into four genera (alphacoronavirus, betacoronavirus, gammacoronavirus, and deltacoronavirus). They are responsible for multiple diseases of the respiratory tract ranging from a

simple, common cold to bronchiolitis and pneumonia. CoVs can infect a wide variety of species from mammals to avian species as well companion animals. In particular, Human Coronaviruses (HCoVs) such as HCoV-229E and HCoV-OC43 and the newer HCoV-NL63 and HCoV-HKU1, cause milder symptoms. On the other hand, highly pathogenic HCoVs appeared over the last 20 years in different world sites which have given rise to major fatal human pneumonia epidemics. We here recall the Severe SARS-CoV that appeared in 2002 at Foshan, China, the Middle East Respiratory Syndrome Coronavirus (MERS-CoV), after a decade in Jeddah, Saudi Arabia, and the recent SARS-CoV-2 in 2019 at Wuhan, China (Kirtipal et al., 2020). Their pathogenicity is caused by high recombination and nucleotide substitution rates, which is an obvious selective advantage. By infecting the first respiratory tract, i.e. epithelial and bronchial cells and pneumocytes, HCoVs can cause severe and unresolvable respiratory diseases (V'kovski et al., 2021). Viruses, as obligate intracellular parasites, have developed several tricks to hijack the host's machinery (Lim et al., 2016) and favor their own cycle of replication and pathogenesis.

The most recent SARS-CoV-2 is the causative agent of coronavirus disease (COVID)-19, which was declared a global pandemic by The World Health Organization (WHO) on March 11, 2020. The structural proteins that characterize the virions are Envelope (E), Membrane (M), Nucleocapsid (N) and Spike (S). The first two are important in the assembly of the viral particles, while N encapsulates the genome. Spike is a trimeric glycoprotein composed of two main subunits, S1containing the Receptor Binding Domain (RBD) and S2 involved in the fusion with host cells (Fig. 7).

The infection phase begins when S trimer protrudes from the host-derived viral envelope and provides specificity for cellular input receptors. The best known is the Angiotensin-Converting Enzyme 2 (ACE2) widely distributed on epithelial cells of trachea, bronchi, bronchial serous glands and alveoli (Liu et al., 2011), alveolar monocytes and macrophages (Kuba et al., 2005) as well as on renal epithelial cells and mucous cells of the intestine (Hikmet et al., 2020). The conformational change induced by receptor binding exhibits S2 internal cleavage site to proteolytic action performed by the serine protease TMPRSS2, or endosomal cysteine proteases cathepsin B (CatB) and CatL (Senapati et al., 2021; Gkogkou et al., 2020). Once the interaction has occurred, proteolytic cleavage of Spike separates the RBD from the S2 domain, promoting its fusion on the cell or endosomal membrane (Takeda 2022). In addition to ACE2, Spike basic residues interact also with Heparan Sulfate Proteoglycans (HSPGs) negative charged molecules contributing to SARS-CoV-2 infectivity (Walls et al., 2020). In addition, a recent study suggested TfR1 as SARS-CoV-2 transporter shuttling between the inside and outside of cells (Tang et al., 2020). During intracellular life, coronaviruses replicate their RNA genome and incorporate it into new viral particles (Fig. 7). Following infection, the innate immune system of the host acts as the first defense line to prevent viral propagation. The severity of

the disease is closely related to the host defense immune response and to the release of proinflammatory cytokines, including IL-6 (Liu et al., 2020). An excessive release of this cytokine can cause tissue and organ damage although the mechanism for initiation of a hyper-inflammatory response is poorly understood.

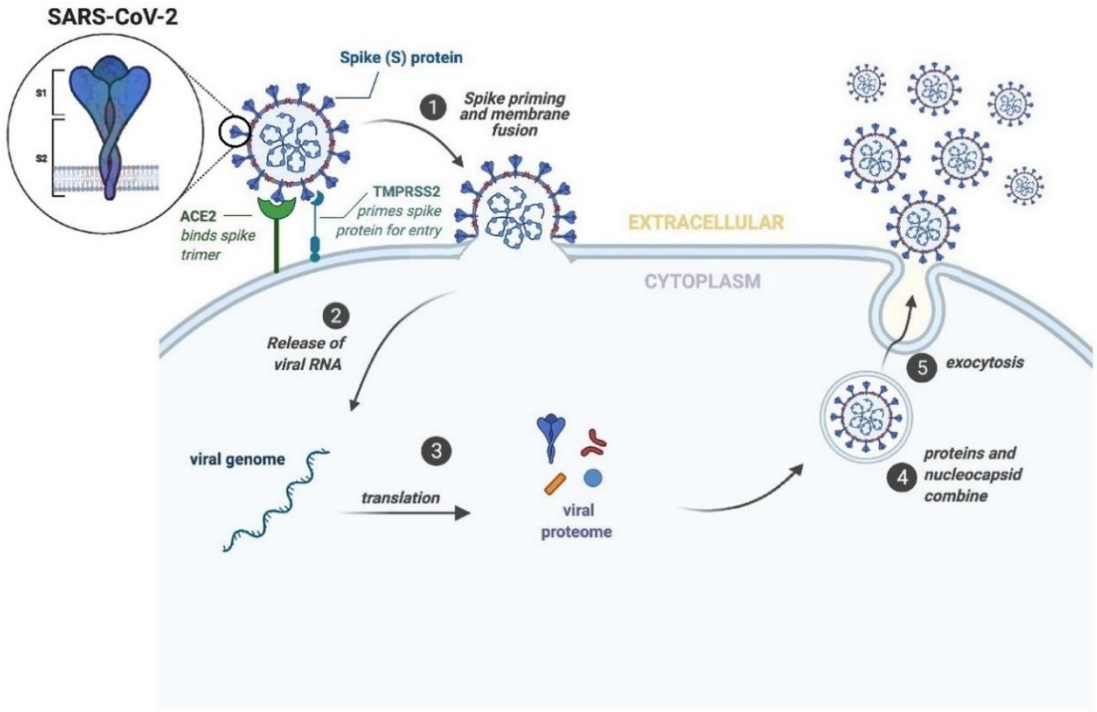

Figure 7. Schematic representation of SARS-CoV-2 Spike glycoprotein and crucial stages of the SARS-CoV-2 life cycle. SARS-CoV-2 uses the Spike(S) glycoprotein to bind to the host cell's ACE2 receptor, TMPRSS2 primes Spike glycoprotein and trigger fusion events between the virus and the host membrane (**1**). The virus is internalized through receptor-mediated endocytosis or through clathrin-mediated pathways. Once in the cytoplasm, viruses release their genomes (**2**) to allow replication of their genetic material (**3**). After production of the SARS-CoV-2 structural proteins, the nucleocapsids are assembled in the cytoplasm (**4**) and the viruses are released from the infected cell through exocytosis (**5**). Abbreviations: S1, subunit 1; S2, subunit 2; ACE2, Angiotensin-Converting Enzyme 2; TMPRSS2, Transmembrane Protease Serine 2 (Modify from Grobbelaar et al., 2021; Modified from Johansen-Leete et al., 2022).

Recent studies have shown that SARS-CoV-2 virulence factors act on the immune system. Spike is a molecular pattern associated with viral pathogens (PAMPs) that is recognized by toll-like receptor 2 (TLR2), which dimerizes to activate the NF-κB pathway, and an over response characterized by the so-called proinflammatory cytokine storm is triggered (Patra et al., 2020) (Fig. 8). As already described, the increase of IL-6 significantly modulates iron metabolism, indeed it is now known that SARS-CoV-2 infection is related to dysregulation of iron metabolism. In Covid-19 patients, numerous alterations have been reported including high hepcidin levels associate to systemic inflammation as well hyperferritinemia (Banchini et al., 2021). Serum ferritin levels can predict COVID-19-related severity and mortality, as high levels are related to poor prognosis (Suriawinata et al., 2022). The

increase in serum hepcidin is related to a reduction in serum iron but also to oxidative stress that has been proposed as a marker for COVID-19 pathogenesis (Michels et al., 2015; Nai et al., 2021). In the serum of critically ill COVID-19 patients, hepcidin over expression is related to decreased serum iron, which is not accessible to pathogens in the circulation, and also related to oxidative stress (Bayraktaret al., 2022). Host response to SARS-CoV-2 infection generates a vicious cycle between viral infection, inflammation, dysregulation of iron metabolism and oxidative stress. Within this framework, the identification of a molecule able to counteract such vicious cycle would be of utmost importance.

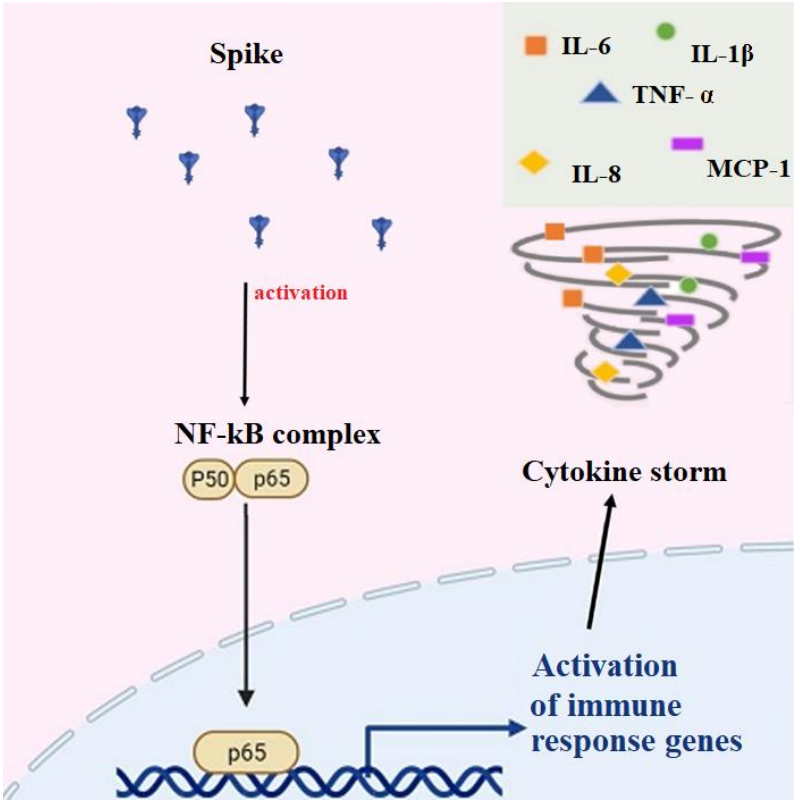

Figure 8. Spike as a virulence factor is able to activate NF-kB complex and induce immune response associated to a storm of pro-inflammatory cytokines. Abbreviations: NF-Kb, Nuclear Factor kappa B; Interleukin (IL)-6; IL-8; IL-1β; Tumor Necrosis Factor-α (TNF-α); Monocyte chemoattractant protein-1 (MCP-1) (Modified from: Tumpara et al., 2021).

1.4. Lactoferrin: structure, properties and related functions

Lactoferrin is a whey glycoprotein discovered around the 1940s by Sorensen and Sorensen (Sorensen and Sorensen et al., 1940) and subsequently purified from human and bovine milk and defined as iron-binding red protein (Johanson 1960). Lf is secreted by mucosal epithelial cells, and it is present in many biological fluids such as saliva, tears, semen, CSF, urine, bronchial secretions, vaginal discharge, synovial fluid (Czosnykowska-Lukacka et al., 2019). The highest Lf concentration is found

in human colostrum (around 6-8 mg/ml) and the amount decreases by about one third in mature milk (Alexander et al., 2012). As a glycoprotein of the innate immunity, Lf is also found in the secondary granules of neutrophils (15 μg/10^6neutrophils) (Lepanto et al., 2019a) and released into the plasma following their degranulation. The majority of Lf is liberated directly at inflamed or infected sites, therefore it can be considered a marker for inflammatory diseases as its plasma concentration increases from 0.2-2 mg/L (Levay and Viljoen 1995) up to 200 mg/l in the case of septicemia. Lf, also known as Lacto-transferrin, is a member of the Transferrin family together with serum Transferrin (sTf) and ovo Transferrin (oTf), all expressed as a single polypeptide chain of approximately 80 kDa organized into two halves, the N- and C-lobes (N and C) connected by a linker peptide (Fig. 9A, B, C). Each lobe is further divided into two subdomains, N1 and N2 and C1 and C2. Since the ancestor Tf is single-lobed, it is likely that a gene duplication event gave rise to the fusion of the two lobes (Williams et al., 1982) which share about 40% homology. To date, triple lobed Tfs, typical of algae, are also known, leading to an understanding of evolutionary adaptation according to the requirements of each species (Lambert et al., 2005). In sTf, Lf and oTf, each lobe is capable to bind one ferric ion (Baker et al., 2001) with high affinity ($K_d \sim 10^{-20}$ M) (Lambert 2012). The metal binds in the space between N1 and N2 and between C1 and C2, where highly conserved amino acid residues are present, including Asp and His in subdomain 1 (N1 or C1) and two Tyr in domain 2 (N2 or C2). It is known that of the six iron coordination sites, four are engaged in binding with these conserved residues, the other two by a bidentate carbonate anion (Mizutani et al., 2001) (Fig. 9D). The carbonate binds first in the binding pocket, neutralizing the positive charge due to the Arg residue and allowing the binding of iron to Tyr. The associated conformational change allows Asp and His to meet iron, switching from an open "Apo" to a closed "Holo" conformation (Pakdaman et al., 1998). As Lf is concerned, it should be noted that under physiological conditions it is present in the Native form with an iron saturation rate ranging from 10% to 20%, therefore there is a prevalence of monoferric and apo/iron-free form molecules. In inflamed/infectious sites it is found mainly in the Holo form with an iron saturation rate around 95%. By binding free iron in biological fluids and inflamed or infected sites, Lf reduces ROS production and the availability of the metal to pathogens. Moreover, each form can activate different metabolic pathways (Jiang et al., 2012; Cutone et al., 2020a). Since it has been experimentally shown that iron saturation affects Lf biological activity in vivo and in vivo, these characteristics must be taken into account.

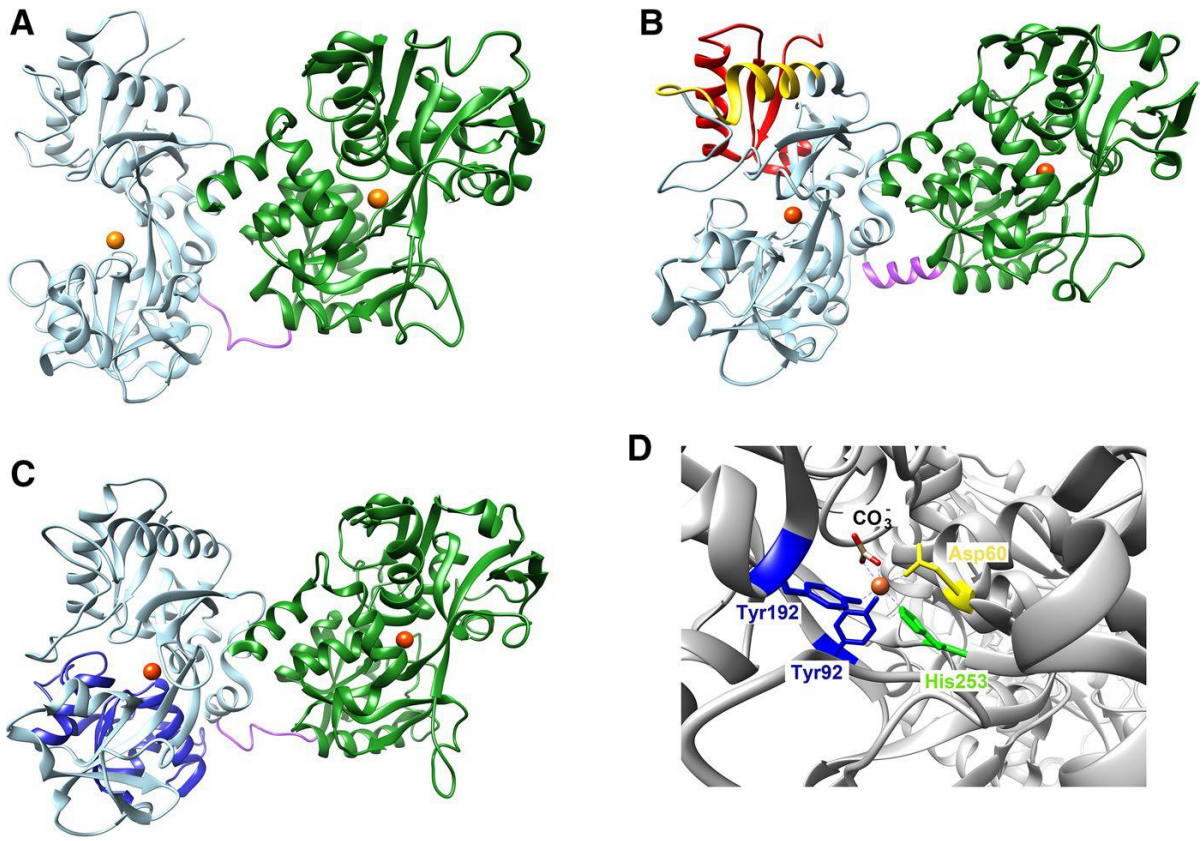

Figure 9. (**A**) (PDB code = 3QYT), human lactoferrin (hLf) (**B**) (PDB code = 1SQY), hen ovotrasferrin (oTf) (**C**) (PDB code = 1OVT) and the conserved iron binding site (as representative, iron binding site in the N-lobe of hLf was reported) (**D**). For each protein, the N-lobe is highlighted in light-blue and the C-lobe in green, the connecting peptide (aa. 332–338 for hTf, 334– 344 for hLf and 334–342 for oTf) in violet, and the ferric irons are depicted as orange spheres. The peptides produced by tryptic digestion are evidenced as follows: the lactoferricin (aa.1–47 of hLf) and lactoferrampin (aa. 269–285 of hLf) regions are highlighted in red and yellow, respectively (**B**), the OTAP- 92 (aa. 109–200 of oTf) in blue (**C**). Ferric iron binds as a bidentate carbonate complex, coordinated by four amino acidic residues: an Aspartate, a Histidine and two Tyrosines (D60, H253, Tyr92 and Tyr192 for the N-lobe of hLf) (**D**) (Ianiro et al., 2022)

The members of the Tf family share many characteristics but present some divergent physicochemical properties, such as different iron binding stability at low pH and different pI. At an acidic pH, carbonate protonation facilitates the loss of the ferric ion (Baker and Baker 2004). In particular, sTf releases iron around pH 5, while Lf has a high iron-binding stability at an even lower pH (around 3.0). This is reflected in the different functions performed by the two proteins. Tf is used to transport iron into tissues and after receptor-mediated endocytosis, at a pH of around 5.5, iron is released into the endosome. In contrast, Lf acts as an iron competitor for pathogens in inflammatory and/or infected sites, where the pH can reach lower values, around 3. This iron binding stability could be attributed to the cooperativity between the NH_2- and COOH-terminal lobes, as suggested by Ward and colleagues in 1996 (Ward et al., 1996). In addition, the peptide linking the two lobes is found as a

flexible, irregular non-folded loop in Tf, whereas it is organized in a rigid three-turn alpha helix in Lf, possibly ensuring a stronger interaction between the two lobes and a better stabilization of iron binding.

The second evolutionary gap among Tf members regards their isoelectric points. Despite sTf and oTf present a slightly acidic pI around 6.0, Lf is far away from such a value, approaching very basic values close to 9. This difference is likely linked to the multiple functions of Lf, and not possessed by the other two Tfs. As a matter of fact, beyond their ancestral capacity of iron binding, Lf has evolved its repertoire of activities towards functions usually possessed by niched and specialized macromolecules. Lf embraces all the selected capabilities, adding unique ones, shown by the members of the Tf family. It shares antimicrobial, antiviral, antioxidant and immunomodulatory activity with oTf (Giansanti et al., 2015) and modulates energy metabolism, cell proliferation and survival as melanoTf (Suryo Rahmanto et al., 2007), whereas it peculiarly shows anticancer action against a wide range of tumors (Cutone et al., 2020a), as well as DNA and RNA-binding ability, thus suggesting a direct role in gene expression (Lepanto et al., 2019a), and it is emerging as a natural modulator of iron homeostasis, in both physiological and pathological conditions (Cutone et al., 2014, 2017, 2019; Rosa et al., 2017; Bonaccorsi et al., 2018). Such properties of Lf have highlighted its potential as a functional food supplement, being characterized by both nutritional benefits and protective functions. However, its bioavailability is strictly dependent on two main aspects: a good natural source to draw from and the existence of intestinal receptors to target.

Regarding the source, Lf has been characterized in numerous species. Human Lf (hLf) is a single polypeptide chain constituted of 691 amino acids (Anderson et al., 1990), while bovine Lf (bLf) is constituted of 689 amino acids (Moore et al., 1997). As a result of tryptic digestion, two peptides are obtained: Lactoferricin (Lfcin, aa. 1-47 in hLf and 17-41 in bLf) and Lactoferrampin (Lfampin, aa. 269-285 in hLf and 268-284 in bLf). Both are positively charged and have potent antimicrobial (Van der Kraan et al., 2004; Gifford et al., 2005), antifungal (Fernandes et al., 2017), antiviral (Berlutti et al., 2011), anti-inflammatory (Drago-Serrano et al., 2018) and anticancer (Arias et al., 2017) properties. The positive charge that characterizes them favors their interaction with the negatively charged membrane structures of prokaryotes and eukaryotes, favoring lysis and cell death (Epand and Vogel 1999). Lf has dislocated regions that can undergo various post-translational modifications, such as phosphorylation, acetylation, lipidation, ubiquitination or glycosylation. The latter affects protein folding, protein solubility, proteolysis resistance, immunogenicity and Lf specific receptors binding (Albar et al., 2014). HLf has two main sites of N-glycosylation Asn 138 and Asn 479 (Haridas et al., 1995; Thomassen et al., 2005) but different N-glycan patterns (Le Parc et al., 2014) while bLf has five potential sites (Asn 233, 281, 368, 476 and 545). Glycans added to hLf consist of complex

branched structures, rich in sialic acid and fucose (Yu et al., 2011). Besides this diversity which could have effects on the functions performed, bLf has been classified as a functionally bioequivalent to hLf. It has also been defined as "generally recognized as safe" (GRAS) by the Food and Drug Administration of the United States, in fact many in vitro (Sessa et al., 2017, Lepanto et al., 2019b), in vivo (Valenti et al., 2017; Cutone et al., 2019) and clinical studies (Paesano et al., 2014; Lepanto et al., 2018) use bLf, since it is more easily commercially available. The use of recombinant hLf, produced by different systems, ranging from microorganisms to higher eukaryotic organisms, plants and transgenic cattle, requires high industrial costs, and its functionality can depend on differences in iron-saturation rate, glycosylation patterns, purity and stability, with respect to the natural product (Cutone et al., 2020b).

As far as receptors are concerned, Tfs are designed for extracellular functions, aimed at addressing both physiological needs and pathological conditions. However, Tfs are able to bind to specific cell receptors and transduce their biological message intracellularly. STf receptors are the most well-characterized at both structural and functional levels; their role in iron metabolism and homeostasis will be detailed in the next section. Concerning Lf, several receptors (hLfRs) have been characterized in different cell types, including Intelectin-1 (ITLN1), LDL receptor-related protein (LRP), asialoglycoprotein receptor (ASGPR), CD14 and nucleolin (Suzuki et al., 2005; Mancinelli et al., 2018). Generally, upon binding to the receptor, Lf can both trigger intracellular pathways (Jiang et al., 2011) or undergo clathrin-mediated endocytosis and, depending on the cell type, subsequent nuclear translocation (Ashida et al., 2004), thus allowing Lf to act as a regulator or transregulator of cell gene expression (Legrand 2016). Studies on Lf bioavailability have identified ITLN1 to be expressed on the apical side of enterocytes and functioning as the main gate for Lf internalization in the intestinal mucosa (Kawakami and Lonnerdal 1991; Suzuki et al., 2005). Importantly, it has been demonstrated that orally administered Lf can enter systemic circulation through intestine via lymphatic pathway (Kitagawa et al., 2003; Fischer et al., 2007). Of note, the heterologous interaction between bLf and hLfRs was demonstrated (Shin et al., 2008) as well as its ability to enter the cell nucleus in human cells (Paesano et al., 2012; Cutone et al., 2020c), thus partially clarifying the reason why bLf exerts similar functions to its human homologue.

1.4.1. Antiviral function of Lf

Several functions have been attributed to Lf, dependent on and/or independent from its iron binding ability. In addition to activities directed against pathogens, including viruses, Lf has been shown to affect different cell and metabolic processes such as wound repair, gene transcription, bone formation,

intestinal iron absorption, and to exert antitumoral, anti-inflammatory, immunomodulatory and antioxidant activities (Fig. 10).

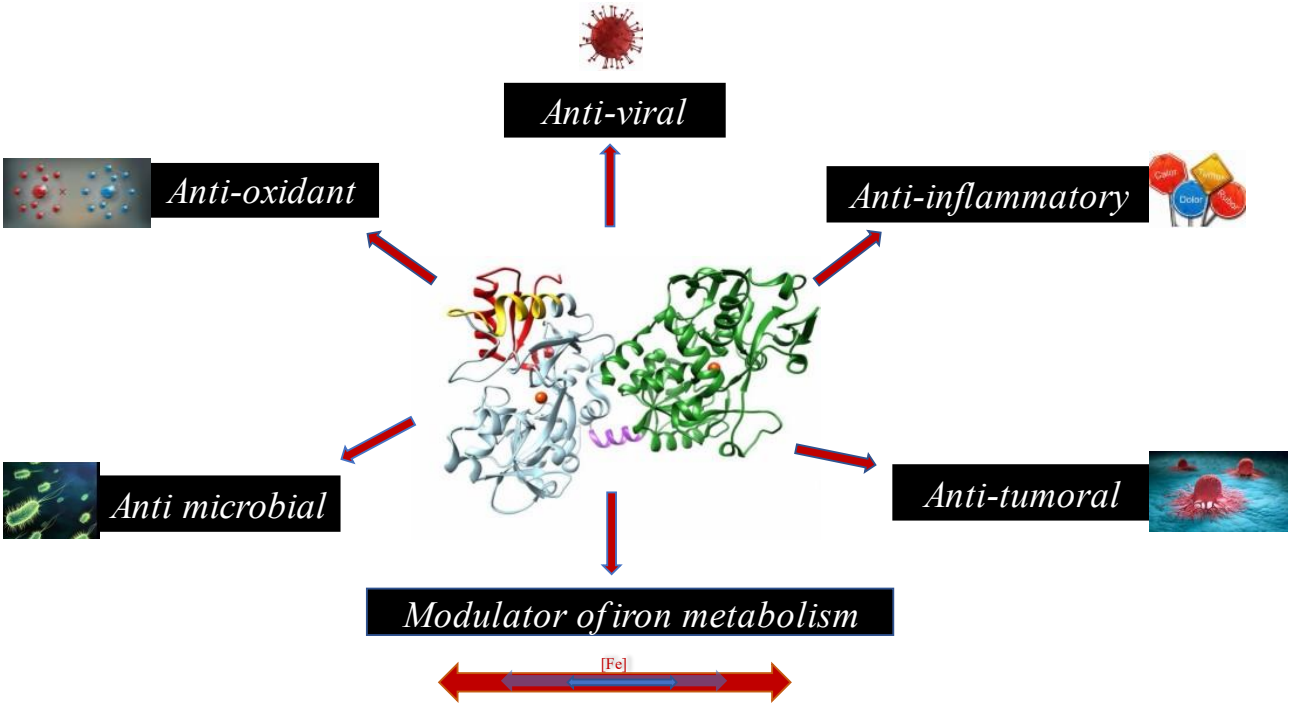

Figure 10. Schematic picture of the main representative Lf functions.

The antiviral activity of Lf was first demonstrated in 1987 in mice infected with the polycythaemia-inducing Friend virus complex (Lu et al., 1987). Its activity is conserved against both enveloped and naked viruses (Berlutti et al., 2011; Wakabayashi et al., 2014). In vitro studies have shown antiviral action of both Nat and Holo forms of bLf, thus indicating that its capacity is not only dependent on its ability to chelate iron (Marchetti et al., 1998; Marchetti et al., 1999; Siciliano et al., 1999; Superti et al., 2001; Berlutti et al., 2011). Many studies indicate that Lf antiviral activity occurs during the early phase of infection, preventing viral particles from entering the host cell through two mechanisms: (i) by binding to host cell receptors, making them no longer available for virus-host cell interaction; (ii) by binding to viral particles (Beljaars et al., 2002; Hasegawa et al., 1994; Marchetti et al., 1999) (Fig. 11). Furthermore, Lf is poised to suppress virus growth once host cells have been infected (Ikeda et al., 2000; Superti et al., 1997) (Fig. 11). Due to its properties, Lf can bind to negatively charged compounds as previously mentioned, such as glycosaminoglycans (GAGs), especially HSPGs. In addition, Lf may inhibit viral infection through its binding to the dendritic cell

adhesion molecule non-integrin 3 and LDL receptors (Groot et al., 2005; Chien et al., 2008). In this way, Lf avoids viral infection by preventing the interaction between cell receptor and the viral particle (Van der Strate et al., 2001).

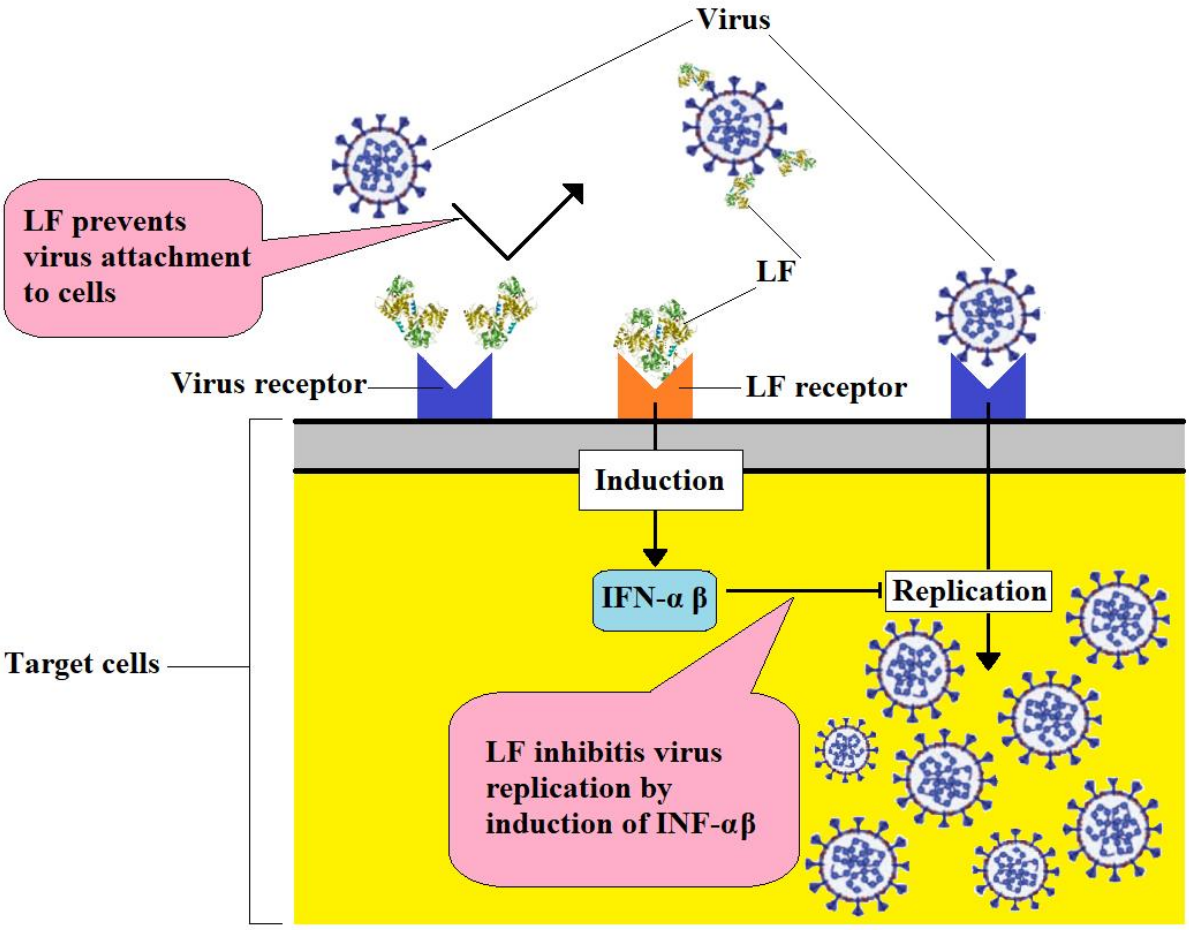

Figure 11. **Mechanism of the antiviral effect of lactoferrin.** LF blocks virus attachment to target cells by binding to the virus receptor on the host cells or by attaching itself to the virus. In addition, lactoferrin leads to the production of IFN α/β and thereby inhibits the replication of the virus after it enters the cells. Abbreviations: LF, Lactoferrin; IFN α/β, Interferon α/β (Modified from Wakabayashi et al., 2014).

Lf has been demonstrated to exert antiviral activity against Cytomegalovirus (CMV), Herpes Simplex Virus (HSV), Poliovirus (PV), Hepatitis B Virus (HBV), Hepatitis B Virus (HCV), Parainfluenza Virus (PIV), Human Papillomavirus (HPV), as well HIV and SARS-CoV (Berlutti et al., 2011; Wakabayashi et al., 2014; Campione et al., 2021). Concerning HIV, numerous studies have shown the inhibition of HIV-infection through both hLf and bLf (Harmsen et al., 1995; Puddu et al., 1998;

Swart et al., 1996) and that its antiviral action is carried out in the early phase of infection (Harmsen et al., 1995; Puddu et al., 1998). Lf has been shown to bind the gp120 receptor, which is responsible for virus entry into the host cell (Swart et al., 1996). In addition, Lf binding to C-type lectins on dendritic cells prevents HIV entry and bLf results more efficient than hLf probably due to different glycosylation patterns which affects antiviral activity (Groot et al., 2005). However, such infections can also be counteracted through the inhibition of viral replication, as indicated in other in vitro study (Viani et al., 1999). Regarding SARS-CoV, Lang and colleagues studied the role of Lf on the entry route of the SARS pseudovirus into Myc cells. Results showed that Lf was able to block binding of Spike protein to host cells, indicating an inhibitory function exerted in the viral adhesion phase (Lang et al., 2011). However, Lf blocks Spike binding to host cells (Lang et al., 2011) by an ACE2-independent pathway. In silico and in vitro studies have shown that Lf exerts anti-SARS-CoV-2 activity by binding to both viral components and host surface molecules. In silico analysis suggested that viral entry is hindered by Spike direct recognition to Lf, thus restricting both viral entry into host cells and infection (Campione et al., 2021). However, the currently accepted model suggests that Lf could block viral entry by interacting with HSPG, (Hu et al., 2021; Mirabelli et al., 2021), thereby mediating the transport of extracellular viral particles from low-affinity anchoring sites to specific high-affinity entry such as ACE2.

1.4.2. Anti-inflammatory and antioxidant functions of Lf

Lf is described as a potent molecule in the treatment of common inflammatory diseases. The anti-inflammatory activity of Lf is in part related to its ability to chelate iron that accumulates into inflamed tissues and promotes the production of tissue-toxic hydroxides. At inflamed/infected sites, Lf is released from the secondary granules of neutrophils (PMN) and, due to its iron-binding stability, it chelates the metal even at low pH (Wiesner and Vilcinskas 2010; Sagel et al., 2009; Pfefferkorn et al., 2010). The consequent restricted availability of iron for pathogens inhibits their growth as well as the expression of virulence factors (Reyes et al., 2005). The anti-inflammatory activity is also related to the ability of Lf to interact with negatively charged molecules such as proteoglycans on immune cells and activate anti-inflammatory response signaling pathways (González-Chávez et al., 2009; Legrand, 2016). In addition, its action can be explained by its ability to enter cells and translocate into the nucleus (Ashida et al., 2004), where it can modulate gene expression by acting as a regulator or trans-regulator of gene expression (Legrand 2016). The molecular mechanisms by which Lf exerts its action are diverse. In particular, the activation of pro-inflammatory cytokines, such as TNF-α, IL-1β, IL-6 and IL-8, is hindered by the Lf neutralizing effect against exogenous

molecules such as bacterial lipopolysaccharides (LPS). Indeed, Lf was found to bind to lipid A of LPS with high affinity through its lactoferricin domain (Appelmelk et al., 1994; Elass-Rochard et al., 1995). The interaction between lactoferricin and lipid A (Zhang et al., 1999) prevents LPS from binding to key players in LPS signaling, such as serum LPS-binding protein (LBP), soluble CD14 (sCD14), membrane CD14 (mCD14) on monocytes and L-selectin on PMNs (Elass-Rochard et al., 1998, Baveye et al., 2000). In addition, Lf has been shown to reduce the production of cytokines released by THP-1 cells following LPS-challenging through its nuclear translocation and interference with NF-kB signaling (Haversen et al., 2002). The neutralizing effect mediated by Lf-LPS binding affects not only the activation of immune system but also of endothelial cells. These latter, upon LPS-induction, up-express adhesion molecules, selectins and IL-8, which are necessary for the local recruitment of immune cells to inflammatory sites, and Lf has been shown to inhibit the production of such molecules (Elass et al., 2002).

The anti-inflammatory action of Lf under both aseptic and septic conditions has been reported in several in vitro and in vivo studies. For instance, during *Chlamydia trachomatis* infection, a sexually transmitted pathogen that causes acute and chronic infections and thus inflammation, Lf has been shown to be a potent anti-inflammatory molecule. Incubation with bLf of a human epithelial cell line at the time of infection resulted in a reduction of *C. trachomatis* entry (Sessa et al., 2017). In addition to inhibiting bacterial entry into cells, Lf exerts potent anti-inflammatory activity by down-regulating the synthesis of IL-6 and IL-8 by infected cells.

In cystic fibrosis (CF), the respiratory tract is susceptible to infection, particularly by *Pseudomonas aeruginosa* (Lipuma 2010; Salsgiver et al., 2016). Even before bacterial infection, a major inflammatory response is triggered with up-regulation of NF-kB and activator protein (AP)-1 and overproduction of pro-inflammatory cytokines (Dakin et al., 2002; Verhaeghe 2007; Bragonzi et al., 2018). BLf treatment of infected bronchial epithelium significantly reduced pro-inflammatory cytokines levels (Frioni et al., 2014). In addition, aerosolised bLf administration in mice infected with *P. aeruginosa* was found to exert a protective function by reducing bacterial load, cytokines and pro-inflammatory chemokines (Valenti et al., 2017).

On the other hand, aseptic inflammation can be triggered by physical, chemical, metabolic stimuli of a certain magnitude and in detail by the rupture of cell membranes and spillage of contents. However, persistence of anti-inflammatory response causes the host to face more damages than benefits.

In individuals with Alzheimer's disease, there is elevated deposition of extracellular β-amyloid (Aβ) protein and hyperphosphorylation of microtubule-associated tau proteins in neurons (Colvez et al., 2002). In addition, a chronic inflammatory process, mainly around amyloid plaques of activated microglia, promotes the synthesis of several pro-inflammatory cytokines, such as IL-1β, IL-6, TNF-

α and interferon (IFN)-γ (Cunningham et al., 2005; Dal Prà et al., 2015), and an increase in free iron content in the brains of AD patients is found (Du et al., 2018 manca), which impairs brain function due to the associated induction of oxidative stress (Cunningham et al., 2005; Dal Prà et al., 2015). In the brains of AD patients, endogenous hLf content increases but it is not sufficient to suppress pathogenesis. Oral treatment with bLf (250 mg/day for three months) in AD patients has been shown to be significantly effective in reducing serum IL-6 and increasing serum IL-10 (Mohamed et al., 2019 manca). The results obtained may be related to the anti-inflammatory and antioxidant activity due to Lf iron binding capacity.

During inflammation, neutrophils, monocytes and lymphocytes trigger oxidative stress through the release of ROS/NOS and pro-inflammatory cytokines. Therefore, the two processes are intertwined in such a way that one can easily induce the other and vice versa. It is typical of chronic diseases including neurocognitive disorders, but also cancer, infections (Marnett 2000; Misonou et al., 2020) including HIV-1 (Ivanov et al., 2016) and SARS-CoV-2 (Suhail et al., 2020). The rate and extent of ROS formation and their elimination depend on the action of enzymes such as SOD, CAT, and GPX. As already discussed, free iron can promote the production of hydroxyl radicals which can oxidize any group in the vicinity. Lf, due to its ability to bind Fe^{3+}, can protect against ROS-mediated damaging effects. In addition, Lf has an important antioxidant role in that it promotes the upregulation of key antioxidant enzymes such as GPX and SOD1 (Kruzel et al., 2013). The antioxidant property of bLf was demonstrated in a rat model, in which oxidative damage of the renal tubule was induced by ferric nitrilotriacetate (Okazaki et al., 2012). Protective effects against renal tubular oxidative damage and maintenance of antioxidant enzyme activities were observed in the Lf-treated group. The authors suggested that Lf intake is beneficial for the prevention of iron-mediated renal tubular oxidative damage. In addition, Lf reduced LPS-induced oxidative stress levels in mice (Kruzel et al., 2010); this was demonstrated by reduced mitochondrial DNA damage and H_2O_2 release (Kruzel 2017). Overall, Lf co-exhibits anti-inflammatory and antioxidant activity independently from its iron binding ability thus favoring the rescue from the pathological disorders described.

1.4.3. Lf as a natural modulator of iron homeostasis

Acquired disorders of iron homeostasis, mainly associated to pathological states including inflammation, infection and cancer, result in both systemic iron deficiency, causing anemia and depletion of iron-containing enzymes essential for many biological processes, and tissue iron overload, which enhances the production of deleterious ROS that cause tissue damage and organ failure. As mentioned above, upon inflammation or infection, Fpn is degraded through hepcidin-dependent or independent mechanisms involving the activation of pro-inflammatory cytokines, such

as IL-6 and IL-1β, provoking a significant decrease in iron export from cells to plasma (Andrews 2000). Consequently, at the cellular level, iron uptake by enterocytes is impaired, macrophages fail to recyclie iron from senescent erythrocytes and hepatocytes become inefficient in releasing iron stores. Thus, intracellular iron overload is established, and systemic iron deficiency (ID), ID anemia (IDA) and anemia of inflammation (AI) occur (Andrews 2000; Frazer and Anderson 2003). The persistence of inflammatory stimuli exacerbates the anemic status by inhibiting erythroid cell differentiation, thus worsening AI (Weiss et al., 2019). Hence, it is critical to counteract the persistence of the inflammatory state by rebalancing physiological iron levels between tissues/secretions and blood. In this frame, Lf is emerging as a natural orchestrator of iron homeostasis, due to its multi-target activities, including iron-withholding, immunomodulatory, anti-inflammatory, anti-microbial, anti-viral and anticancer abilities (Sokolov et al., 2012; Kruzel et al., 2017; Rosa et al., 2017; Lepanto et al., 2019a; Cutone et al., 2020a). First, Lf iron saturation rate seems to crucially influence its impact in regulating intracellular iron content, which is intrinsically associated with the modulation of iron-related proteins, also in cancer cells (Zhang et al., 2021). In addition, Lf capacity to enter the cell nucleus suggests a direct implication of the glycoprotein in modulating gene expression. Lf possesses two DNA binding sites able to interact with specific and non-specific DNA sequences (Guschina et al., 2013) and the capacity to act as a transcription factor (Furmanski et al., 1989). Of note, recombinant hLf has been demonstrated to activate, directly or indirectly, nuclear translocation of Nrf2 (Zakharova et al., 2018), a master regulator of cell antioxidant response, also involved in the transcriptional up-regulation of Fpn (Harada et al., 2011). Moreover, Lf has been described to directly interact with Cp (Zakharova et al., 2000; Sokolov et al., 2014), the functional partner of Fpn in most cells.

Since AI is a secondary manifestation of inflammatory disorders, anti-inflammatory therapeutic approaches should be mainly addressed to restore physiological iron homeostasis. Among the putative innovative therapies, the use of Fpn agonists or hepcidin antagonists has been proposed (Wessling-Resnick 2010; Casu et al., 2018). In this scenario, bLf has been repeatedly described to counteract inflammatory disorders by down-regulating IL-6 and, at the same time, by up-regulating Fpn expression, rebalancing endogenous iron between tissue/secretions and blood (Frioni et al., 2014; Cutone et al., 2014; Paesano et al., 2014; Cutone et al., 2017; Lepanto et al., 2018).

As a matter of fact, in several in vitro and in vivo models, bLf has been shown to be affective in counteracting the down-regulation Fpn induced by inflammatory or infection stimuli. A study on infected enterocytes reports the efficiency of bLf treatment in reverting both Fpn degradation and pro-inflammatory activation (Frioni et al., 2014). Concordantly, in inflamed human macrophages, bLf treatment determines a macrophagic shift from the pro-inflammatory M1 to tolerogenic M2

phenotype (Cutone et al., 2014; Cutone et al., 2017). After inflammatory stimuli, macrophages polarize into M1 phenotype, characterized by the synthesis of pro-inflammatory cytokines, including IL-6 and IL-1β, as well as by the dysregulation of the main iron-related proteins, as the downregulation of Fpn/Cp axis, TfR1 and the up-regulation of cytosolic Ftn (Corna et al., 2010; Recalcati et al., 2010; Cutone et al., 2017). All these changes lead to the blockade of iron recycling to blood by macrophages, the main iron source for the body deriving from the lysis of senescent erythrocytes (Cutone et al., 2017). Treatment with bLf reverts iron disorders induced by inflammatory stimuli by down-regulating IL-6 synthesis and up-regulating Fpn expression, thus restoring the physiological cell-to-blood iron export (Cutone et al., 2014; Cutone et al., 2017). Importantly, bLf, in addition to Fpn expression, is also able to modulate all the iron-related proteins, up-regulating TfR1, Cp and down-regulating cytosolic Ftn (Cutone et al., 2017) (Fig. 12). Most of the clinical studies about the efficacy of bLf supplementation in counteracting systemic iron disorders have been carried out in anemic pregnant women, a peculiar physiological state often presenting dysregulation of iron homeostasis. The first clinical study on the efficacy of bLf oral administration, in comparison with the classical ferrous sulfate therapy, has represented a milestone in the bLf experimentation against anemia (Paesano et al., 2006). In this clinical trial conducted on pregnant women treated with 100 mg of 20–30% iron-saturated bLf (corresponding to 70–84 μg/day of elemental iron) two times a day before meals, a significant rescue of both serum Hb and total serum iron (TSI) was reported, when compared to pregnant women treated with 329,7 mg of ferrous sulfate (about 105 mg of elemental iron), once a day during meals. The discrepancy between the elemental iron supplementation and the registered efficacy of bLf, with respect to ferrous sulfate administration, led to speculate that bLf could modulate iron and inflammatory homeostasis through more sophisticated mechanisms. The efficacy of bLf was also tested in pregnant and non-pregnant women suffering from and affected by AI (Lepanto et al., 2018). In this respect, bLf treatment was found to be significantly efficient in curing AI in HT pregnant and non-pregnant women compared to the classical ferrous iron therapy (Paesano et al., 2014; Lepanto et al., 2018). In particular, after 30 days of bLf treatment, both HT pregnant and non-pregnant women showed a significant recovery in the total number of RBCs as well as in the concentration of serum Hb, TSI and Ftn. Notably, bLf management was also efficient in significantly reducing serum IL-6 and hepcidin levels with respect to the higher basal ones (Paesano et al., 2014; Lepanto et al., 2018). Hence, even if more studies are needed to unveil the molecular mechanisms underlying bLf anti-inflammatory activity, this evidence strongly supports the bLf efficacy in curing AI through its ability to decrease IL-6 synthesis (Rosa et al., 2017; Lepanto et al., 2019a) thus modulating hepcidin and/or Fpn, the most pivotal actors in systemic iron homeostasis (Wessling-Resnick 2010; Casu et al., 2018).

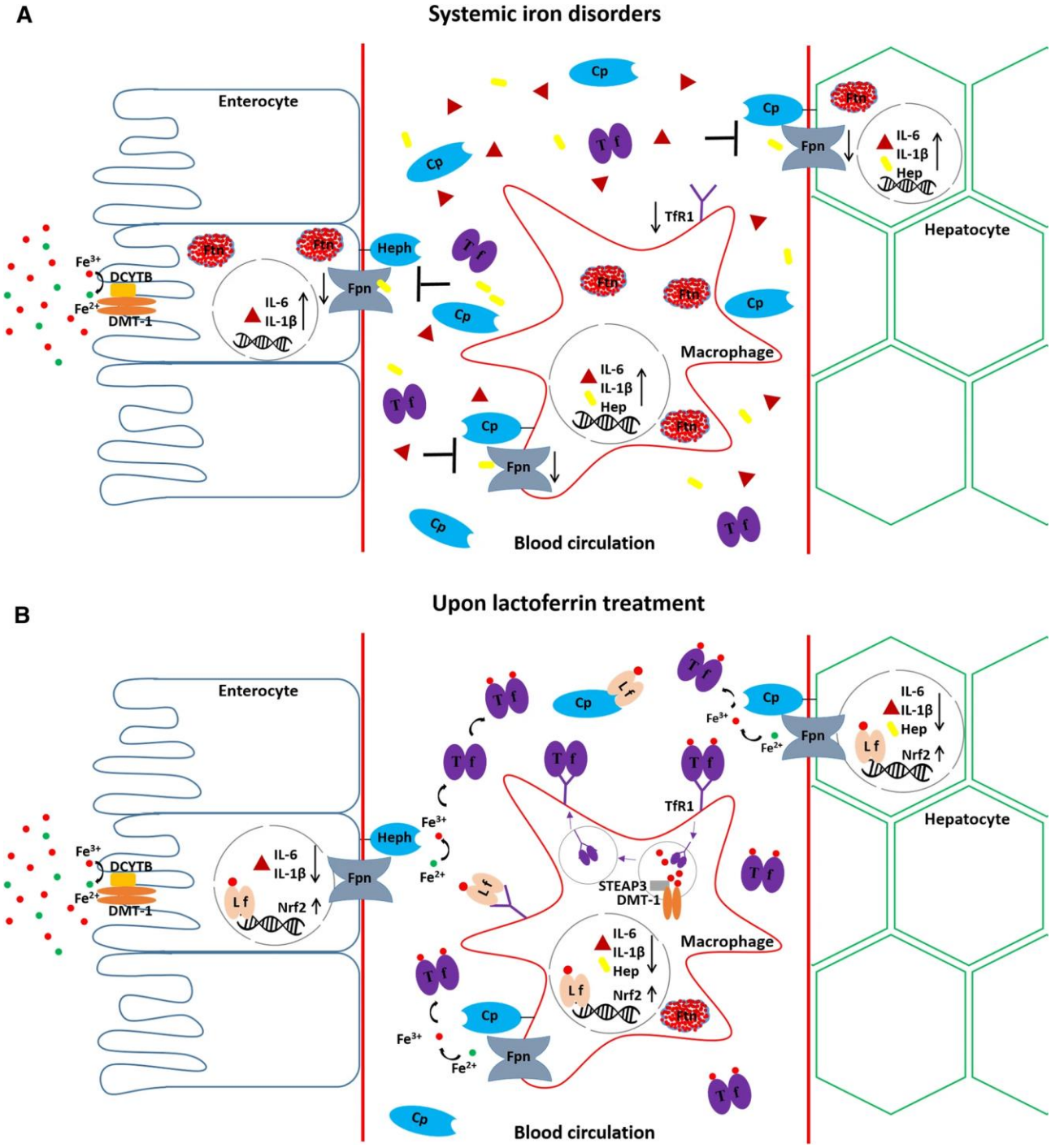

Figure 12. Schematic representation of systemic iron disorders in the absence (A) or presence (B) of lactoferrin. **A**) Upon infection or inflammation, enterocytes, macrophages and hepatocytes, the main cell types involved in iron homeostasis, upregulate the expression of pro-inflammatory cytokines and of the peptidic hormone hepcidin, negative regulators of Fpn. The blockade of iron export induces an increase of intracellular iron and, hence, of ferritin, with a consequent decrease in Tf-bound iron import through TfR1. In these conditions, anemia sets in and intracellular iron engulf takes place. **B**) Lactoferrin treatment can trigger different protective effects, from downregulation of pro-inflammatory cytokines and hepcidin, to the up-regulation of Nrf2, a positive regulator of Fpn expression. Rescued iron export drives the decrease of intracellular iron and the recovery of iron import through TfR1. Other interactors of lactoferrin are also reported in the scheme. See text for further details. Abbreviations: DMT-1, Divalent Metal Transporter-1; DCYTB, Duodenal Cytochrome b; Ftn, Ferritin; Fpn, Ferroportin; Heph, Hephestin; Cp, Ceruloplasmin; Tf, Transferrin; TfR1, Transferrin Receptor 1; Interleukin (IL)-6; IL-1β; Nrf2, erythroid nuclear factor 2-related factor; Lf, Lactoferrin (Ianiro et al., 2022).

2. AIM

The viral proteins Tat of HIV and Spike of SARS-CoV-2 have been described as a neurotoxin and a virulence factor respectively, able to induce by themselves metabolic dysregulation into host cells, independent from the viral infection.

Tat is a multifunctional protein able to activate chemokine expression or act as a neurotoxin in SNC, depending on cell types. Tat can enter cells, including neurons, and modulate gene expression thus promoting viral spread, neuroinflammation and oxidative stress (Dhillon et al., 2007; Asensio and Campbell 2001; Mastrantonio et al., 2019).

Spike is capable of driving host viral pathogenesis, which in turn is the critical regulator of viral infection and disease outcome. Spike is recognized by TLR2 which activates the NF-κB pathway and can trigger an over response characterized by the so-called "proinflammatory cytokine storm" (Patra et al., 2020). As already mentioned, the increase of IL-6 significantly modulates iron metabolism. It has been shown that SARS-CoV-2 infected patients present iron deficiency and elevation in serum ferritin and hepcidin (Sonnweber et al., 2020).

Overall, both Tat and Spike induce pathological states worsened by pro-inflammatory cytokines production. Several studies have indicated that the inflammatory response leads to high intracellular iron content which facilitates viral spreading (Mancinelli et al., 2020) and oxidative stress (Galaris et al., 2019). Therefore, these processes are intertwined in such a way that one can easily induce the other and vice versa. Hence, present therapies demand a specifically targeted approach to counteract the adverse effects of these viral proteins. Whitin this framework, lactoferrin, a cationic glycoprotein of innate immunity which exerts multiple functions both dependent and independent from its iron-withholding ability, could play an important role. Numerous studies have evidenced its efficacy against inflammation (Lepanto et al., 2019a), oxidative stress (Kruzel et al., 2013) and iron homeostasis disorders (Frioni et al., 2014; Cutone et al., 2014; Paesano et al., 2014; Cutone et al., 2017; Lepanto et al., 2018), typical of diverse pathological conditions, including viral infections (Berlutti et al., 2011).

The aim of the present research work was to evaluate the efficacy of Lf in counteracting inflammatory and iron disorders, as well as oxidative stress, induced by Tat and Spike viral proteins in different in vitro models.

Specifically, regarding Tat, the aim was to evaluate the effects of bLf on HIV-1 Tat-mediated oxidative stress and neurotoxicity in the astrocytoma cell line U373 and in co-cultures with neuroblastoma cells (SH-SY5Y). Since iron saturation of Lf can influence its functions, experiments were conducted employing both the Nat and Holo forms of the glycoprotein.

As for Spike, in order to unravel the mechanism underlying the antiviral activity of lactoferrin, a neutralizing assay against a pseudovirus expressing the SARS-CoV-2 Spike glycoprotein was carried out with both bLf and hLf in different cellular models. To demonstrate the effective binding between Lf and Spike, an in-vitro pull-down assay was performed. Furthermore, the putative protective role of Lf on inflammatory and iron disorders in epithelial and macrophage models stimulated with the SARS-CoV-2 Spike glycoprotein was investigated.
The above two parts will be treated separately.

❖ **Part 1**

Effects of bovine Lactoferrin on HIV-1 Tat-mediated oxidative stress, iron disorders and neurotoxicity

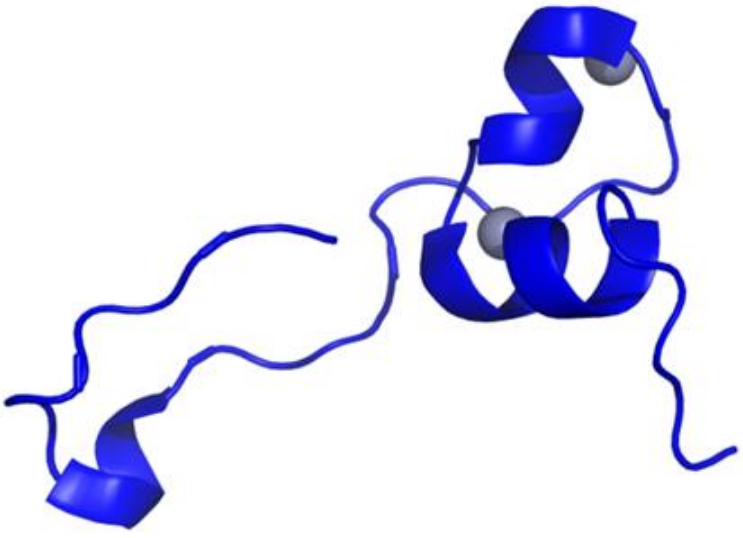

PDB: 6CYT

3/1. Materials and methods

3/1.1. Reagents

DMEM (Dulbecco's modified Eagle's medium), FBS (Fetal Bovine Serum), Trypsin–EDTA 0.25% solution, gentamicin 50 mg/ml solution, sulfasalazine (SSZ; a specific inhibitor of System Xc^-), MK-801 hydrogen maleate (MK-801; an NMDA receptor an-tagonist), N-Acetyl-L-cysteine (NAC) and kit for MTT assay were obtained from Sigma–Aldrich (Milan, Italy). The reagent for Bradford assay was from Bio-Rad Italia (Milan, Italy). TRIzol Reagent was from Life technologies Italia-Invitrogen, (Monza, Italy). The Go Taq 2-Step RT-qPCR System kit was obtained from Promega Italia Srl, (Milan, Italy) and SsoAdvanced universal SYBR green supermix was purchased from Bio-Rad Italia (Milan, Italy).

3/1.2. Bovine lactoferrin

Highly purified bLf (Saputo Dairy, Australia) was generously supplied by Vivatis Pharma Italia s.r.l. Protein purity was about 99% as checked by SDS-PAGE and silver nitrate staining. The concentration of bLf solutions was assessed via UV spectroscopy with an extinction coefficient of 15.1 (280 nm, 1% solution). Iron saturation was about 11% as determined via optical spectroscopy at 468 nm using an extinction coefficient of 0.54 for a 1% solution of 100% iron saturated protein. LPS contamination, assessed via Limulus Amebocyte assay (Pyrochrome kit, PBI International, Italy), was 0.5 ± 0.06 ng/mg. Before each in vitro assay, bLf solutions were sterilized using a 0.2 μm Millex HV filter at low protein retention (Millipore Corp., Bedford, MA, United States).

Holo-bLf was prepared by incubating Native bLf (20 mg/ml in 0.1 M sodium bicarbonate) with 5 mM ferric citrate for 2 h under stirring. The resultant Holo-bLf was then dialyzed against 0.1 M sodium bicarbonate for 48 h to remove unbound iron. The obtained Holo-bLf, >95% iron-saturated, was frozen and stored at -20 °C prior to experimental usage.

3/1.3. Cell Cultures, Transfection and Treatments

Human glioblastoma astrocytoma cells (U373-MG) and human neuroblastoma cells (SH-SY5Y) were purchased from American Type Culture Collection (ATCC, Manassas, VA, USA). Both cell lines were maintained in culture at 37 °C, in 5% CO_2 atmosphere, using Dulbecco's Modified Eagle's Medium (DMEM) supplemented with 10% Fetal Bovine Serum (FBS), 2 mM L-glutamine, 40 μg/ml gentamicin. Confluent monolayers were sub-cultured by conventional trypsinization.

U373-MG cells were transfected with pcDNA3.1 (U373-mock) or pcDNA3.1-HIV-Tat (U373-Tat) expression vectors as previously reported (Mastrantonio et al., 2019; Capone et al., 2013). For the maintenance of transfected cells in culture, G418 (200 μg/ml) was added to the culture medium. Treatments with Nat-Lf (100 μg/ml) and Holo-bLf (100 μg/ml) were performed in DMEM without FBS for different time as indicated. Pre-treatments with Sulfasalazine (300 μM), NAC (2mM) or MK-801 (10 μM), where indicated, were performed 30 min before the addition of lactoferrin to the cell cultures.

3/1.4. Co-Cultures and cell viability assay

SH-SY5Y cells were grown in co-cultures with U373-mock or U373-Tat using a transwell culture system as previously reported (D'Ezio et al., 2021). For each sample in co-cultures, $1{,}5x10^4$ neuronal cells were seeded in transwell insert and $3x10^4$ astroglial cells were plated in the lower compartment of 6-well plate and allowed to grow for 24 h. U373 and SH-SY5Y cell viability was assessed by MTT assay at the end of the incubation period. MTT solution (0.5 mg/ml MTT dissolved in Phosphate Buffered Saline (PBS)) was added to the cell culture at the final concentration of 10%, and the cells were left in incubator at 37 °C for 4 hours. Formazan crystals were dissolved in MTT solvent (4 mM HCl, 0.1% NP40 in isopropanol) and samples were incubated at 37 °C for 30 minutes. The optical density (OD) of each sample was then measured at a wavelength of 570 nm using the Tecan Spark10M reader. In some experiments, where indicated, Trypan blue exclusion assay has been used to quantify viable cells.

3/1.5. Quantitative Real-Time Reverse Transcription-Polymerase Chain Reaction

Total RNA was purified by using Trizol Reagent and reverse transcribed into cDNA with GoTaq 2-step RT-qPCR system. cDNA was then amplified for system Xc^- gene (xCT subunit, NM_014331.4) and Glyceraldehyde 3-phosphate dehydrogenase (GAPDH, NM_002046.7) mRNA was examined as the reference cellular transcript. The sequences of primers were as previously reported (D'Ezio et al., 2021). PCR products were quantified by the SYBR-Green method. Reactions were performed in Agilent Aria Mx machine (Agilent technologies) using the following program: 45 cycles of 95 °C for 15 s, 60 °C for 60 s, 72 °C for 20 s. GAPDH mRNA amplification products were present at equivalent levels in all cell lysates. Values were calculated relative to the internal housekeeping gene according to the second derivative test (delta–delta Ct ($2\text{-}\Delta\Delta CT$) method).

3/1.6. Total and Nuclear Extracts

Preparation of total extracts was performed by adding 1% TEEN triton buffer (10 mM tris HCl pH 7.4, 1 mM EDTA, 1 mM EGTA, 150 mM NaCl, 1% Triton X-100, protease inhibitor cocktail dissolved 1:100) to the cell pellets. Samples were kept at 4°C for 20 minutes, shaking every minute. Subsequently, samples were centrifuged at 14000 rpm, 4°C for 20 minutes and then the supernatant containing the cellular proteins was removed and stored in aliquots at -80°C.

Preparation of nuclear extracts was performed by adding buffer A (10 mM Hepes pH 7.9, 10 mM KCl, 1.5 mM $MgCl_2$, 0.5 mM DTT, 0.1% NP40, protease inhibitor cocktail dissolved 1:100) to the cell pellets to separate nuclei from cytosol. After incubation for 10 min on ice, samples were centrifuged at 12000 rpm for 10 min at 4 °C. Thereafter, pellets containing nuclear fractions were resuspended in buffer C (20 mM Hepes pH 7.9, 420 mM NaCl, 1.5 mM $MgCl_2$, 25% glycerol, 1 mM EDTA, 1 mM EGTA, 0.5 mM DTT, 0.05% NP40, protease inhibitor cocktail dissolved 1:50) and incubated on ice for 30 min. A final centrifugation at 14000 rpm was carried out, and the supernatants were collected and stored at -80 °C.

The total protein content was determined according to Bradford method.

3/1.7. Western Blotting

Proteins were separated by SDS-PAGE and electroblotted onto nitrocellulose (GE Healthcare, Life Sciences, Little Chalfont, Buckinghamshire, UK). Following transfer, each membrane was incubated in TBS-T (Tris Buffer Saline: 20 mM Tris-HCl pH 7.4; 137 mM NaCl; 0.1% Tween 20) containing 5% non-fat dried milk powder (Blotting-Grade Blocker, PanReac AppliChem, ITW reagents) for 1 h at room temperature. The membrane was incubated overnight at 4 °C with primary antibody dissolved in TBS-T containing 5% milk.

The following primary antibodies were employed: polyclonal anti-actin (A2066 Sigma-Aldrich; Milan, Italy) (1:1000), polyclonal anti-System Xc^- (Ab175186 Abcam, Milan, Italy) (1:1000), polyclonal anti-Nrf2 (16396-1-AP Protein Tech; Manchester, United Kingdom) (1:1000), polyclonal anti-Ftn (sc25617, Santa Cruz, CA, USA) (1:1000), polyclonal anti-HCP (A0031, Dako, Santa Clara, CA, USA) (1:1000), polyclonal anti-lamin A (Ab26300 Abcam; Milan, Italy) (1:1000), monoclonal anti-vinculin (sc-73614, Santa Cruz, CA, USA) (1:1000), monoclonal anti-ARA70 (NCOA4) (sc-373739, Santa Cruz, CA, USA) (1:1000), monoclonal anti-bLf (sc-53498, Santa Cruz CA, USA) (1:1000), monoclonal anti-Fpn 31A5 (1:1000), generously provided by T. Arvedson (Amgen), monoclonal anti-TfR1 (sc-32272, Santa Cruz, CA, USA) (1:1000), monoclonal anti- p-Histone H2A.X (Ser 139) (sc-517348, Santa Cruz, CA, USA) (1:1000).

The membrane was then incubated with the appropriate HRP-conjugated secondary antibody (Biorad) (1:1000) in TBS-T containing 2.5% milk for 1 h at room temperature. The reagent used for detection was Clarity Western ECL substrate (170-5061, Biorad).
Differences between samples with respect to the presence of the proteins of interest were normalized using actin protein for total extracts and lamin A protein for nuclear extracts as reference.

3/1.8. Cytokine analysis

Quantitation of IL-6 and IL-1β was performed on cell supernatants by ELISA, using Human ELISA Max Deluxe Sets (BioLegend, USA).

3/1.9. Immunocytochemistry and confocal analysis

Cells were grown on coverslips and fixed with 4% PFA in PBS, followed by permeabilization with 0.1% Triton X-100 in PBS. TfR1 and Ftn primary antibodies (1:100) were incubated overnight at 4 °C and visualized by means of Alexa Fluor (Invitrogen, Carlsbad, CA, USA). Coverslips were stained with the fluorophore-conjugated secondary antibodies (Alexa Fluor™ 546 and Alexa Fluor™ 488, Invitrogen, Carlsbad, CA, USA) and Hoechst for nuclei visualization, were mounted in antifade (SlowFade; Invitrogen, Carlsbad, CA, USA) and examined under a confocal microscope (TCS SP8; Leica, Wetzlar, Germany), equipped with a 40 ×1.40–0.60 NA HCX Plan Apo oil BL objective at RT.

3/1.10. Measurements of Glutamate Concentration in Cell Supernatants

To evaluate glutamate release in supernatants of co-cultures, Glutamate Assay (Abcam) was performed as indicated by manufacturer's instructions. Briefly, 20 µl of each sample supernatant were collected in a 96-well plate and assay buffer was added up to 50 µl final volume. Then 100 µl of the reaction mix were added to each well, the plate was incubated for 30 min at 37 °C, protected from light, and optical density (OD) was measured at 450 nm in a microplate reader. Glutamate concentration of each sample was calculated using glutamate standard curve (0, 1.3, 6.5, 13, 26, 40, 53, 67 µM).

3/1.11. Statistical Analysis

All data are expressed as mean ± standard error of the mean (SEM) of n observations. Statistical analysis of the data was performed using Graph Pad PRISM software. Statistical significance was assessed by the one-way ANOVA test, followed by the Tukey post-test. Differences are considered statistically significant at $p \leq 0.05$.

4/1. Results

4/1.1. Native and Holo bovine lactoferrin are internalized by U373 cells

Previous studies have shown that bLf performs its numerous functions either by entering the nucleus or by initiating signal transduction cascades (Jiang et al. 2011; Suzuki et al. 2005). To investigate the molecular mechanism by which bLf exerts its action in our experimental system, we first examined its subcellular localization. In this research work U373 pcDNA3.1 (U373), as control cells, and U373 pcDNA3.1-Tat (U373-Tat) cells were treated with 100µg/mL of bLf, in its Nat- and Holo form. As shown in Figure 13, both Nat and Holo forms are internalized by U373-mock and U373-Tat cells. Both forms are mainly localized at the nuclear level, with Holo-bLf showing higher levels than the Native form (Fig. 13).

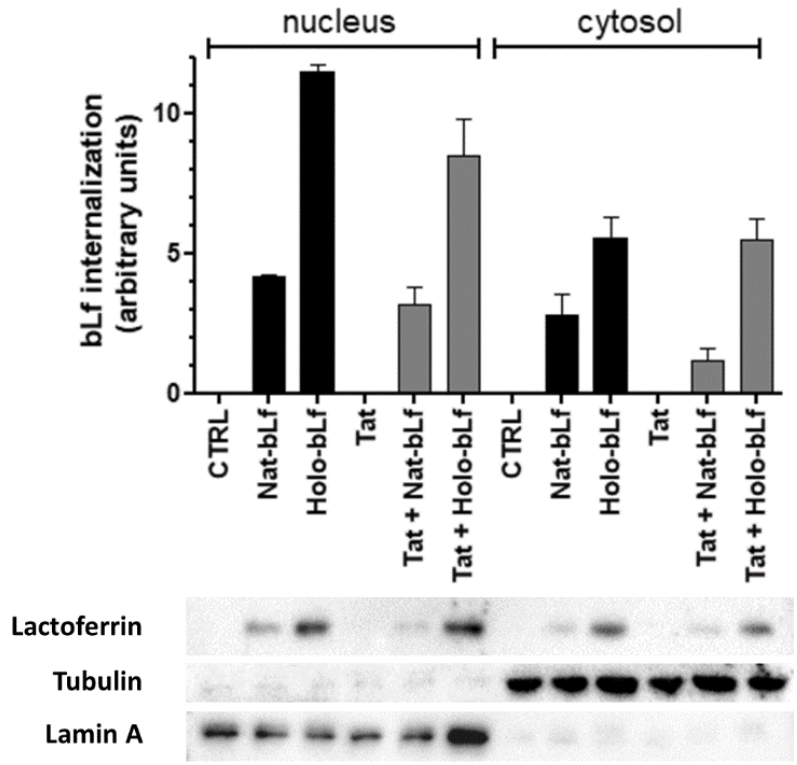

Figure 13. Analysis of bLf internalization and sub-cellular localization in U373 and U373-Tat cells. Western blot of bLf in cytosolic (C) and nuclear (N) fractions after 24 h of treatment with 100 µg/ml of Nat-bLf or Holo-bLf. Data are calculated relative to the internal housekeeping gene (Tubulin for cytosolic fraction and Lamin A for nuclear fraction) and are expressed as the means ± SEM.

4/1.2. Bovine lactoferrin modulates cell antioxidant response

To better elucidate the role of bLf in maintaining the physiological balance of ROS, analyses of Nrf2 nuclear translocation and of the expression of System Xc^- were performed in U373-mock and U373-Tat cells (Fig. 14, 15, 16). The results show an approximately 50% increase of Nrf2 nuclear expression in U373-Tat cells, as compared to the control (Fig. 14). Treatment with bLf has a positive effect on Nrf2 traslocation, with the Holo form more efficient than the native counterpart (Fig. 14).

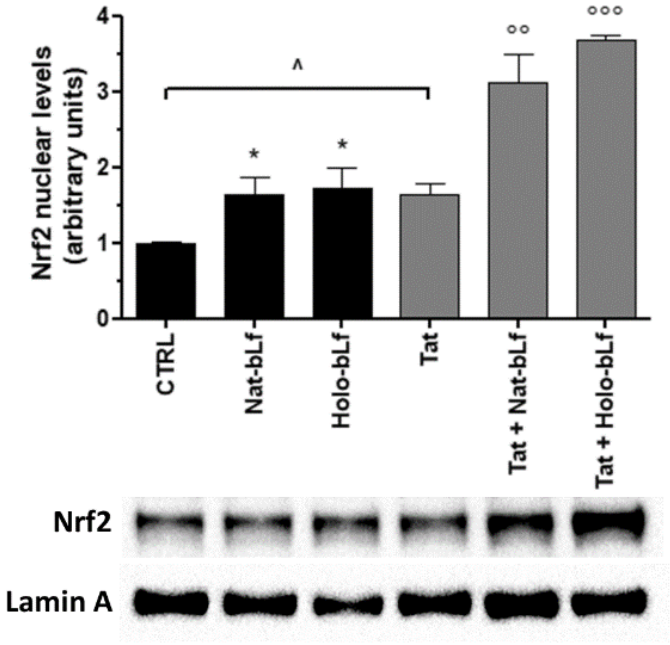

Figure 14. Analysis of Nrf2 nuclear translocation. Western blot and densitometric analysis of Nrf2 protein levels in nuclear extracts of U373 and U373-Tat cells after 4 h of treatment with 100 μg/ml of Nat-bLf or Holo-bLf. Data are calculated relative to the internal housekeeping gene (Lamin A) and are expressed as the means ± SEM. One-way ANOVA, followed by Tukey's test, was used to determine signif-icant differences. *$p \leq 0.05$ vs CTRL; °°$p \leq 0.01$ and °°°$p \leq 0.001$ vs Tat; ^$p \leq 0.05$ between Tat and CTRL

Gene expression of System Xc^- was assessed by qPCR on total RNA extracts. In agreement with Nrf2 nuclear expression, the System Xc^- was also found to be up-regulated in Tat-expressing cells, as already reported (Mastrantonio et al., 2019) (Fig. 15**C** inset). Again, bLf enhances the expression of the System Xc^- with a peak between 4-8 h post-treatment; differences are detected according to iron saturation rate and Tat expression. The effect over time of both Lf forms is depicted in Figures 15 **A-D**.

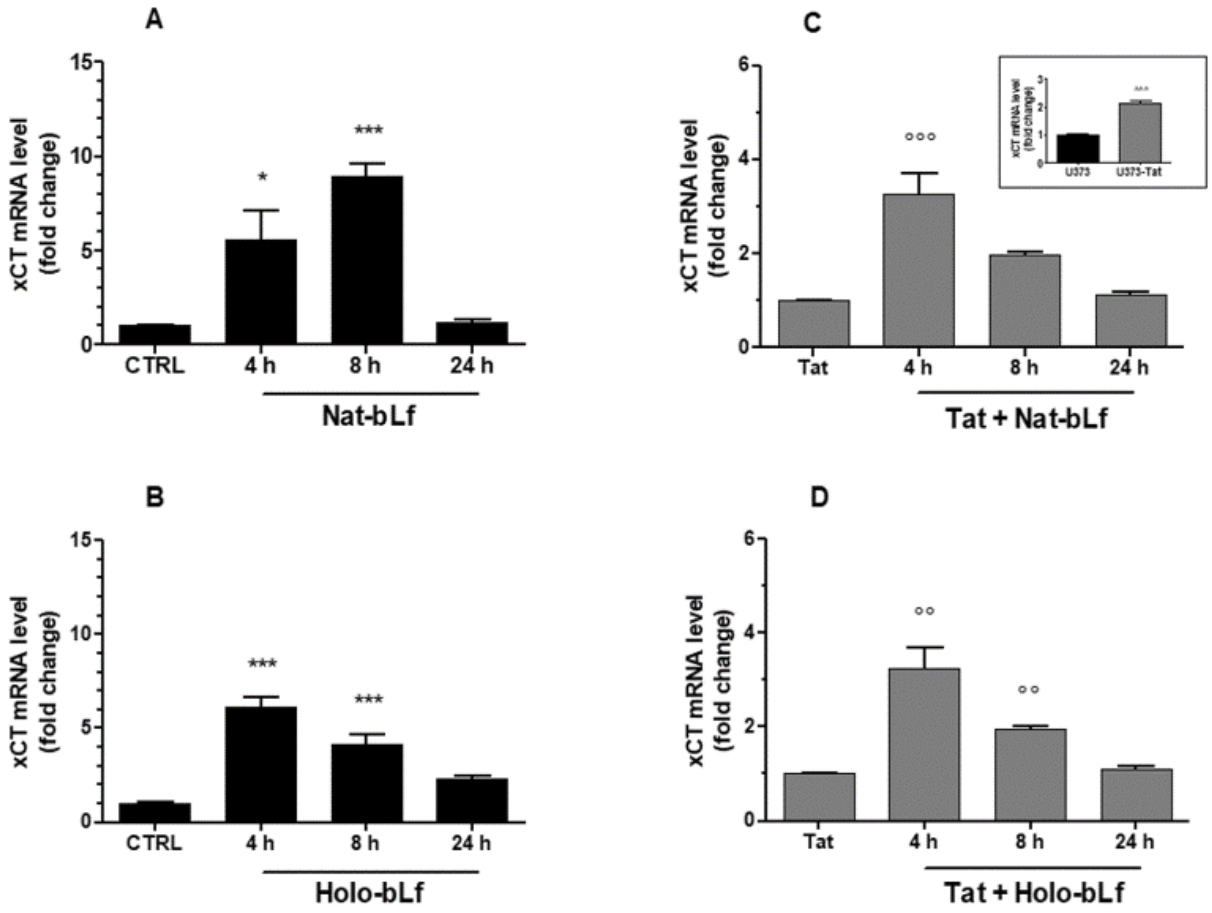

Figure 15. Analysis of System Xc^- transcript levels. Real-Time qPCR analysis of System Xc^- mRNA in U373 (**A**, **B**) and U373-Tat (**C**, **D**) cells after 4, 8 and 24 h of treatment with 100 µg/ml of Nat-bLf or Holo-bLf. Data are calculated relative to the internal housekeeping gene (GAPDH) and are expressed as the means ± SEM. One-way ANOVA, followed by Tukey's test, was used to determine significant differences. *$p \leq 0.05$ and ***$p \leq 0.001$ vs CTRL; °°$p \leq 0.01$ and °°°$p \leq 0.001$ vs Tat; ^^^$p \leq 0.001$ between U373-Tat and U373 (inset).

To corroborate the results obtained at the transcript level, protein expression was also evaluated. Western blots confirme the enhanced expression of System Xc^- in U373-Tat cells, with respect to control cells and the potentiating effect exerted by bLf, which, globally, acts as a positive regulator for System Xc^- (Fig. 16). Consistent with the transcriptional data in Figure 15, a significant up-regulation of System Xc^- production is obtained following treatment with Holo-bLf in both U373 and U373-Tat cells.

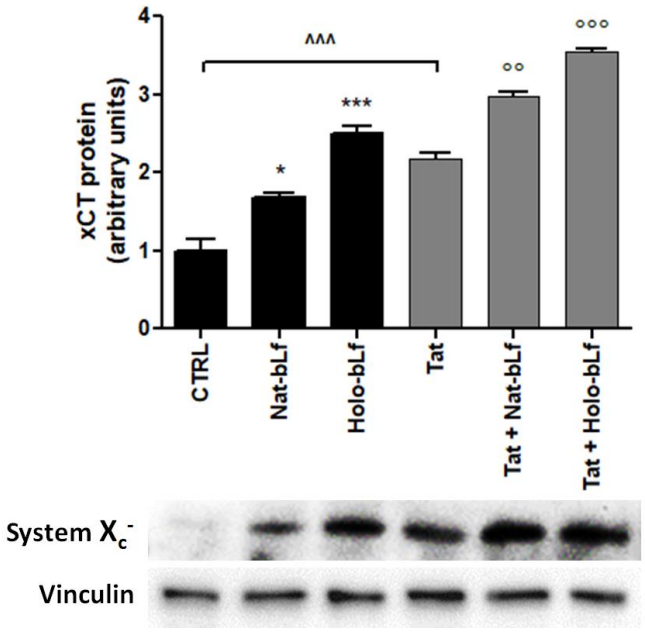

Figure 16. Western blot and densitometric analysis of System Xc^- in U373 and U373-Tat cells treated with 100 µg/ml of Nat-bLf or Holo-bLf after 24h. Data are calculated relative to the internal housekeeping gene (Vinculin) and are expressed as the means ± SEM. One-way ANOVA, followed by Tukey's test, was used to determine significant differences. *p ≤ 0.05 and ***p ≤ 0.001 vs CTRL; °°p ≤ 0.01 and °°°p ≤ 0.001 vs Tat; ^^^p ≤ 0.001 between Tat and CTRL.

4/1.3. Bovine lactoferrin potentiates cell defense against intracellular iron overload

Due to the tight correlation between oxidative stress and iron disorders, the expression of the main proteins involved in iron homeostasis was then assessed. The expression of the iron storage protein Ftn and of the receptor required for its degradation, NCOA4, were measured. As shown in Figure 17 **A** and **B**, a significant decrease in Ftn expression and a concomitant upregulation of NCOA4 is observed in U373-Tat cells. This effect would suggest the activation of a ferritinophagy process, which is not affected by bLf treatment (Fig. 17**A, B**).

Next, the expression of TfR1 and Fpn, involved in iron uptake and export, respectively, was assessed. As shown in Figure 17 **C** and **D,** cells expressing Tat show a reduction in TfR1 and an increase in Fpn compared to U373-mock cells. In U373-Tat cells, Nat-bLf treatment increases the sole Fpn expression, whereas the saturated form boosted the effect of Tat on both TfR1 and Fpn.

In addition, Fpn-coupled ferroxidase Cp is decreased in the presence of Tat (Fig. 17**E**). Treatment with Holo- bLf reduces the levels in control cells, while both Nat- and Holo-bLf do not reverse the effect of Tat. Next, to investigate Tat-induced inflammatory disorders, the expression of IL-6 and IL-1β, the main cytokines involved in iron disorders, was analyzed under the same experimental conditions. Tat does not promote any increase in IL-6 expression, whereas treatment with Holo-bLf induces significant upregulation of IL-6 in U373-Tat cells compared with Nat-bLf, which has no

effect (Fig. 17A). On the other hand, no detectable levels of IL-1β are found in all conditions tested (data not shown).

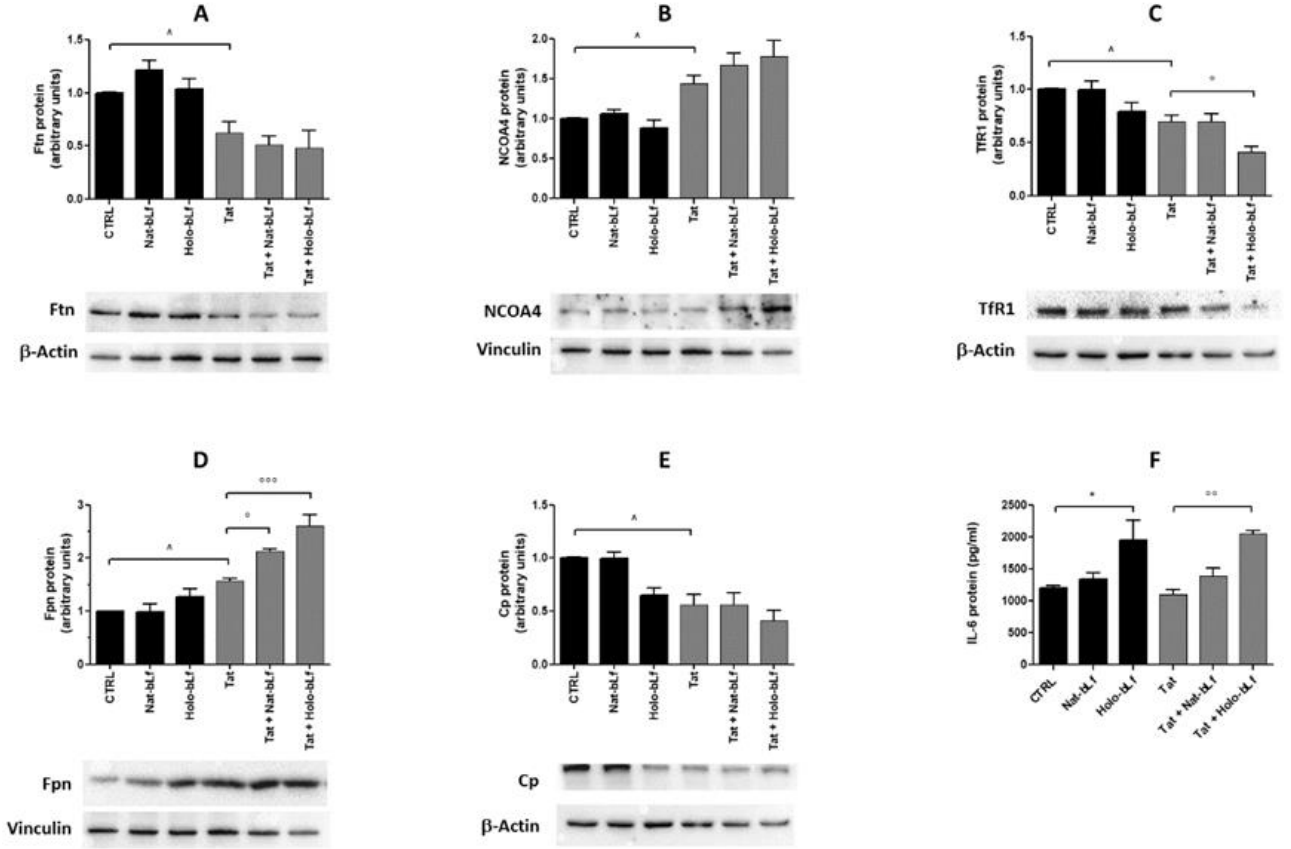

Figure 17. Western blot and densitometric analysis of Ftn(**A**), NCOA4 (**B**), TfR1 (**C**), Fpn (**D**), Cp (**E**), and ELISA quantification of IL-6 (**F**) in U373 and U373-Tat cells treated with 100 μg/ml of Nat-bLf or Holo-bLf for 48h. Data are calculated relative to the internal housekeeping gene (β-Actin or Vinculin) and are expressed as the means ± SEM. One-way ANOVA, followed by Tukey's test, was used to determine significant differences. *$p \leq 0.05$ vs CTRL; °$p \leq 0.05$, °°$p \leq 0.01$ and °°°$p \leq 0.001$ vs Tat; ^$p \leq 0.05$ between Tat and CTRL.

Confocal microscopy reveales a perinuclear localization of TfR1 and Ftn in U373-mock, unaffected by bLf treatments (Fig. 18). In the presence of the viral protein Tat, TfR1 localizes predominantly to the membrane, and bLf treatments restores its perinuclear re-localization. Ftn signal in bLf-treated U373-Tat cells is reduced compared with U373-mock cells, in agreement with western blots data (Fig. 17 A).

Overall, the data suggest that bLf treatment counteracts pro-oxidant intracellular iron accumulation, likely caused by Tat-induced ferritinophagy. This response results in increased Fpn-mediated iron release and reduced Tf-bound metal entry.

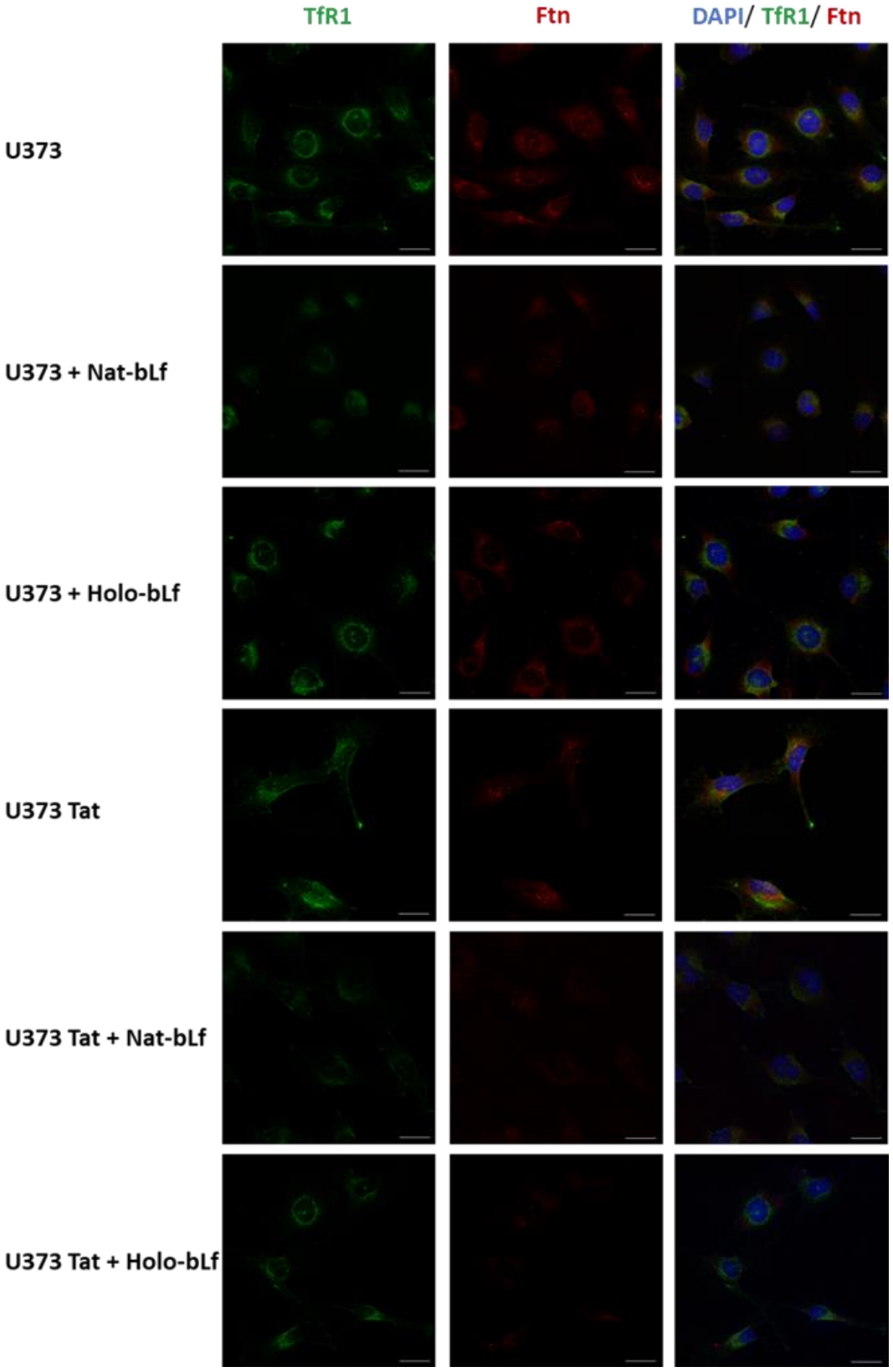

Figure 18. Immunofluorescence and confocal analysis for TfR1(green) and Ftn (red) subcellular lo-calization in U373 and U373-Tat cells treated with 100 μg/ml of Nat-bLf or Holo-bLf for 48 h. DAPI was used to stain nuclei (blue). Scale bar,10 μm.

4/1.4. Bovine lactoferrin counteracts Tat-mediated lipid peroxidation and DNA damage in astroglial cells

To clarify the efficacy of bLf against oxidative stress, ROS production was evaluated by testing lipid peroxidation. As shown in Figure 19**A**, expression of Tat induces a significant increase in lipoperoxidation compared with control cells. Treatment with bLf, in both Native and Holo forms, effectively restores lipid peroxidation to control levels (Fig. 19**A**), suggesting an important antioxidant activity of bLf. The significant reduction of lipid peroxidation in U373-mock cells suggests a protective role that bLf plays against ROS that is independent of Tat presence. Consistent with Bodipy analysis, there is a significant increase in histone variant ɣ-H2AX, a selective marker of DNA damage in U373-Tat. Treatment with bLf reduces Tat-induced ɣ-H2AX expression, suggesting a potential protective effect on DNA damage (Fig. 19**B**).

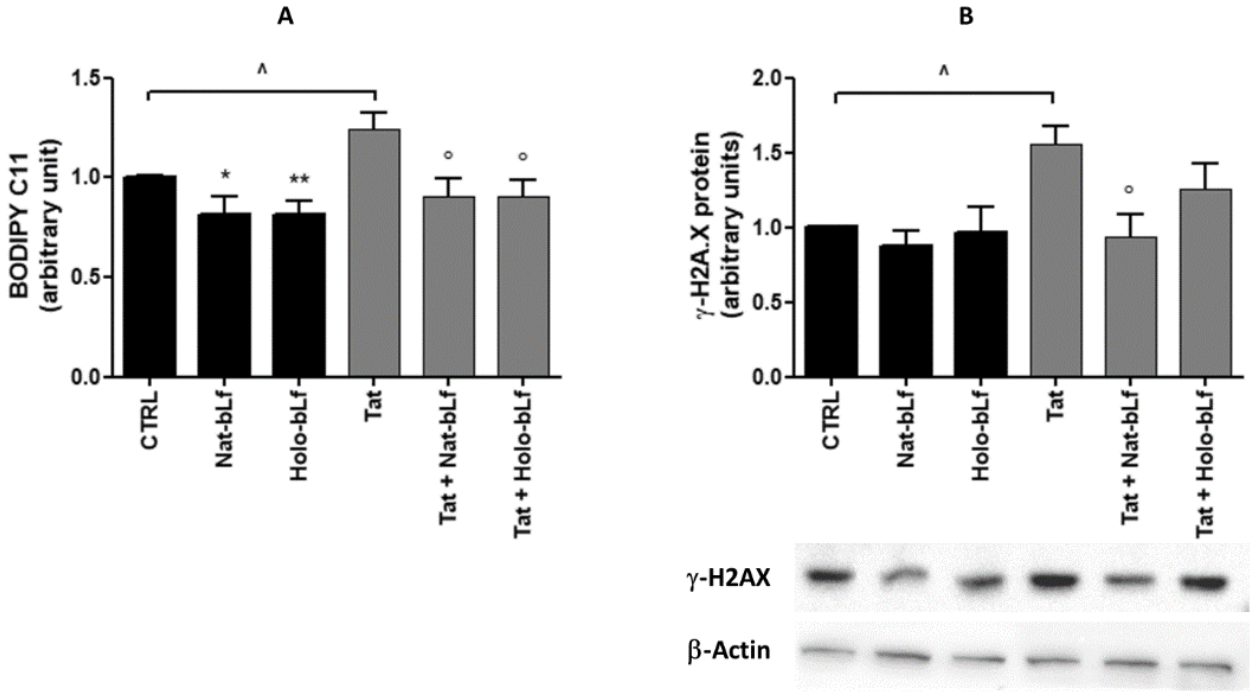

Figure 19. Analysis of lipid peroxidation by Bodipy assay (**A**) and Western blotting of ɣ-H2AX (**B**) in U373 and U373-Tat cells treated with 100 μg/ml of Nat- or Holo-bLf for 24 h. Data are calculated relative to the internal housekeeping gene (β-Actin) and are expressed as the means ± SEM (b). One-way ANOVA, followed by Tukey's test, was used to determine significant differences. *p ≤ 0.05 and **p ≤ 0.01 vs CTRL; °p ≤ 0.05 vs Tat; ^p ≤ 0.05 between Tat and CTRL.

4/1.5. Holo-bLf exacerbates Tat-induced neurotoxicity via System Xc^-

Given the close interconnection between astroglial metabolism and neuronal function, co-cultures of U373 and U373-Tat cells with SH-SY5Y neuronal cells were set up. The co-cultures have been treated with Nat- and Holo-bLf at a concentration of 100 μg/ml for 24 hours, and viability tests were carried out by MTT assay and cell counts.

In agreement with a previous study (Mastrantonio et al., 2019), a significant reduction in the viability of neurons cultured with U373-Tat is recorded (Fig 20**A**). Treatment with both forms of bLf exacerbates this effect in cells expressing Tat, most consistently for the Holo form. The same results are obtained by cell counts (Fig. 20**C**).

On the other hand, treatment with bLf does not affect the viability of astroglial cells both in the presence and absence of Tat expression (Fig. 20 panels **B**, **D**).

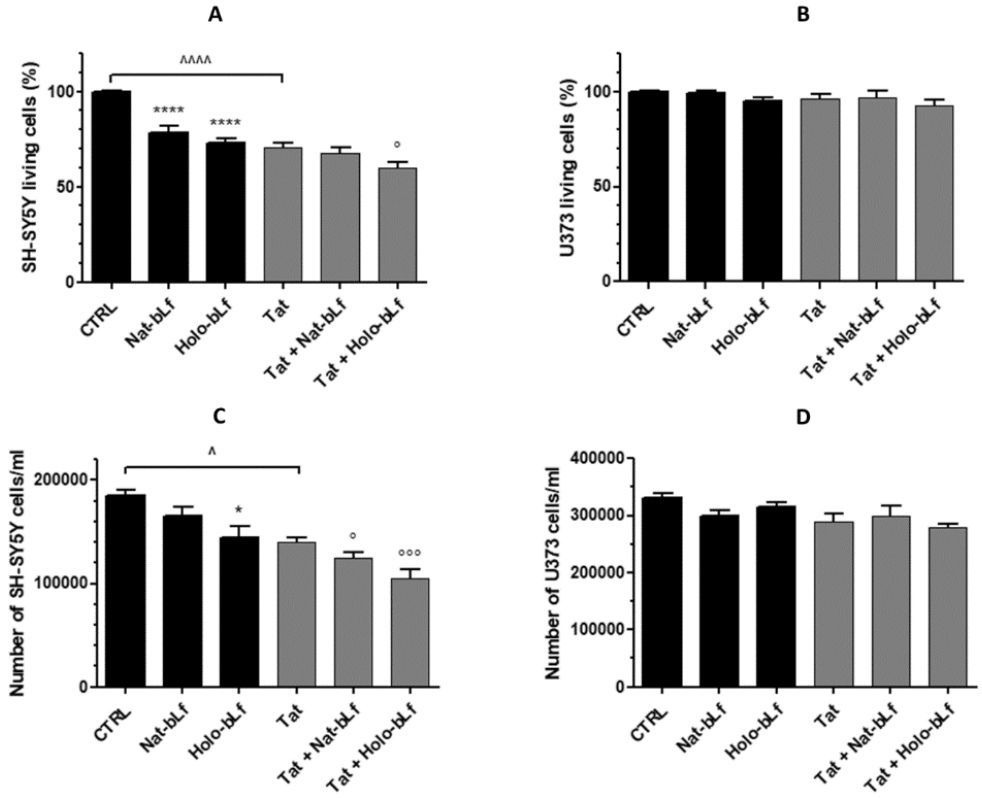

Figure 20. Cell viability measurement by MTT assay (**A, B**) and trypan blue exclusion assay (**C, D**) on co-cultures of SH-SY5Y and U373 or U373-Tat cells untreated or treated with 100 μg/ml Nat- or Holo-bLf for 24 h. The histograms in (**A**) and (**B**) show the percentage of living cells, and the rate of reduction was calculated by setting the control (CTRL) equal to 100%. One-way ANOVA, followed by Tukey's test, was used to determine significant differences. *$p \leq 0.05$ and ****$p \leq 0.0001$ vs CTRL; °$p \leq 0.05$ and °°°$p \leq 0.001$ vs Tat; ^$p \leq 0.05$ and ^^^^$p \leq 0.0001$ between Tat and CTRL.

In addition, to elucidate the molecular mechanism involving neurotoxicity, the experiments were repeated using N-acetylcysteine (NAC) as a scavenger of ROS. Co-cultures were treated for 30 min

with NAC and then with bLf for 24 h. The MTT results show that NAC restores neuronal viability in both U373 and U373-Tat co-cultures (Fig. 21**A**). In contrast, astroglial cell viability is not modulated by NAC under any condition (Fig. 21**B**).

To clarify a possible correlation between increased System Xc^- and neurotoxicity, experiments were conducted in the presence of sulfasalazine (SSZ), a specific inhibitor of the antyporter. Again, cells were pretreated for 30 min with SSZ and subsequently incubated with both forms of bLf. The results show that, under all conditions, neuronal viability is restored by treatment with SSZ (Fig. 21**C**). In the presence of the inhibitor, U373 cell viability is not modulated in any condition, while it is reduced by 30% in U373-Tat compared with control. Of note, treatment with Nat-bLf restores viability to control levels (Fig. 21**D**).

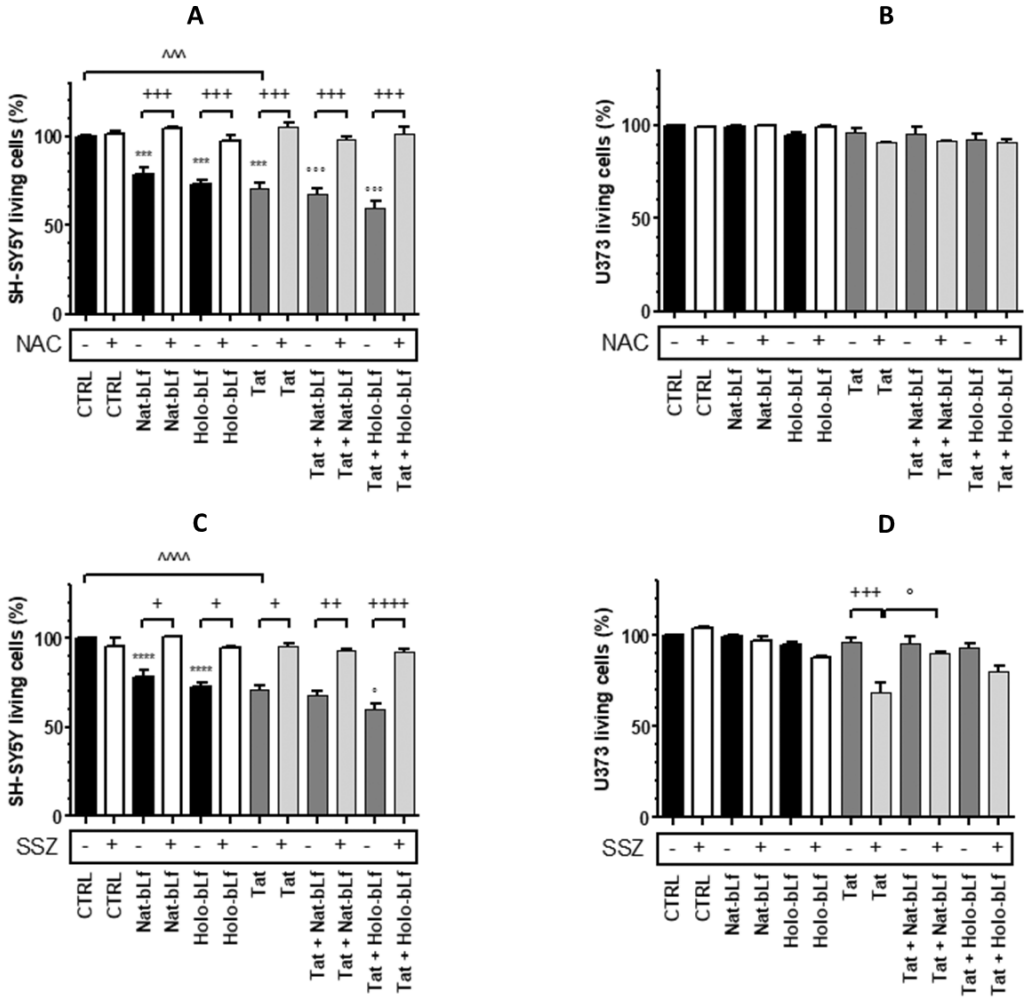

Figure 21. Cell viability measurement by MTT assay on co-cultures of SH-SY5Y and U373 or U373-Tat cells, pre-treated with 2 mM N-acetyl cysteine (NAC) (**A, B**) or 300 μM sulfasalazine (**C, D**), untreated or treated with 100 μg/ml Nat- or Holo-bLf for 24 h. The histograms show the percentage of living cells, and the rate of reduction was calculated by setting the control (CTRL) equal to 100%. One-way ANOVA, followed by Tukey's test, was used to determine significant differences. ***$p \leq 0.001$ and ****$p \leq 0.0001$ vs CTRL; °$p \leq 0.05$ and °°°$p \leq 0.001$ vs Tat; ^^^$p \leq 0.001$ and ^^^^$p \leq 0.0001$ between Tat and CTRL; +$p \leq 0.05$, ++$p \leq 0.01$, +++$p \leq 0.001$ and ++++$p \leq 0.0001$ between treatment with SSZ or NAC and without SSZ or NAC.

To better understand the molecular mechanism, the amount of glutamate in the culture medium was measured. Glutamate release was normalized to the number of viable astrocytes (Fig. 22**A**) by setting the ratio as 1 for untreated U373-mock cells.

Treatment with bLf-Holo induces a marked increase in glutamate in co-cultures with astroglial cells expressing or not the viral protein (Fig.22**A**, **B**). In contrast, the Native form results in a slight increase only in U373-Tat cells. Treatment with SSZ reduces the amount of glutamate in all conditions tested, thus further demonstrating the role of System Xc^- in neuronal excitotoxicity (Fig. 22**A** e **B**)

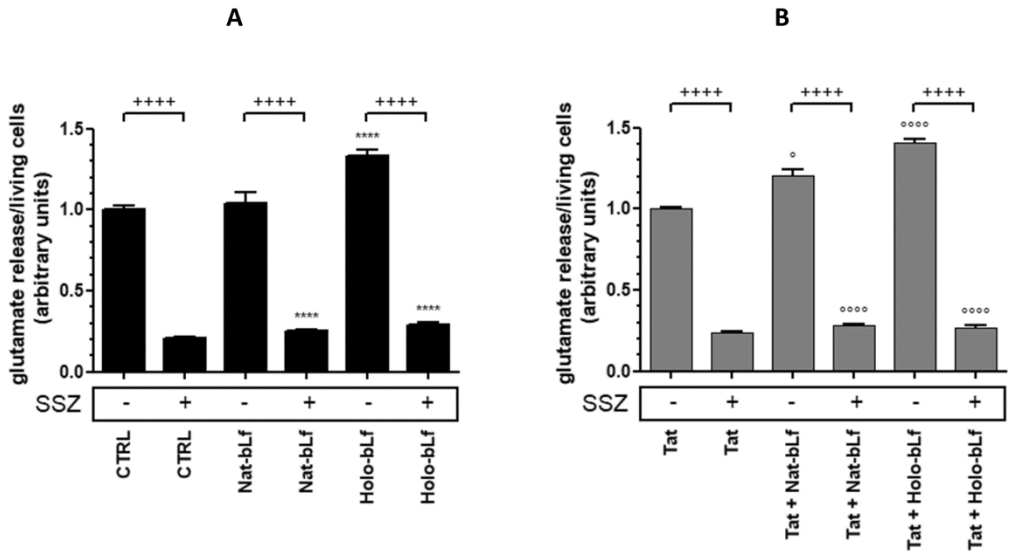

Figure 22. Measurement of glutamate release in co-culture supernatants of SH-SY5Y with U373 (**A**) or U373-Tat (**B**) cells untreated or treated with 300 μM sulfasalazine and 100 μg/ml Nat- or Holo-bLf for 24 h. One-way ANOVA, followed by Tukey's test, was used to determine significant differences. ****$p \leq 0.0001$ vs CTRL; °$p \leq 0.05$ and °°°°$p \leq 0.0001$ vs Tat; ++++$p \leq 0.0001$ between treatment with or without SSZ.

In addition, viability was also analyzed in the presence of MK801, a specific NMDA receptor antagonist. As shown, viability of U373 cells is unaffected, whereas NMDA treatment counteracts the reduction in neuronal viability induced by Holo-bLf treatment, again confirming the role of Systema Xc^-, and thus the increased glutamate release, in the induction of excitotoxicity (Fig 23 **B**, **C**).

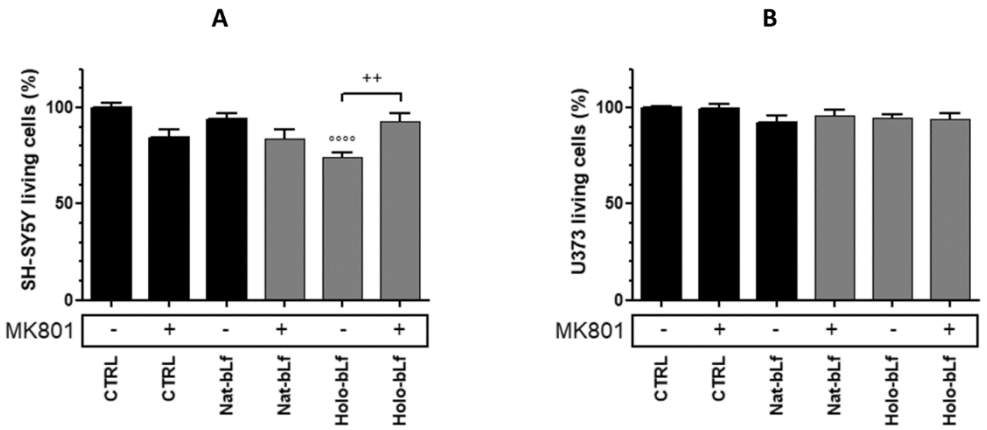

Figure 23. Cell viability measurement by MTT assay on SH-SY5Y cells (**A**) and U373-Tat cells (**B**) in co-cultures, untreated or treated with 10 μM MK801 and 100 μg/ml Nat- or Holo-bLf for 24 h. The histograms show the percentage of living cells, and the rate of reduction was calculated by setting the control (CTRL) equal to 100%. One-way ANOVA, followed by Tukey's test, was used to determine significant differences. ****$p \leq 0.0001$ vs CTRL; ++$p \leq 0.01$ between treatment with or without MK801.

Finally, Nat-bLf does not induce lipoperoxidation in SH-SY5Y co-cultured with U373-Tat; on the other hand, Holo bLf significantly increases lipoperoxidation in neuronal cells compared with control (Fig. 24**A**), thus supporting an iron role in ROS-mediated excitotoxicity. Interestingly, neither form of bLf induces lipid peroxidation in monocultures of SH-SY5Y cells (Fig. 24**B**).

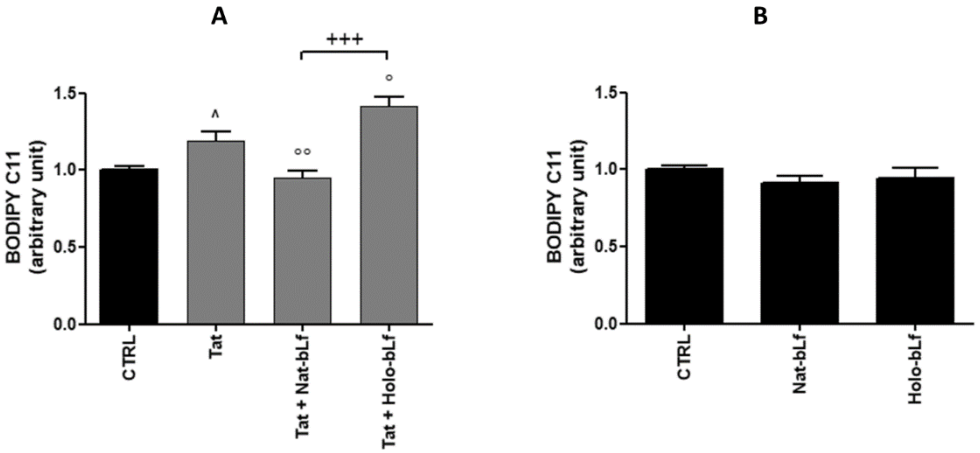

Figure 24. Analysis of lipid peroxidation by bodipy assay in co-cultures of SH-SY5Y with U373-Tat cells (**A**) or in SH-SY5Y monocultures (**B**) untreated or treated with 100 μg/ml Nat- or Holo-bLf for 24 h. One-way ANOVA, followed by Tukey's test, was used to determine significant differences. °$p \leq 0.05$ and °°$p \leq 0.01$ vs Tat; ^$p \leq 0.05$ between Tat and CTRL; +++$p \leq 0.001$ between treatment with Nat- and Holo-bLf.

5/1. Discussion

Viruses are obligate intracellular parasites that exploit host cell systems for their own propagation. RNA viruses exhibit the highest mutation rate (Drake et al., 1999), which gives them a selective advantage, thus it is more difficult to develop an effective therapy. Several studies have highlighted the role of oxidative stress in viral pathogenesis, including apoptosis, altered immunological function, virus replication, and inflammatory response (Pace and Leaf 1995; Paracha et al., 2013). In HIV infection, oxidative stress plays a crucial role in the spread of the virus by activating NF-kB, which is required for viral replication (Staal et al., 1990) and at the same time for inflammatory response (Lenardo and Baltimor 1989). Under infection, the host activates antioxidant pathways governed by Nrf2 factor to preserve cellular redox homeostasis (Pillai et al., 2022). The systemic inflammatory state in infected individuals leads to intracellular iron accumulation and anemia, which have been associated with increased viral replication and worse prognosis in HIV+ patients (Chang et al., 2015; Drakesmith et al., 2008). To this end, iron depletion may have a marked anti-HIV effect; indeed, overexpression of Fpn is a contributing factor to HIV-1 limitation (Kumari et al., 2016). Emerging evidence suggests that viruses take advantage from intracellular iron in order to guide their own replication (Mancinelli et al., 2020; Schmidt 2020).

Viral proteins are the causal agents of neuronal death observed in HIV-infected patients (Marino et al., 2020), inducing oxidative stress and neuroinflammation (Capone et al., 2013; Mangino et al., 2015; Persichini et al., 2016). However, in HAND, the correlation between oxidative stress and dysregulation of iron metabolism is unclear.

The results shown concern the cellular response in astroglial cell lines constitutively expressing the viral protein Tat. The antioxidant defense response promotes the activation of Nrf2 factor and consequently the transcriptional and translational overexpression of the System Xc^-. When Tat is present, modulation of iron protein expression suggests that a ferritinophagy process takes place. In addition, increased expression of Fpn and decreased expression of TfR1 are observed compared with control, favoring reduction of intracellular iron. Tat protein, as also demonstrated for Nef (Madrid et al., 2005), appears to reduce Tf receptor expression, thus limiting viral replication. It must be recalled that TfR1 has been defined as a secondary receptor for virus entry, including SARS-CoV-2 (Wessling-Resnick 2010; Tang et al., 2020).

Overall, the data suggest that astrocytes try to reply to Tat-mediated effects by counteracting the accumulation of ROS and intracellular iron. However, significant increases in lipoperoxidation and DNA damage are still recorded. Treatment with both Nat- and Holo-forms of bLf reduced lipid peroxidation, and only Nat-bLf played a protective role against DNA damage. Both forms of bLf promoted antioxidant response and intracellular iron depletion, but with different efficacy. Holo-bLf

was significantly more efficient than the Native counterpart in promoting the expression of System Xc^- and Fpn. However, Nat-bLf reduced the expression of the DNA damage marker ɣ-H2AX and did not induce the expression of IL-6. The different function exerted by the two forms could be related to the different iron content which, in turn, influences bLf physico-chemical features. The stability of Holo-bLf is greater than the Apo and Nat forms; indeed, it is more resistant to proteolysis (Rosa et al., 2018). Similar to what was reported in a human glioblastoma model (Cutone et al., 2020a), the saturated form is able to localize more efficiently in the nucleus than its counterpart and persist longer, suggesting possible gene regulation over time. Importantly, Native form can act as an iron chelator, reducing potentially reactive free iron and ROS formation.

In the CNS of HIV+ patients, astrocytes can actively contribute to neurotoxicity characterizing the disease. These cells release excessive amounts of glutamate, pro-inflammatory cytokines, and nitric oxide that collectively promote ROS production, mediating neuronal damage (Persichini et al., 2014). Infected patients compared to healthy ones have five times higher levels of glutamate in CSF (Ferrarese et al., 2001), and in patients with HAND the levels are still higher despite ART (Cassol et al., 2014). The malfunction of the glutamate-glutamine shuttle system could explain the extracellular accumulation of this neurotransmitter. In this context, a promising pharmacological target in neurodegenerative diseases could be System Xc^-.

In this research work, it was shown that Holo-bLf acts as a positive regulator of the Nrf2 pathway by promoting the prolonged expression of System Xc^-, thereby exacerbating the neurotoxic effect on neuronal cells. Standardization of nutraceuticals is needed since currently available Lf-based products show high variability in the downstream effects. Quality control of Lf is essential for effective function to be claimed. The iron content, as shown in this work, greatly affects bLf biological activities. Indeed, Nat-bLf turns out to be protective against oxidative stress, does not induce excitotoxicity, protects the host from DNA damage, and does not increase IL-6 expression. On the other hand, Holo-bLf, although able to promote antioxidant cellular response, exacerbates System Xc^--mediated neurotoxicity, does not protect against DNA damage, and induces IL-6 production. To date, the neurotoxic effect of Lf has never been described in the literature. Our results emphasize the importance of glycoprotein saturation and its implications in the success or failure of clinical therapies.

❖ **Part 2**

Effects of Lactoferrin on SARS-CoV-2 Spike-mediated cell fusion, inflammation and iron disorders

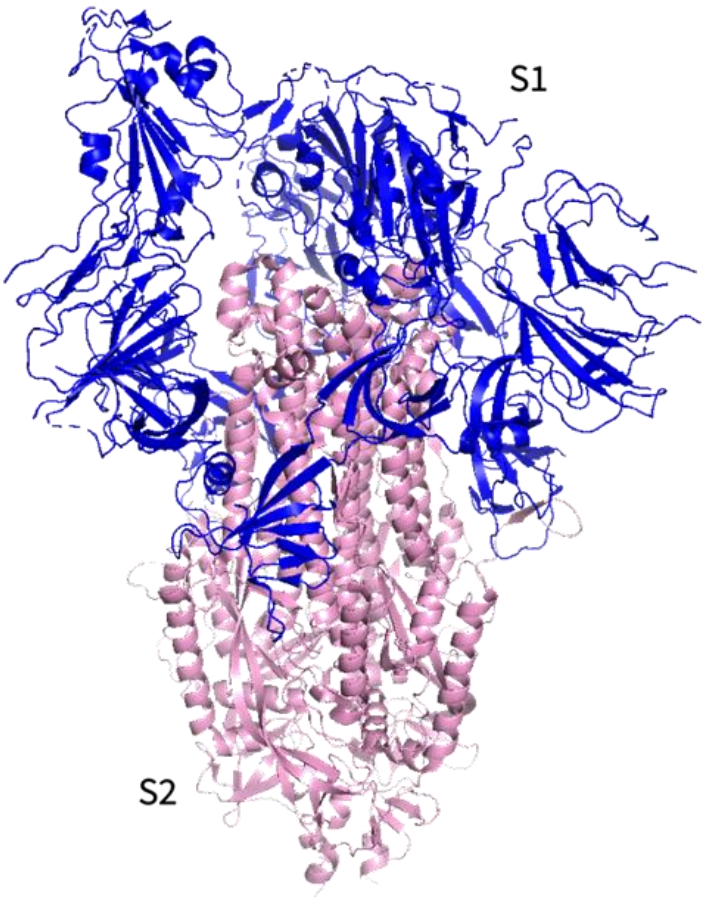

PDB: 6VSB

3/2. Materials and Methods

3/2.1. Bovine and Human Lactoferrin

For bLf, the same commercial preparation described in the section 3/1.1. was employed. Highly purified hLf was purchased from Sigma Aldrich (Milan, Italy). HLf purity was about 97%, as checked by SDS-PAGE and silver nitrate staining. Iron saturation of hLf was about 9%, as determined via optical spectroscopy at 468 nm using an extinction coefficient of 0.54 for a 1% solution of 100% iron saturated protein. LPS contamination, assessed via Limulus Amebocyte assay (Pyrochrome kit, PBI International, Milan, Italy), was 0.3 ± 0.07 ng/mg. Before each in vitro assay, bLf and hLf solutions were sterilized using a 0.2 μm Millex HV filter at low protein retention (Millipore Corp., Bedford, MA, USA).

3/2.2. Cell Culture and Pseudovirus

The African green monkey kidney-derived Vero E6 and human colon carcinoma–derived Caco-2 cells were purchased from American Type Culture Collection (ATCC), Human Bronchial Epithelial (16HBE14o-) cell line was purchased from Millipore Sigma (St. Louis, MO, USA), while THP-1 cells were purchased from European Collection of Cell Cultures (ECACC). Vero E6 and Caco-2 cells were cultured in high-glucose Dulbecco's Modified Eagle's Medium (DMEM) (Euroclone, Milan, Italy) with 10% Fetal Bovine Serum (FBS) (Euroclone, Italy) in a humidified incubator with 5% CO_2 at 37 °C. 16HBE14o- Human Bronchial Epithelial cells were cultured in minimum essential medium (MEM) with 10% FBS at 37 °C in a humidified incubator with 5% CO_2. THP-1 cells were maintained in RPMI 1640 medium (Euroclone, Italy), supplemented with 10% FBS and 2 mM glutamine, at 37 °C in a humidified incubator with 5% CO_2. THP-1 cells, which grow spontaneously in loose suspension under these conditions, were subcultured twice a week by gentle shaking, followed by pelleting and reseeding at a density of approximately 5×10^5 cells/mL.

SARS-CoV-2 Spike Pseudovirus (hereafter referred to as "Pseudovirus"), an HIV-based luciferase lentivirus pseudotyped with SARS-CoV-2 full length Spike protein of Wuhan strain, was purchased from Creative Biogene (New York, NY, USA) (SARS-CoV-2 S Pseudotyped Luciferase Lentivirus, cat. CoV-002). The Pseudovirus presents SARS-CoV-2 Spike as the only surface protein that mediates viral fusion with host cells.

3/2.3. Pseudovirus Neutralization Assay

For neutralization assays, cells were seeded in 96-well tissue culture plates (1×10^4 cells/well) for 24 h (Vero E6) or 48 h (Caco-2 and 16HBE14o-) at 37 °C in a humidified incubator with 5% CO_2. THP-1 cells were differentiated in macrophages by incubation in 96-well tissue culture plates at a density of 2×10^4 cells/well in RPMI medium containing 0.16 μM phorbol myristate acetate (PMA) (Sigma Aldrich, Italy) for 48 h at 37 °C in a humidified incubator with 5% CO_2. Cell confluence conditions were set following instructions provided by the Pseudovirus manufacturer. To evaluate the inhibition of Pseudovirus fusion to the host membrane, 1.25 and 6.25 μM of bLf or hLf, corresponding to 100 and 500 μg/mL, were used on Vero E6 cells; the higher concentration was used on 16HBE14o-, Caco-2 and THP-1 cells. For studies on the interaction of Lf with pseudoviral particles and/or host cells, the neutralization assay was carried out with a multiplicity of infection (MOI) of 10 in the presence or absence of bLf or hLf, according to the following experimental plan: (i) to evaluate the entry efficiency of the pseudoviral particles, cells were treated with Pseudovirus for 8 h at 37 °C; (ii) to evaluate whether Lf interferes with the viral fusion rate by binding viral surface components, the Pseudovirus was preincubated with bLf or hLf for 1 h at 37 °C and then the cells were treated with these suspensions for 8 h at 37 °C; (iii) to evaluate whether Lf interferes with viral attachment to host cells, cells were preincubated with bLf or hLf for 1 h at 37 °C. The cells were then washed with PBS and treated with Pseudovirus for 8 h at 37 °C; (iv) to assess whether Lf interferes with both viral and host cell components, bLf or hLf was added together with Pseudovirus to the cell monolayer for 8 h at 37 °C.

For experiments on the contribution of TfR1 to pseudoviral fusion to the cell membrane, two different approaches were followed: (i) cells were preincubated with an antibody against human TfR1 (sc-32272, Santa Cruz, CA, USA) for 1 h at 37 °C. The cells were then washed with PBS and treated with Pseudovirus for 8 h at 37 °C; (ii) the Pseudovirus was preincubated with a soluble form of TfR1 (11020-H01H, Sino Biological, China) for 1 h at 37 °C and then the cells were treated with this suspension for 8 h at 37 °C.

At the end of the incubation, cells were washed twice with PBS, covered with the appropriate culture medium with 2% of FBS and incubated for 48 h at 37 °C in a humidified incubator with 5% CO_2. After 48 h, cells were washed, lysed with cell culture lysis reagent (Promega, Italy) and the transduction efficiency was determined by luminescence analysis using firefly luciferase assay kit (Promega, Italy). The relative luciferase unit (RLU) in each well was detected using a Cytation 5 Cell Imaging Multi-Mode Reader (BioTek, Winooski, VT, USA).

3/2.4. Sepharose 6B Pull-Down

CNBr-activated Sepharose 6B (GE Healthcare, Chalfont St Giles, Buckinghamshire, UK) was employed for conjugation of bLf, hLf or human Tf (hTf, Fluka Sigma Aldrich, Milan, Italy). The resin (100 mg) was washed with 1 mM HCl and coupled to 0.5 mL of a 10 mg/mL protein solution in PBS by overnight incubation at room temperature under continuous shaking. The resin was fully inactivated by incubation in 1 mL of Tris-HCl 0.5 M pH 8.0 for 2 h at room temperature. After five washes with 1 mL of PBS, the resins were resuspended in an equal volume of PBS. An amount of 40 µL of the resuspended resins was added to 200 µL of full-length stabilized trimeric Spike of Wuhan strain (P2020-025, Trenzyme GmbH, Konstanz, Germany) (20 µg/mL) or its S1 domain (40591-V08H, Sino Biological, Eschborn, Germany) (20 µg/mL) and incubated for 2 h at room temperature under continuous shaking. The resins were then washed five times with 1 mL of PBS and eluted in 50 µL of SDS sample buffer. An amount of 20 µL of the eluted fractions was analyzed by SDS-PAGE and Western blot (monoclonal anti-His-HRP, Sigma, 1:10,000).

3/2.5. Stimulation of Caco-2 and Differentiated THP-1 Cells with Spike

For the stimulation assay, Caco-2 cells were seeded in 6-well tissue culture plates in complete DMEM medium at a density of 7×10^5 cells/well for 48 h at 37 °C in a humidified incubator with 5% CO_2, while THP-1 cells were differentiated in macrophages by incubation in 6-well tissue culture plates at a density of 2×10^6 cells/well in complete RPMI medium containing 0.16 µM PMA for 48 h at 37 °C in a humidified incubator with 5% CO_2. Caco-2 cells and differentiated THP-1 cells were washed twice with PBS and treated or not with full-length stabilized trimeric Spike and/or with bLf according to one of the following experimental procedures: (i) untreated cells; (ii) cells treated with 1.25 µM bLf; (iii) cells treated with 20 nM Spike; (iv) cells pre-treated with 20 nM Spike for 1 h and subsequent addition of 1.25 µM bLf; (v) cells pretreated with 1.25 µM bLf for 1 h and subsequent addition of 20 nM Spike and (vi) cells treated with a mixture of 1.25 µM bLf and 20 nM Spike preincubated for 1 h. For all conditions, cells were incubated for 48 h at 37 °C in a humidified incubator with 5% CO_2.

After 48 h from treatments, cytokines were quantified on the supernatants. Adherent cells were scraped in PBS with 1 mM phenylmethylsulfonyl fluoride (PMSF), pelleted at 5000× g for 5 min and stored at −80 °C for protein analysis.

3/2.6. Cytokine Analysis

Quantification of IL-1β and IL-6 was performed on cell monolayer supernatants using Human ELISA Max Deluxe Sets (BioLegend, San Diego, CA, USA).

3/2.7. Western Blots

Caco-2 cells and THP-1 cells were lysed in 300 µL of 25 mM MOPS pH 7.4, 150 mM NaCl, 1% Triton, 1 mM PMSF, 2 µM leupeptin and pepstatin in ice for 1 h. Total protein content was quantified by Bradford assay. An amount of 20 µg of total protein, in SDS sample buffer containing DTT, was heat-treated (except for Fpn (Tsuji 2020)) and loaded onto SDS-PAGE. For Western blot analysis, the following primary antibodies were employed: monoclonal anti-TfR1 (anti-TfR) (sc-32272, Santa Cruz, CA, USA) (1:5000), monoclonal anti-Fpn 31A5, (Amgen) (1:10,000), polyclonal anti-Ftn (sc25617, Santa Cruz, CA, USA) (1:10,000), polyclonal anti-HCP (A0031, Dako, Santa Clara, CA, USA) (1:10,000), anti-hephaestin (sc-365365, Santa Cruz, CA, USA) (1:10,000), anti-DMT-1 (sc-166884, Santa Cruz, CA, USA) (1:10,000) and monoclonal anti-actin (sc1616, Santa Cruz, CA, USA) (1:10,000). After incubation with the appropriate secondary horseradish peroxidase-conjugated antibody, blots were developed with Enhanced Chemi Luminescence (ECL Prime) (GE Healthcare, UK). Protein levels were normalized on actin by densitometry analysis, performed with ImageJ.

3/2.8. Statistical Analysis

For fusion experiments, Western blots and ELISA assays, statistically significant differences were assessed by one-way ANOVA and the post-hoc Tukey test. All statistical analyses were run using Prism v7 software (GraphPad Software, San Diego, CA, USA). Results were expressed as mean ± standard deviation (SD) of three independent experiments. A p-value ≤ 0.05 was considered statistically significant.

4/2. Results

4/2.1. Antiviral activity of bLf and hLf

The efficacy of bLf and hLf at different concentrations (1.25 and 6.25 μM, corresponding to 100 and 500 μg/mL respectively) in inhibiting SARS-CoV-2 Spike Pseudovirus fusion was examined firstly on Vero E6 cells, an epithelial cell line extensively employed in studies of SARS-CoV-2, according to the experimental scheme described in Materials and Methods.

Lf concentrations of 1.25 μM and 6.25μM were chosen based on published data in the literature. Specifically, the lower concentration is usually used for anti-inflammatory studies (Elass et al., 2002; Hwang et al., 2007; Inubushi et al., 2012), while the higher concentration is used to evaluate the antiviral activity of Lf (Campione et al., 2021; Mirabelli et al., 2021; Hasegawaet al., 1994; Oda et al., 2021; Wotring et al., 2022). Although in inflamed/infected sites the Lf concentration can rise around 1.25-2.5 μM (Bennett and Mohla 1976), it is still necessary to add exogenous Lf for effective antiviral activity. Preincubation of reagents allows discrimination of the mechanism of action, based on the order of addition, and makes the effect independent from the kinetics of interaction. BLf shows a dose-dependent inhibition of pseudoviral fusion under all experimental conditions compared with control, especially when bLf was preincubated with pseudovirus and when this glycoprotein was added at the time of infection (Fig. 23**a**, **b**). HLf induces, at both concentrations, a significant inhibition of pseudoviral entry into Vero E6 cells under all experimental conditions (Fig. 23**c**, **d**), even if its effect is milder than that exerted by bLf.

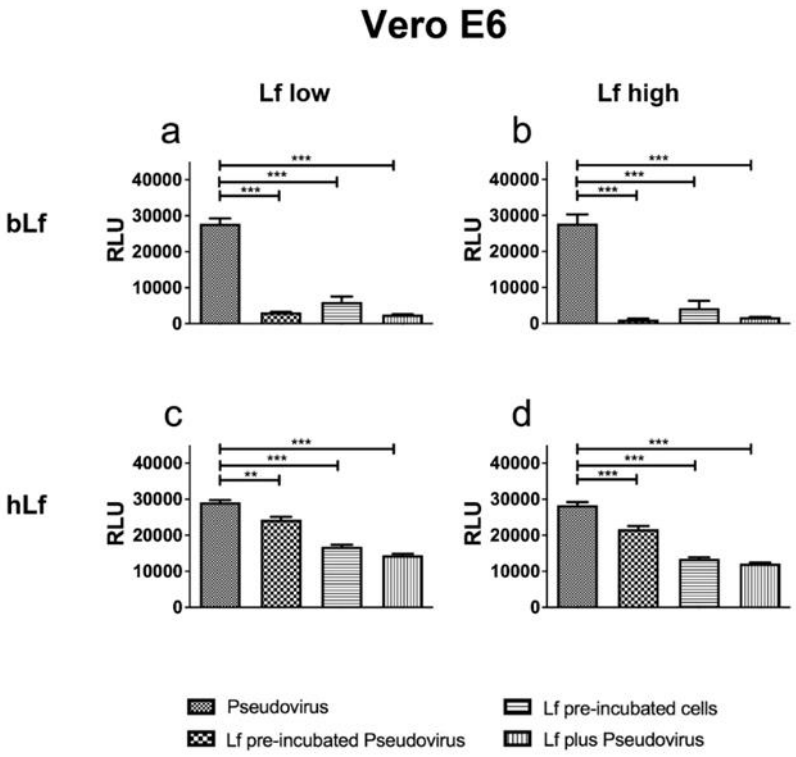

Figure 23. Luminescence of Pseudovirus observed in Vero E6 cells infected at multiplicity of infection (MOI) of 10 in the presence or absence of 1.25 (**a,c**) or 6.25 μM (**b,d**) of bovine lactoferrin (bLf) (**a,b**) or human lactoferrin (hLf) (**c,d**). See text for details. Data represent the mean values of three independent experiments. Error bars: standard error of the mean. Statistical significance is indicated as follows: **: $p < 0.01$; ***: $p < 0.001$ (one-way ANOVA with post-hoc Tukey test). RLU = Relative Luminescence Units.

To verify that Lf is also effective on a cell line heavily targeted by the virus, experiments were conducted using the highest concentration of bLf and hLf on human 16HBE14o$^-$derived bronchial epithelial cells. As shown in Figure 24, both forms are efficient in preventing pseudoviral fusion, but bLf is more efficient in the condition in which it is preincubated with pseudovirus (Fig. 24**a**, **b**). Lf activity was also evaluated on intestinal Caco-2 epithelial cells which mimic intestinal absorption of Lf and are also involved in iron homeostasis. The results obtained (Fig. 24**c**, **d**) are comparable to previous ones, in which bLf (Fig. 24**c**) was more effective than hLf (Fig. 24**d**) in counteracting pseudovirus fusion. Similar results are obtained on THP-1 cells (Fig. 24**e**, **f**).

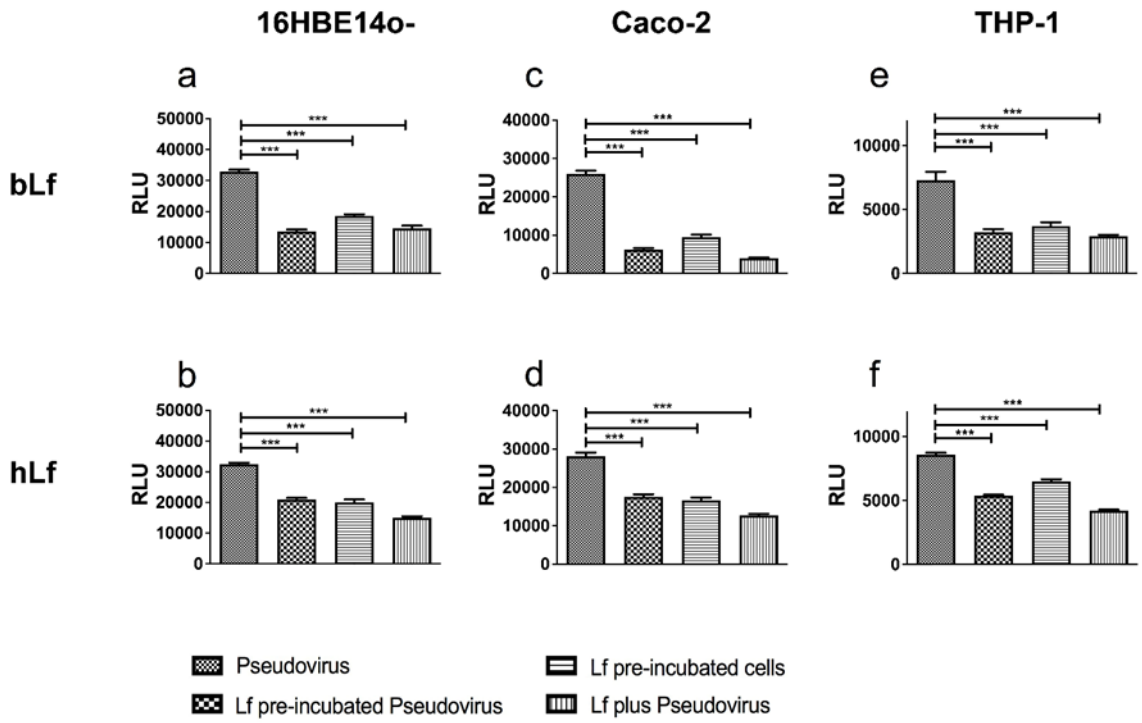

Figure 24. Luminescence of Pseudovirus observed in 16HBE14o- (**a,b**), Caco-2 (**c,d**) and THP-1 (**e,f**) cells infected at multiplicity of infection (MOI) of 10 in the presence or absence of 6.25 μM of bovine lactoferrin (bLf) (**a,c,e**) or human lactoferrin (hLf) (**b,d,f**). See text for details. Data represent the mean values of three independent experiments. Error bars: standard error of the mean. Statistical significance is indicated as follows: ***: $p < 0.001$ (one-way ANOVA with post-hoc Tukey test). RLU = Relative Luminescence Units.

bLf and hLf binding to SARS-CoV-2 Spike glycoprotein

To demonstrate the effective binding between bLf/ hLf and the SARS-CoV-2 Spike, an in vitro pull-down assay was performed (Fig. 25). For this purpose, unconjugated Sepharose 6B resins conjugated with bLf, hLf and hTf were incubated with full length trimeric Spike or its S1 domain. The resin conjugated with hTf was employed as a control of binding specificity, since Tfs belongs to the same family of Lfs. As shown in Figure 25**a**, an immunoreactive band around 250 kDa, corresponding to the monomeric form of the Spike glycoprotein, is recorded in the eluted SDS fractions of the resins conjugated with bLf and hLf. No reactive bands are recorded for both unconjugated and hTf-conjugated resins, thus demonstrating the specificity of binding between Spike and bLf/hLf. Interestingly, the S1 domain alone is not sufficient to allow binding between Lfs and Spike (Fig. 25**b**). With this assay, it is shown that bLf is able to bind to the Spike glycoprotein and that this interaction depends on its oligomerization state.

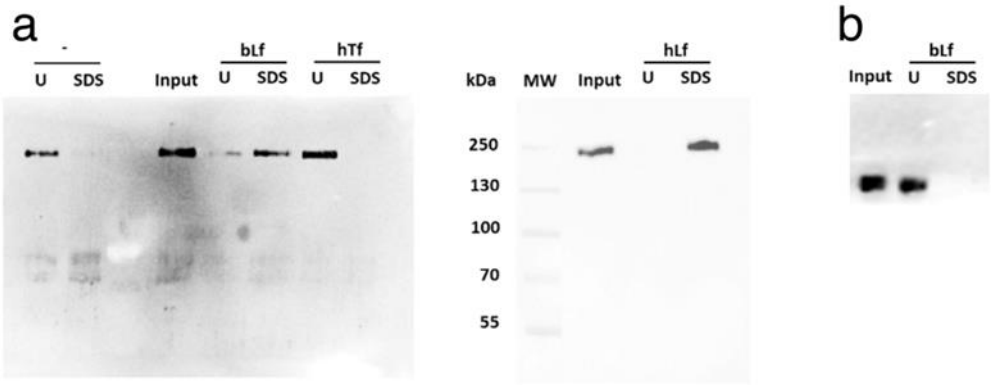

Figure 25. Sepharose 6B pull down of full-length stabilized trimeric (**a**) and S1 domain (**b**) SARS-CoV-2 Spike. Unconjugated (-), bovine Lactoferrin (bLf)-, human Lactoferrin (hLf)- and human Transferrin (hTf)-conjugated Sepharose 6B resins were employed. Input, unbound (U) and SDS eluted fractions were analyzed through Western blot.

bLf counteracts inflammatory and iron homeostasis disorders induced by the glycoprotein Spike

To investigate the role of the SARS-CoV-2 Spike on inflammatory and iron disorders and the potential protective effect of bLf, the expression of key iron management proteins and interleukins was evaluated in in vitro models of both macrophages and enterocytes. For this purpose, THP-1 and Caco-2 cells were untreated or treated with 20 nM full-length SARS-CoV-2 glycoprotein Spike in the absence or presence of 1.25μM bLf, according to the experimental scheme described in Materials and Methods. For this study, the experiments were performed only with bLf, which was more efficient in antiviral activity as described previously. BLf shares functions with hLf although it has greater commercial availability, making it a better candidate for in vitro, in vivo, and even clinical studies.

Regarding THP-1 cells, Spike stimulation induces a significant down-regulation of the iron exporter Fpn, whereas a significant up-regulation of both TfR1 and membrane-bound Cp is observed compared with untreated cells. BLf is able to counteract Spike-induced iron dysregulation under all experimental conditions tested, hindering the Fpn down-regulation and both Cp and TfR1 increase (Fig. **26b**, **c**, **d**). Notably, no modulation of Ftn is detected following Spike stimulation (Fig. 26**e**). In addition to iron management proteins, the expression of IL-1β and IL-6, the main cytokines involved in iron disorders, was tested under the same experimental conditions. As shown in Figure 26**f**, Spike treatment induces a significant up-regulation of both IL-1β and IL-6, with bLf contrasting such an increase in all experimental conditions, reaching significant values for both interleukins when pre-incubated with the Spike glycoprotein and, only for IL-6, when pre-incubated with cells.

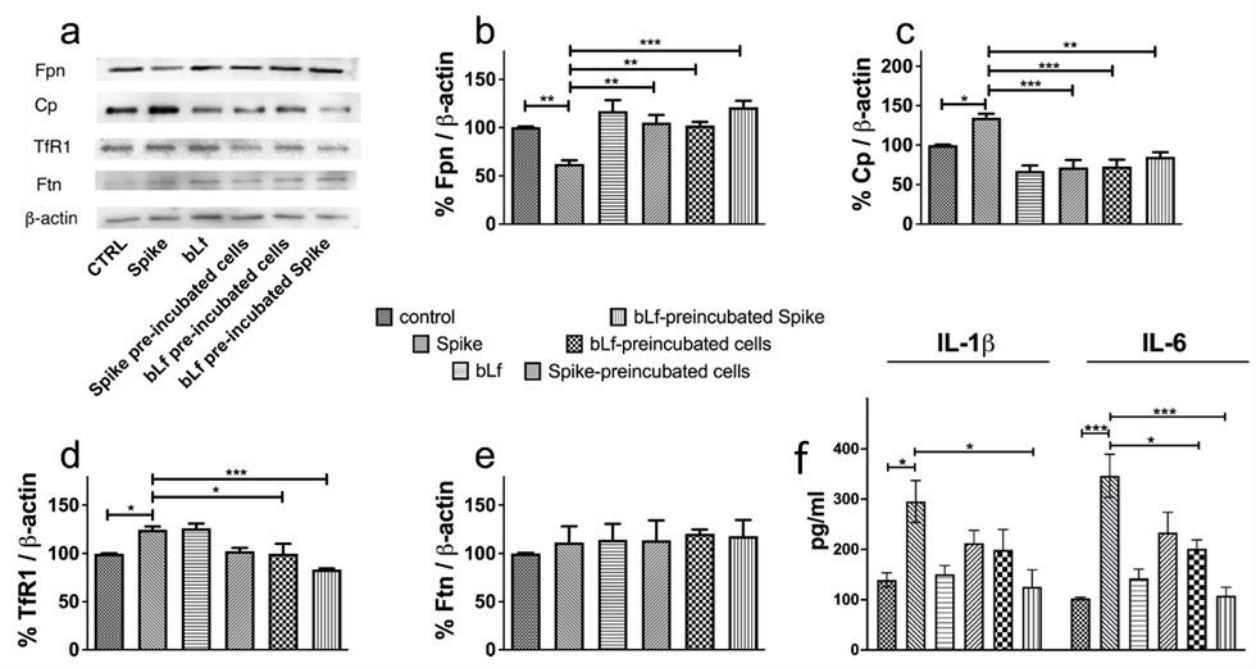

Figure 26. Protective effect of bovine lactoferrin (bLf) against iron and inflammatory disorders induced by SARS-CoV-2 Spike glycoprotein on THP-1 cells. Western blot (**a**) and densitometry analysis of ferroportin (Fpn) (**b**), membrane-bound ceruloplasmin (Cp) (**c**), transferrin receptor 1 (TfR1) (**d**) and ferritin (Ftn) (**e**) levels and ELISA quantitation of IL-1β and IL-6 production (**f**) in THP-1 cells untreated or treated with 20 nM Spike glycoprotein in the absence or presence of 1.25 μM bLf. See text for details. Error bars: standard error of the mean. Statistical significance is indicated as follows: *: $p < 0.05$; **: $p < 0.01$; ***: $p < 0.001$ (one-way ANOVA with post-hoc Tukey test).

As Caco-2 cells are concerned, Spike treatment significantly reduces Fpn, Heph and DMT-1 (Fig. 27**b**, **c**, **e**), while no significant effect is recorded for TfR1 and Ftn (Fig. 27**d**, **f**). Again, bLf is able to significantly counteract iron dysregulation when it is pre-incubated with the Spike glycoprotein for Fpn, Heph and DMT-1, indicating that the two proteins interact. Significant levels for Fpn and Heph are achieved when bLf was pre-incubated with the cells, and for Heph and DMT-1 when bLf was added one hour after stimulation with Spike. The latter result indicates that bLf can revert the effects even after they are triggered by Spike. No significant effect of bLf on the expression of TfR1 and Ftn is observed. Of note, no detectable levels of IL-1β and IL-6 are recorded under both basal and Spike/bLf-stimulated conditions.

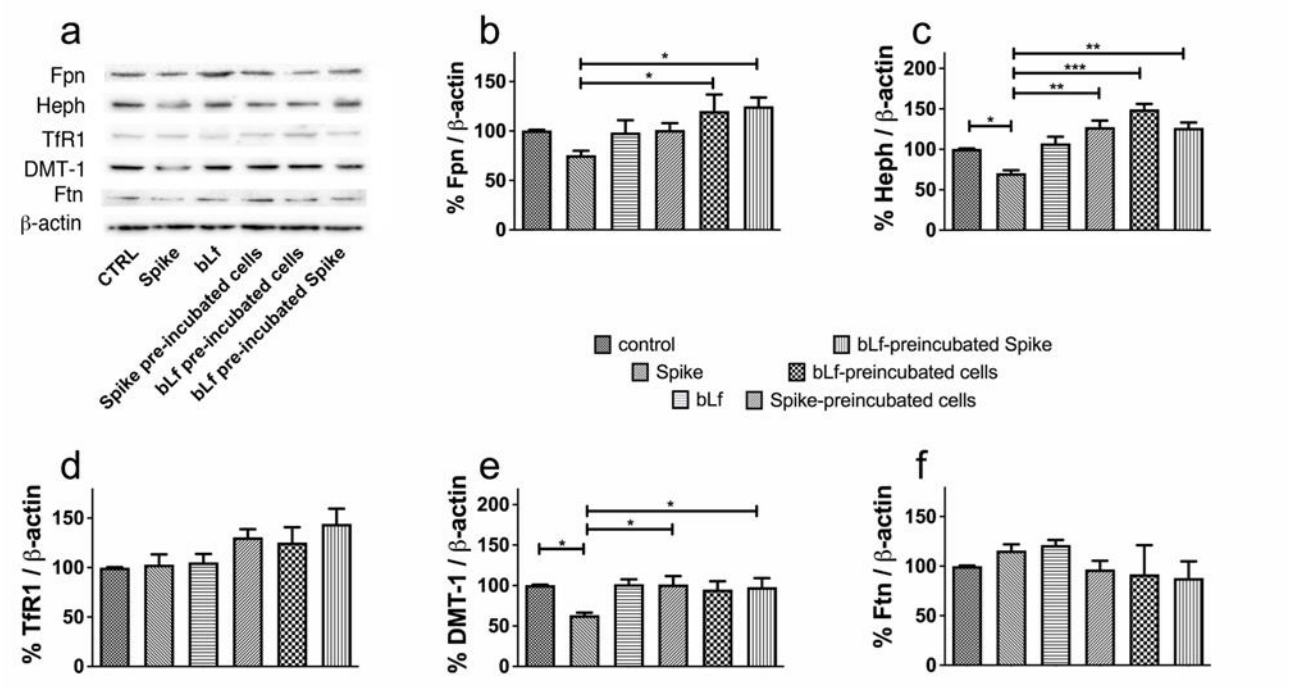

Figure 2. Protective effect of bovine lactoferrin (bLf) against iron and inflammatory disorders induced by SARS-CoV-2 Spike glycoprotein on Caco-2 cells. Western blot (panel (**a**) and densitometry analysis of ferroportin (Fpn) (**b**), hephaestin (Heph) (**c**), transferrin receptor 1 (TfR1) (**d**), DMT-1 (**e**) and ferritin (Ftn) (**f**) levels in Caco-2 cells untreated or treated with 20 nM Spike glycoprotein in the absence or presence of 1.25 μM bLf. See text for details. Error bars: standard error of the mean. Statistical significance is indicated as follows: *: $p < 0.05$; **: $p < 0.01$; ***: $p < 0.001$ (one-way ANOVA with post-hoc Tukey test).

4/2.4. TfR1 as a secondary gate for SARS-CoV-2 Spike Pseudovirus

As mentioned above, it has been reported that SARS-CoV-2 exploits several cell surface receptors for its entry, including TfR1 (Tang et al., 2020). To explore the possible contribution of TfR1 in promoting the entry of SARS-CoV-2 on novel models, the neutralization assay was done on bronchial and intestinal epithelial cells and a macrophage cell line in the presence of a monoclonal antibody that recognizes ectodomains of human TfR1 or a soluble form of TfR1. Both significantly reduce pseudoviral fusion in all three cell lines (Fig. 28), although the most prominent effect is seen with soluble TfR1 in 16HBE14o- respiratory cells (Fig. 28 **a**).

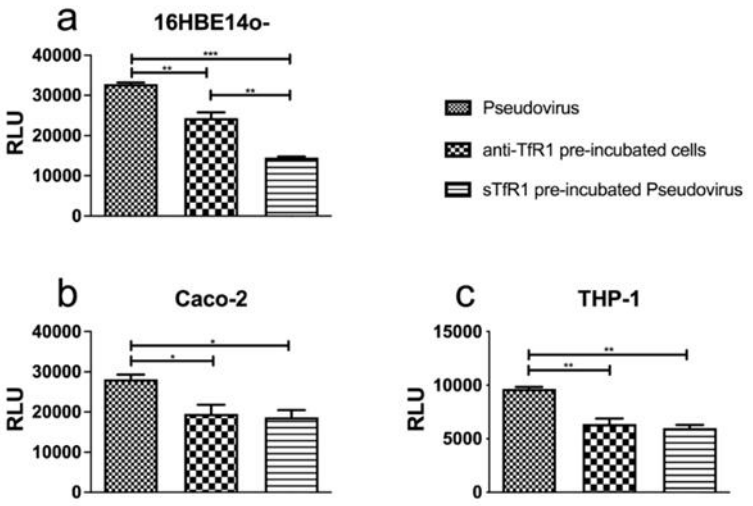

Figure 28. Luminescence of Pseudovirus observed in in 16HBE14o- (**a**), Caco-2 (**b**) and THP-1 (**c**) cells infected at multiplicity of infection (MOI) of 10 in the presence or absence of 200 nM monoclonal antibody recognizing the ectodomains of human transferrin receptor 1 (TfR1) (anti-TfR1) or 200 nM soluble human TfR1 (sTfR1). See text for details. Data represent the mean values of three independent experiments. Error bars: standard error of the mean. Statistical significance is indicated as follows: *: $p < 0.05$; **: $p < 0.01$; ***: $p < 0.001$ (one-way ANOVA with post-hoc Tukey test). RLU = Relative Luminescence Units.

5/2. Discussion

Structural glycoprotein Spike, which decorates the surface of virions, is an essential target for the development of therapies and vaccines. SARS-CoV and SARS-CoV-2 have 79% genomic identity associated with similar structural and pathogenic features (Tang et al., 2020). However, both viruses show significant differences in their ability to infect humans. Although the Spike glycoprotein of both viruses share about 75% amino acid identity in the RBD domain, the presence of new insertions and deletions in the Spike of SARS-CoV-2 resulted in a gain of function by enhancing virus transmission. For instance, the binding affinity to the ACE2 receptor is 10-20 times higher in SARS-CoV-2 (Saadi et al., 2021). Spike is emerging as the major virulence factor capable of triggering the immunopathological response (Saadi et al., 2021). The extent of such response underlies the viral spread as well as the outcome and severity of the disease. For this reason, many studies aimed at finding an effective therapy, target the inhibition of Spike activity, including possible molecules capable of interacting with it.

Results obtained in silico from Campione group (Campione et al., 2021) showed a direct interaction between Lf and Spike glycoprotein. In this work, the interaction between Lf and Spike of SARS-CoV-2 was experimentally demonstrated. The antiviral activity of Lf was demonstrated by a neutralization assay of bLf and hLf against Spike-decorated pseudoviruses. Both Lf are able to perform this function in all three cell lines analyzed, with little difference depending on the concentration used. However, bLf exerts a more effective action than hLf, particularly when bLf and pseudovirus are added together, with or without pre-incubation of the same. This is a good indication that bLf thorough the interaction with Spike could block virus entry. BLf, by competing with Spike-mediated binding to the host cell receptor, would exert its action with an efficacy depending on the type of receptors expressed on the cell surface.

Until now, the effectiveness of Lf in inhibiting SARS-CoV-2 entry was attributed to its ability to prevent virus binding to HSPG membrane receptors (Hu et al., 2021). Here, an in vitro pull-down assay allowed us to confirm the in-silico model (Campione et al. 2021) as well as demonstrate that Lfs can block SARS-CoV-2 entry via direct binding to Spike in the trimeric form.

Purified SARS-CoV and SARS-CoV-2 Spike glycoproteins are potent inducers of the inflammatory response. Spike of SARS-CoV promotes NF-kB activation and thereby the expression of pro-inflammatory cytokines such as IL-6 and IL-8 in peripheral blood monocyte macrophages and THP-1 (Dosch et al., 2009). Similarly, SARS-CoV-2 Spike activates the NF-kB AP-1/c-Fos pathway and thus the production of IL-6 in epithelial cells (Patra et al., 2020). Activation of pro-inflammatory pathways can modulate iron protein expression, leading to a decrease in Fpn (Ginzburg 2019) and increase in TfR1 (Tacchini et al., 2008).

Iron is involved in numerous biological processes that make it indispensable. High metal levels have been found in several disease states associated with inflammation (Kernan and Carcillo 2017), as well as viral infections (Hsu et al., 2022). Iron is not only required for viral spreading, being involved in processes such as dNTP biosynthesis, reverse transcription, translation, and viral assembly (Schmidt et al., 2020; Sienkiewicz et al., 2022), but also in ROS production and NF-kB activation (Xiong et al., 2003).

In this research work, it was shown that Spike can induce alteration of key proteins involved in iron metabolism in both macrophage and intestinal epithelial cell lines. Down regulation of Fpn was observed in both cell lines, indicating a phenotype of intracellular iron accumulation. To support this hypothesis, down regulation of DMT-1 and Heph in enterocytes as well as upregulation of TfR1 in macrophages was also detected. The observed changes are in line with previous in vitro (Recalcati et al., 2010; Cutone et al., 2017) and in vivo (Liu et al., 2005; Willemetz et al., 2017) studies in which decreased Fpn expression has been reported in inflammatory states. Such modulation is often accompanied by elevated production of pro-inflammatory cytokines such as IL-1β and IL-6 (Lepanto et al., 2018).

Spike stimulation also led to upregulation of Cp and downregulation of Heph in enterocytes. This different modulation of Fpn partners must consider that Cp exerts not only ferrosidase activity, but also copper transport, antioxidant activity, and amine oxidation (Bonaccorsi et al., 2018). Cp is defined as an acute phase protein, the expression of which can be induced by TNF-α in alveolar macrophages (Tisato et al., 2018), by IFN-γ in monocytic cell lines (Mazumder et al., 1997) as well as by stimulation with IL-1β in glial cells (Persichini et al., 2010). As for TfR1, its significant up-regulation in THP-1 cells after Spike treatment is consistent with other studies reporting increased expression during the acute phase response (Tacchini et al., 2008; Malik et al., 2011). Despite its role in iron uptake, TfR1 is also hijacked by numerous viruses to enter the cell (Mancinelli et al., 2020), and SARS-CoV-2 appears to be no exception (Tang et al., 2020). The observed modulation of Fpn partners is in line with a pro-inflammatory response in macrophages and enterocytes respectively, as already reported in some studies (Sheikh et al., 2007; Bergamaschi et al., 2017).

Following stimulation with Spike, an increase in TfR1 is observed in THP-1, in agreement with a previously observed acute phase response (Tacchini et al., 2008; Malik et al., 2011). Of note, TfR1 is used by many viruses for its own entry, including SARS-CoV-2 (Tang et al., 2020). While the role of TfR1 may be to promote iron entry and ensure viral replication, the data obtained in this study confirm that TfR1 contributes to Spike-mediated fusion on epithelial and macrophage cells.

However, intracellular Ftn does not appear to be modulated in any of our models. Hepatocytes, macrophages, and Kupffer cells have been shown to secrete Ftn (Wesselius et al., 1994); in particular,

administration of IL-1β or TNF-α in differentiated rat hepatoma cells doubled the amount of ferritin released into the culture medium, but did not affect intracellular levels (Tran et al., 1997). In patients with COVID-19, serum Ftn levels increase as the disease progresses, prognosis is worse when levels are higher (Mehta et al., 2020; Phua et al., 2020). Our data demonstrated that bLf counteracts the dysregulation of iron metabolism proteins, but it also downregulated IL-6 production.

Overall, we showed that i) Lf competes with binding to surface receptors when incubated with cell monolayer or Spike; ii) Lf can block pathogenesis by binding directly to Spike; iv) bLf can restore physiological balance by counteracting iron disorders and inflammation. The bLf efficacy as regulator of iron homeostasis has been reported in several inflamed/infected models in vitro (Cutone et al., 2017; Frioni et al., 2014) and in vivo (Cutone et al., 2019), as well as in clinical studies (Lepanto et al., 2018). During viral infection, Lf, by chelating free iron, may act on iron disorders and consequently potentiate antioxidant response of the host as well downregulate pro-inflammatory cytokines, such as IL-1β and IL-6. Taken together, our findings support the results of preliminary clinical studies where, Lf treatment reduces time of SARS-CoV-2 RNA negativization (Rosa et al., 2021; Campione et al., 2021), recovery of clinical symptoms as well as serum levels of IL-6, Ftn and D-dimer (Campione et al., 2021).

In conclusion, the results provide evidence for an effective link between Lf and Spike, which interferes with Spike-mediated pseudovirus fusion and Spike-triggered iron disorders (Fig. 29). These results give hope for the use of Lf as an adjuvant to current therapies in patients with COVID-19, however, the in vivo efficacy is yet to be evaluated.

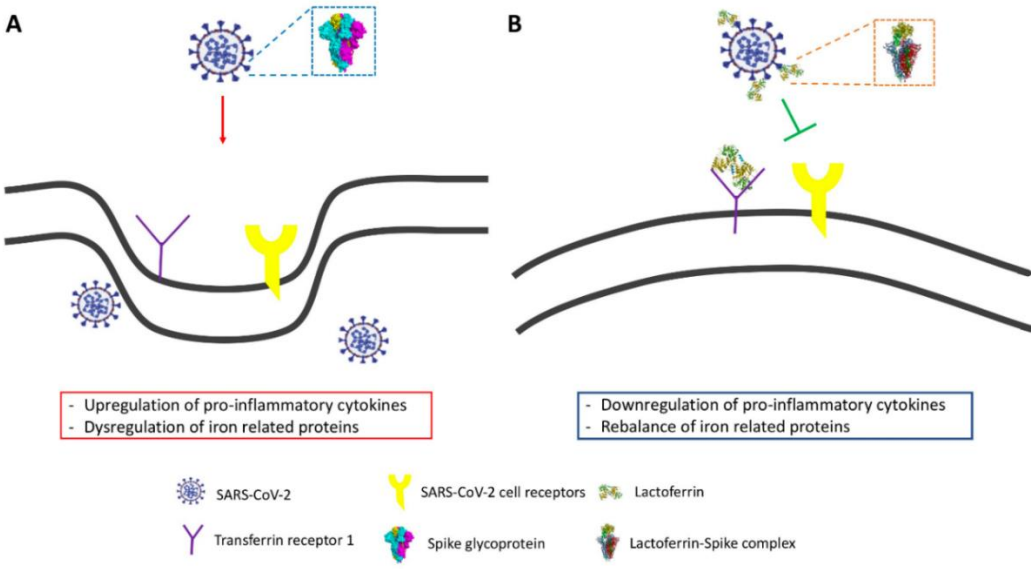

Figure 29. Schematic representation of viral infections in absence (**A**) and presence of Lf (**B**). **A**) Upon SARS-CoV-2 infections, the binding between Spike and SARS-CoV-2 receptors as well TfR1 allows viral particles internalization into the host cell, thus enhancing the upregulation of pro-inflammatory cytokines and dysregulation of iron related proteins; **B**) The binding between Lf and Spike affects with Spike-mediated pseudoviral entry and Spike-induced iron dysregulation.

6. CONCLUSIONS

Increased virus infectivity, transmissibility, disease severity and the development of immunity against infection are mediated by structural and non-structural viral proteins. The latter have emerged as crucial molecules in infection-associated disorders. Tat of HIV-1 and Spike of SARS-CoV-2 have been described as a neurotoxin and virulence factor, respectively. Both can induce an inflammatory response associated with oxidative stress and iron disorders. Therefore, current treatment requires a novel approach to counteract these negative effects.

This study showed that Lf, as a multifunctional protein, can both prevent viral infection at an early stage by blocking virus entry, and counteract viral protein-induced disturbances by restoring physiological-like conditions. Nat-Lf has been shown to counteract iron dysregulation by improving iron recycling from cells, increasing iron release, and reducing iron uptake in cells subjected to Tat and Spike. In addition, the Native form reduces the production of pro-inflammatory cytokines, thus showing an overall protective effect. On the other hand, the iron-saturated form would appear to have some functions shared with the Native, such as antioxidant activity, and some divergent ones that cannot be underestimated. Holo-Lf transports iron and is more stable than the unsaturated forms and this could diversify the cellular response over time, explaining the differential effects observed. These results highlight a current problem with commercial preparations of Lf. There is great variability and discrepancy between Lf products and the associated effects, precisely because the physico-chemical parameters, including iron saturation, are only partially characterized. Quality control is therefore necessary prior to Lf treatment for in vitro and in vivo experiments and for dietary supplementation. In addition, natural compounds are emerging as a promising alternative or support to treatment.

In this context, Lf, as a natural glycoprotein, has been proposed as an adjuvant to antiviral treatments. Current therapies for HIV-1 and SARS-CoV-2 do not suppress the expression of viral proteins and their negative effects. In this regard, the present research work highlights the importance of Lf as a novel and effective therapeutic strategy to restore iron and inflammatory disorders induced by viral proteins.

7. REFERENCES

1. Abbott, N. J. Astrocyte-Endothelial Interactions and Blood-Brain Barrier Permeability. *J Anat* 2002, 200 (6), 629–638. https://doi.org/10.1046/j.1469-7580.2002.00064.x.
2. Armitage, A. E.; Stacey, A. R.; Giannoulatou, E.; Marshall, E.; Sturges, P.; Chatha, K.; Smith, N. M. G.; Huang, X.; Xu, X.; Pasricha, S.-R.; Li, N.; Wu, H.; Webster, C.; Prentice, A. M.; Pellegrino, P.; Williams, I.; Norris, P. J.; Drakesmith, H.; Borrow, P. Distinct Patterns of Hepcidin and Iron Regulation during HIV-1, HBV, and HCV Infections. *Proc Natl Acad Sci U S A* **2014**, *111* (33), 12187–12192. https://doi.org/10.1073/pnas.1402351111.
3. Albar, A. H.; Almehdar, H. A.; Uversky, V. N.; Redwan, E. M. Structural Heterogeneity and Multifunctionality of Lactoferrin. *Curr Protein Pept Sci* **2014**, *15* (8), 778–797. https://doi.org/10.2174/1389203715666140919124530.
4. Alexaki, A.; Liu, Y.; Wigdahl, B. Cellular Reservoirs of HIV-1 and Their Role in Viral Persistence. *Curr HIV Res* **2008**, *6* (5), 388–400. https://doi.org/10.2174/157016208785861195.
5. Alexander, D. B.; Iigo, M.; Yamauchi, K.; Suzui, M.; Tsuda, H. Lactoferrin: An Alternative View of Its Role in Human Biological Fluids. *Biochem Cell Biol* **2012**, *90* (3), 279–306. https://doi.org/10.1139/o2012-013.
6. Al-Refaei, M. A.; Makki, R. M.; Ali, H. M. Structure Prediction of Transferrin Receptor Protein 1 (TfR1) by Homology Modelling, Docking, and Molecular Dynamics Simulation Studies. *Heliyon* **2020**, *6* (1), e03221. https://doi.org/10.1016/j.heliyon.2020.e03221.
7. Alvarez-Carbonell, D.; Ye, F.; Ramanath, N.; Dobrowolski, C.; Karn, J. The Glucocorticoid Receptor Is a Critical Regulator of HIV Latency in Human Microglial Cells. *J Neuroimmune Pharmacol* **2019**, *14* (1), 94–109. https://doi.org/10.1007/s11481-018-9798-1.
8. Andersen, H. H.; Johnsen, K. B.; Moos, T. Iron Deposits in the Chronically Inflamed Central Nervous System and Contributes to Neurodegeneration. *Cell Mol Life Sci* **2014**, *71* (9), 1607–1622. https://doi.org/10.1007/s00018-013-1509-8.
9. Anderson, B. F.; Baker, H. M.; Norris, G. E.; Rumball, S. V.; Baker, E. N. Apolactoferrin Structure Demonstrates Ligand-Induced Conformational Change in Transferrins. *Nature* **1990**, *344* (6268), 784–787. https://doi.org/10.1038/344784a0.
10. Anderson, G. J.; Frazer, D. M.; McKie, A. T.; Vulpe, C. D.; Smith, A. Mechanisms of Haem and Non-Haem Iron Absorption: Lessons from Inherited Disorders of Iron Metabolism. *Biometals* **2005**, *18* (4), 339–348. https://doi.org/10.1007/s10534-005-3708-8.

11. Anderson, C. P.; Shen, M.; Eisenstein, R. S.; Leibold, E. A. Mammalian Iron Metabolism and Its Control by Iron Regulatory Proteins. *Biochim Biophys Acta* **2012**, *1823* (9), 1468–1483. https://doi.org/10.1016/j.bbamcr.2012.05.010.
12. Anderson, G. J.; Frazer, D. M. Current Understanding of Iron Homeostasis. *Am J Clin Nutr* **2017**, *106* (Suppl 6), 1559S-1566S. https://doi.org/10.3945/ajcn.117.155804.
13. András, I. E.; Toborek, M. HIV-1-Induced Alterations of Claudin-5 Expression at the Blood-Brain Barrier Level. *Methods Mol Biol* **2011**, *762*, 355–370. https://doi.org/10.1007/978-1-61779-185-7_26.
14. Andrews, N. C. Disorders of Iron Metabolism. *N Engl J Med* **1999**, *341* (26), 1986–1995. https://doi.org/10.1056/NEJM199912233412607.
15. Andrews, N. C. Iron Metabolism: Iron Deficiency and Iron Overload. *Annu Rev Genomics Hum Genet* **2000**, *1*, 75–98. https://doi.org/10.1146/annurev.genom.1.1.75.
16. Appay, V.; Sauce, D. Immune Activation and Inflammation in HIV-1 Infection: Causes and Consequences. *J Pathol* **2008**, *214* (2), 231–241. https://doi.org/10.1002/path.2276.
17. Appelmelk, B. J.; An, Y. Q.; Geerts, M.; Thijs, B. G.; de Boer, H. A.; MacLaren, D. M.; de Graaff, J.; Nuijens, J. H. Lactoferrin Is a Lipid A-Binding Protein. *Infect Immun* **1994**, *62* (6), 2628–2632. https://doi.org/10.1128/iai.62.6.2628-2632.1994.
18. Araújo-Pereira, M.; Barreto-Duarte, B.; Arriaga, M. B.; Musselwhite, L. W.; Vinhaes, C. L.; Belaunzaran-Zamudio, P. F.; Rupert, A.; Montaner, L. J.; Lederman, M. M.; Sereti, I.; Madero, J. G. S.; Andrade, B. B. Relationship Between Anemia and Systemic Inflammation in People Living With HIV and Tuberculosis: A Sub-Analysis of the CADIRIS Clinical Trial. *Frontiers in Immunology* **2022**, *13*.
19. Arias, M.; Hilchie, A. L.; Haney, E. F.; Bolscher, J. G. M.; Hyndman, M. E.; Hancock, R. E. W.; Vogel, H. J. Anticancer Activities of Bovine and Human Lactoferricin-Derived Peptides. *Biochem Cell Biol* **2017**, *95* (1), 91–98. https://doi.org/10.1139/bcb-2016-0175.
20. Armitage, A. E.; Stacey, A. R.; Giannoulatou, E.; Marshall, E.; Sturges, P.; Chatha, K.; Smith, N. M. G.; Huang, X.; Xu, X.; Pasricha, S.-R.; Li, N.; Wu, H.; Webster, C.; Prentice, A. M.; Pellegrino, P.; Williams, I.; Norris, P. J.; Drakesmith, H.; Borrow, P. Distinct Patterns of Hepcidin and Iron Regulation during HIV-1, HBV, and HCV Infections. *Proc Natl Acad Sci U S A* **2014**, *111* (33), 12187–12192. https://doi.org/10.1073/pnas.1402351111.
21. Aschemeyer, S.; Qiao, B.; Stefanova, D.; Valore, E. V.; Sek, A. C.; Ruwe, T. A.; Vieth, K. R.; Jung, G.; Casu, C.; Rivella, S.; Jormakka, M.; Mackenzie, B.; Ganz, T.; Nemeth, E. Structure-Function Analysis of Ferroportin Defines the Binding Site and an Alternative Mechanism of

Action of Hepcidin. *Blood* **2018**, *131* (8), 899–910. https://doi.org/10.1182/blood-2017-05-786590.

22. Asensio, V. C.; Campbell, I. L. Chemokines and Viral Diseases of the Central Nervous System. *Adv Virus Res* **2001**, *56*, 127–173. https://doi.org/10.1016/s0065-3527(01)56006-6.
23. Ashida, K.; Sasaki, H.; Suzuki, Y. A.; Lönnerdal, B. Cellular Internalization of Lactoferrin in Intestinal Epithelial Cells. *Biometals* **2004**, *17* (3), 311–315. https://doi.org/10.1023/b:biom.0000027710.13543.3f.
24. Bagashev, A.; Sawaya, B. E. Roles and Functions of HIV-1 Tat Protein in the CNS: An Overview. *Virol J* **2013**, *10*, 358. https://doi.org/10.1186/1743-422X-10-358.
25. Baker, H. M.; Mason, A. B.; He, Q. Y.; MacGillivray, R. T.; Baker, E. N. Ligand Variation in the Transferrin Family: The Crystal Structure of the H249Q Mutant of the Human Transferrin N-Lobe as a Model for Iron Binding in Insect Transferrins. *Biochemistry* **2001**, *40* (39), 11670–11675. https://doi.org/10.1021/bi010907p.
26. Baker, H. M.; Baker, E. N. Lactoferrin and Iron: Structural and Dynamic Aspects of Binding and Release. *Biometals* **2004**, *17* (3), 209–216. https://doi.org/10.1023/b:biom.0000027694.40260.70.
27. Baker, S. J.; Rane, S. G.; Reddy, E. P. Hematopoietic Cytokine Receptor Signaling. *Oncogene* **2007**, *26* (47), 6724–6737. https://doi.org/10.1038/sj.onc.1210757.
28. Balakrishna Pillai, A.; JeanPierre, A. R.; Mariappan, V.; Ranganadin, P.; S R, R. Neutralizing the Free Radicals Could Alleviate the Disease Severity Following an Infection by Positive Strand RNA Viruses. *Cell Stress Chaperones* **2022**, *27* (3), 189–195. https://doi.org/10.1007/s12192-022-01269-x.
29. Banchini, F.; Cattaneo, G. M.; Capelli, P. Serum Ferritin Levels in Inflammation: A Retrospective Comparative Analysis between COVID-19 and Emergency Surgical Non-COVID-19 Patients. *World J Emerg Surg* **2021**, *16* (1), 9. https://doi.org/10.1186/s13017-021-00354-3.
30. Banks, W. A.; Robinson, S. M.; Nath, A. Permeability of the Blood-Brain Barrier to HIV-1 Tat. *Exp Neurol* **2005**, *193* (1), 218–227. https://doi.org/10.1016/j.expneurol.2004.11.019.
31. Bansal, A. K.; Mactutus, C. F.; Nath, A.; Maragos, W.; Hauser, K. F.; Booze, R. M. Neurotoxicity of HIV-1 Proteins Gp120 and Tat in the Rat Striatum. *Brain Res* **2000**, *879* (1–2), 42–49. https://doi.org/10.1016/s0006-8993(00)02725-6.
32. Barillari, G.; Ensoli, B. Angiogenic Effects of Extracellular Human Immunodeficiency Virus Type 1 Tat Protein and Its Role in the Pathogenesis of AIDS-Associated Kaposi's Sarcoma. *Clin Microbiol Rev* **2002**, *15* (2), 310–326. https://doi.org/10.1128/CMR.15.2.310-326.2002.

33. Baveye, S.; Elass, E.; Fernig, D. G.; Blanquart, C.; Mazurier, J.; Legrand, D. Human Lactoferrin Interacts with Soluble CD14 and Inhibits Expression of Endothelial Adhesion Molecules, E-Selectin and ICAM-1, Induced by the CD14-Lipopolysaccharide Complex. *Infect Immun* **2000**, *68* (12), 6519–6525. https://doi.org/10.1128/IAI.68.12.6519-6525.2000.
34. Bayraktar, N.; Bayraktar, M.; Ozturk, A.; Ibrahim, B. Evaluation of the Relationship Between Aquaporin-1, Hepcidin, Zinc, Copper, and İron Levels and Oxidative Stress in the Serum of Critically Ill Patients with COVID-19. *Biol Trace Elem Res* **2022**, *200* (12), 5013–5021. https://doi.org/10.1007/s12011-022-03400-6.
35. Beljaars, L.; Bakker, H. I.; van der Strate, B. W. A.; Smit, C.; Duijvestijn, A. M.; Meijer, D. K. F.; Molema, G. The Antiviral Protein Human Lactoferrin Is Distributed in the Body to Cytomegalovirus (CMV) Infection-Prone Cells and Tissues. *Pharm Res* **2002**, *19* (1), 54–62. https://doi.org/10.1023/a:1013655315969.
36. Bennett, R. M.; Mohla, C. A Solid-Phase Radioimmunoassay for the Measurement of Lactoferrin in Human Plasma: Variations with Age, Sex, and Disease. *J Lab Clin Med* **1976**, *88* (1), 156–166.
37. Bergamaschi, G.; Di Sabatino, A.; Pasini, A.; Ubezio, C.; Costanzo, F.; Grataroli, D.; Masotti, M.; Alvisi, C.; Corazza, G. R. Intestinal Expression of Genes Implicated in Iron Absorption and Their Regulation by Hepcidin. *Clin Nutr* **2017**, *36* (5), 1427–1433. https://doi.org/10.1016/j.clnu.2016.09.021.
38. Bergamaschi, G.; Borrelli de Andreis, F.; Aronico, N.; Lenti, M. V.; Barteselli, C.; Merli, S.; Pellegrino, I.; Coppola, L.; Cremonte, E. M.; Croce, G.; Mordà, F.; Lapia, F.; Ferrari, S.; Ballesio, A.; Parodi, A.; Calabretta, F.; Ferrari, M. G.; Fumoso, F.; Gentile, A.; Melazzini, F.; Di Sabatino, A.; Internal Medicine Covid-19 Collaborators. Anemia in Patients with Covid-19: Pathogenesis and Clinical Significance. *Clin Exp Med* **2021**, *21* (2), 239–246. https://doi.org/10.1007/s10238-020-00679-4.
39. Berlutti, F.; Pantanella, F.; Natalizi, T.; Frioni, A.; Paesano, R.; Polimeni, A.; Valenti, P. Antiviral Properties of Lactoferrin--a Natural Immunity Molecule. *Molecules* **2011**, *16* (8), 6992–7018. https://doi.org/10.3390/molecules16086992.
40. Bethel-Brown, C.; Yao, H.; Callen, S.; Lee, Y. H.; Dash, P. K.; Kumar, A.; Buch, S. HIV-1 Tat-Mediated Induction of Platelet-Derived Growth Factor in Astrocytes: Role of Early Growth Response Gene 1. *J Immunol* **2011**, *186* (7), 4119–4129. https://doi.org/10.4049/jimmunol.1002235.
41. Billesbølle, C. B.; Azumaya, C. M.; Kretsch, R. C.; Powers, A. S.; Gonen, S.; Schneider, S.; Arvedson, T.; Dror, R. O.; Cheng, Y.; Manglik, A. Structure of Hepcidin-Bound Ferroportin

Reveals Iron Homeostatic Mechanisms. *Nature* **2020**, *586* (7831), 807–811. https://doi.org/10.1038/s41586-020-2668-z.

42. Bonaccorsi di Patti, M. C.; Polticelli, F.; Tortosa, V.; Furbetta, P. A.; Musci, G. A Bacterial Homologue of the Human Iron Exporter Ferroportin. *FEBS Lett* **2015**, *589* (24 Pt B), 3829–3835. https://doi.org/10.1016/j.febslet.2015.11.025.
43. Bonaccorsi di Patti, M. C.; Cutone, A.; Polticelli, F.; Rosa, L.; Lepanto, M. S.; Valenti, P.; Musci, G. The Ferroportin-Ceruloplasmin System and the Mammalian Iron Homeostasis Machine: Regulatory Pathways and the Role of Lactoferrin. *Biometals* **2018**, *31* (3), 399–414. https://doi.org/10.1007/s10534-018-0087-5.
44. Bragonzi, A.; Horati, H.; Kerrigan, L.; Lorè, N. I.; Scholte, B. J.; Weldon, S. Inflammation and Host-Pathogen Interaction: Cause and Consequence in Cystic Fibrosis Lung Disease. *J Cyst Fibros* **2018**, *17* (2S), S40–S45. https://doi.org/10.1016/j.jcf.2017.10.004.
45. Burckhardt, C. J.; Greber, U. F. Virus Movements on the Plasma Membrane Support Infection and Transmission between Cells. *PLoS Pathog* **2009**, *5* (11), e1000621. https://doi.org/10.1371/journal.ppat.1000621.
46. Cairo, G.; Bernuzzi, F.; Recalcati, S. A Precious Metal: Iron, an Essential Nutrient for All Cells. *Genes Nutr* **2006**, *1* (1), 25–39. https://doi.org/10.1007/BF02829934.
47. Campione, E.; Lanna, C.; Cosio, T.; Rosa, L.; Conte, M. P.; Iacovelli, F.; Romeo, A.; Falconi, M.; Del Vecchio, C.; Franchin, E.; Lia, M. S.; Minieri, M.; Chiaramonte, C.; Ciotti, M.; Nuccetelli, M.; Terrinoni, A.; Iannuzzi, I.; Coppeda, L.; Magrini, A.; Bernardini, S.; Sabatini, S.; Rosapepe, F.; Bartoletti, P. L.; Moricca, N.; Di Lorenzo, A.; Andreoni, M.; Sarmati, L.; Miani, A.; Piscitelli, P.; Valenti, P.; Bianchi, L. Lactoferrin Against SARS-CoV-2: In Vitro and In Silico Evidences. *Front Pharmacol* **2021**, *12*, 666600. https://doi.org/10.3389/fphar.2021.666600.
48. Campos-Escamilla, C. The Role of Transferrins and Iron-Related Proteins in Brain Iron Transport: Applications to Neurological Diseases. *Adv Protein Chem Struct Biol* **2021**, *123*, 133–162. https://doi.org/10.1016/bs.apcsb.2020.09.002.
49. Canali, S.; Zumbrennen-Bullough, K. B.; Core, A. B.; Wang, C.-Y.; Nairz, M.; Bouley, R.; Swirski, F. K.; Babitt, J. L. Endothelial Cells Produce Bone Morphogenetic Protein 6 Required for Iron Homeostasis in Mice. *Blood* **2017**, *129* (4), 405–414. https://doi.org/10.1182/blood-2016-06-721571.
50. Capone, C.; Cervelli, M.; Angelucci, E.; Colasanti, M.; Macone, A.; Mariottini, P.; Persichini, T. A Role for Spermine Oxidase as a Mediator of Reactive Oxygen Species Production in HIV-

Tat-Induced Neuronal Toxicity. *Free Radic Biol Med* **2013**, *63*, 99–107. https://doi.org/10.1016/j.freeradbiomed.2013.05.007.

51. Capone, G.; Calabrò, M.; Lucchese, G.; Fasano, C.; Girardi, B.; Polimeno, L.; Kanduc, D. Peptide Matching between Epstein-Barr Virus and Human Proteins. *Pathog Dis* **2013**, *69* (3), 205–212. https://doi.org/10.1111/2049-632X.12066.
52. Cappellini, M. D.; Musallam, K. M.; Taher, A. T. Iron Deficiency Anaemia Revisited. *J Intern Med* **2020**, *287* (2), 153–170. https://doi.org/10.1111/joim.13004.
53. Carpenter, C. E.; Mahoney, A. W. Contributions of Heme and Nonheme Iron to Human Nutrition. *Crit Rev Food Sci Nutr* **1992**, *31* (4), 333–367. https://doi.org/10.1080/10408399209527576.
54. Casanova, J.-L.; Abel, L. Mechanisms of Viral Inflammation and Disease in Humans. *Science* **2021**, *374* (6571), 1080–1086. https://doi.org/10.1126/science.abj7965.
55. Cassol, E.; Misra, V.; Dutta, A.; Morgello, S.; Gabuzda, D. Cerebrospinal Fluid Metabolomics Reveals Altered Waste Clearance and Accelerated Aging in HIV Patients with Neurocognitive Impairment. *AIDS* **2014**, *28* (11), 1579–1591. https://doi.org/10.1097/QAD.0000000000000303.
56. Casu, C.; Nemeth, E.; Rivella, S. Hepcidin Agonists as Therapeutic Tools. *Blood* **2018**, *131* (16), 1790–1794. https://doi.org/10.1182/blood-2017-11-737411.
57. Chang, H.-C.; Bayeva, M.; Taiwo, B.; Palella, F. J.; Hope, T. J.; Ardehali, H. Short Communication: High Cellular Iron Levels Are Associated with Increased HIV Infection and Replication. *AIDS Res Hum Retroviruses* **2015**, *31* (3), 305–312. https://doi.org/10.1089/aid.2014.0169.
58. Chauhan, A.; Turchan, J.; Pocernich, C.; Bruce-Keller, A.; Roth, S.; Butterfield, D. A.; Major, E. O.; Nath, A. Intracellular Human Immunodeficiency Virus Tat Expression in Astrocytes Promotes Astrocyte Survival but Induces Potent Neurotoxicity at Distant Sites via Axonal Transport. *J Biol Chem* **2003**, *278* (15), 13512–13519. https://doi.org/10.1074/jbc.M209381200.
59. Chauhan, N. K.; Vajpayee, M.; Singh, A. Usefulness of Hemoglobin and Albumin as Prognostic Markers for Highly Active Antiretroviral Therapy for HIV-1 Infection. *Indian J Med Sci* **2011**, *65* (7), 286–296.
60. Chen, H.; Attieh, Z. K.; Syed, B. A.; Kuo, Y.-M.; Stevens, V.; Fuqua, B. K.; Andersen, H. S.; Naylor, C. E.; Evans, R. W.; Gambling, L.; Danzeisen, R.; Bacouri-Haidar, M.; Usta, J.; Vulpe, C. D.; McArdle, H. J. Identification of Zyklopen, a New Member of the Vertebrate Multicopper

Ferroxidase Family, and Characterization in Rodents and Human Cells. *J Nutr* **2010**, *140* (10), 1728–1735. https://doi.org/10.3945/jn.109.117531.

61. Cheng, Y.; Zak, O.; Aisen, P.; Harrison, S. C.; Walz, T. Structure of the Human Transferrin Receptor-Transferrin Complex. *Cell* **2004**, *116* (4), 565–576. https://doi.org/10.1016/s0092-8674(04)00130-8.
62. Chien, Y.-J.; Chen, W.-J.; Hsu, W.-L.; Chiou, S.-S. Bovine Lactoferrin Inhibits Japanese Encephalitis Virus by Binding to Heparan Sulfate and Receptor for Low Density Lipoprotein. *Virology* **2008**, *379* (1), 143–151. https://doi.org/10.1016/j.virol.2008.06.017.
63. Churchill, M. J.; Wesselingh, S. L.; Cowley, D.; Pardo, C. A.; McArthur, J. C.; Brew, B. J.; Gorry, P. R. Extensive Astrocyte Infection Is Prominent in Human Immunodeficiency Virus-Associated Dementia. *Ann Neurol* **2009**, *66* (2), 253–258. https://doi.org/10.1002/ana.21697.
64. Colvez, A.; Joël, M.-E.; Ponton-Sanchez, A.; Royer, A.-C. Health Status and Work Burden of Alzheimer Patients' Informal Caregivers: Comparisons of Five Different Care Programs in the European Union. *Health Policy* **2002**, *60* (3), 219–233. https://doi.org/10.1016/s0168-8510(01)00215-9.
65. Corna, G.; Campana, L.; Pignatti, E.; Castiglioni, A.; Tagliafico, E.; Bosurgi, L.; Campanella, A.; Brunelli, S.; Manfredi, A. A.; Apostoli, P.; Silvestri, L.; Camaschella, C.; Rovere-Querini, P. Polarization Dictates Iron Handling by Inflammatory and Alternatively Activated Macrophages. *Haematologica* **2010**, *95* (11), 1814–1822. https://doi.org/10.3324/haematol.2010.023879.
66. Cunningham, C.; Wilcockson, D. C.; Campion, S.; Lunnon, K.; Perry, V. H. Central and Systemic Endotoxin Challenges Exacerbate the Local Inflammatory Response and Increase Neuronal Death during Chronic Neurodegeneration. *J Neurosci* **2005**, *25* (40), 9275–9284. https://doi.org/10.1523/JNEUROSCI.2614-05.2005.
67. Cutone, A.; Frioni, A.; Berlutti, F.; Valenti, P.; Musci, G.; Bonaccorsi di Patti, M. C. Lactoferrin Prevents LPS-Induced Decrease of the Iron Exporter Ferroportin in Human Monocytes/Macrophages. *Biometals* **2014**, *27* (5), 807–813. https://doi.org/10.1007/s10534-014-9742-7.
68. Cutone, A.; Rosa, L.; Lepanto, M. S.; Scotti, M. J.; Berlutti, F.; Bonaccorsi di Patti, M. C.; Musci, G.; Valenti, P. Lactoferrin Efficiently Counteracts the Inflammation-Induced Changes of the Iron Homeostasis System in Macrophages. *Front Immunol* **2017**, *8*, 705. https://doi.org/10.3389/fimmu.2017.00705.
69. Cutone, A.; Lepanto, M. S.; Rosa, L.; Scotti, M. J.; Rossi, A.; Ranucci, S.; De Fino, I.; Bragonzi, A.; Valenti, P.; Musci, G.; Berlutti, F. Aerosolized Bovine Lactoferrin Counteracts Infection,

Inflammation and Iron Dysbalance in A Cystic Fibrosis Mouse Model of Pseudomonas Aeruginosa Chronic Lung Infection. *Int J Mol Sci* **2019**, *20* (9), 2128. https://doi.org/10.3390/ijms20092128.

70. Cutone, A.; Colella, B.; Pagliaro, A.; Rosa, L.; Lepanto, M. S.; Bonaccorsi di Patti, M. C.; Valenti, P.; Di Bartolomeo, S.; Musci, G. Native and Iron-Saturated Bovine Lactoferrin Differently Hinder Migration in a Model of Human Glioblastoma by Reverting Epithelial-to-Mesenchymal Transition-like Process and Inhibiting Interleukin-6/STAT3 Axis. *Cell Signal* **2020a**, *65*, 109461. https://doi.org/10.1016/j.cellsig.2019.109461.
71. Cutone, A.; Ianiro, G.; Lepanto, M. S.; Rosa, L.; Valenti, P.; Bonaccorsi di Patti, M. C.; Musci, G. Lactoferrin in the Prevention and Treatment of Intestinal Inflammatory Pathologies Associated with Colorectal Cancer Development. *Cancers (Basel)* **2020b**, *12* (12), 3806. https://doi.org/10.3390/cancers12123806.
72. Cutone, A.; Rosa, L.; Ianiro, G.; Lepanto, M. S.; Bonaccorsi di Patti, M. C.; Valenti, P.; Musci, G. Lactoferrin's Anti-Cancer Properties: Safety, Selectivity, and Wide Range of Action. *Biomolecules* **2020c**, *10* (3), 456. https://doi.org/10.3390/biom10030456.
73. Cutone, A.; Rosa, L.; Bonaccorsi di Patti, M. C.; Iacovelli, F.; Conte, M. P.; Ianiro, G.; Romeo, A.; Campione, E.; Bianchi, L.; Valenti, P.; Falconi, M.; Musci, G. Lactoferrin Binding to SARS-CoV-2 Spike Glycoprotein Blocks Pseudoviral Entry and Relieves Iron Protein Dysregulation in Several In Vitro Models. *Pharmaceutics* **2022**, *14* (10), 2111. https://doi.org/10.3390/pharmaceutics14102111.
74. Czosnykowska-Łukacka, M.; Orczyk-Pawiłowicz, M.; Broers, B.; Królak-Olejnik, B. Lactoferrin in Human Milk of Prolonged Lactation. *Nutrients* **2019**, *11* (10), 2350. https://doi.org/10.3390/nu11102350.
75. D'Ezio, V.; Colasanti, M.; Persichini, T. Amyloid-β 25-35 Induces Neurotoxicity through the Up-Regulation of Astrocytic System Xc. *Antioxidants (Basel)* **2021**, *10* (11), 1685. https://doi.org/10.3390/antiox10111685.
76. Dakin, C. J.; Numa, A. H.; Wang, H.; Morton, J. R.; Vertzyas, C. C.; Henry, R. L. Inflammation, Infection, and Pulmonary Function in Infants and Young Children with Cystic Fibrosis. *Am J Respir Crit Care Med* **2002**, *165* (7), 904–910. https://doi.org/10.1164/ajrccm.165.7.2010139.
77. Dal Prà, I.; Chiarini, A.; Gui, L.; Chakravarthy, B.; Pacchiana, R.; Gardenal, E.; Whitfield, J. F.; Armato, U. Do Astrocytes Collaborate with Neurons in Spreading the "Infectious" Aβ and Tau Drivers of Alzheimer's Disease? *Neuroscientist* **2015**, *21* (1), 9–29. https://doi.org/10.1177/1073858414529828.

78. Darbinian, N.; Darbinyan, A.; Merabova, N.; Selzer, M. E.; Amini, S. HIV-1 and HIV-1-Tat Induce Mitochondrial DNA Damage in Human Neurons. *J HIV AIDS* **2020**, *6* (1), 176. https://doi.org/10.16966/2380-5536.176.

79. De Domenico, I.; Ward, D. M.; Kaplan, J. Hepcidin Regulation: Ironing out the Details. *J Clin Invest* **2007**, *117* (7), 1755–1758. https://doi.org/10.1172/JCI32701.

80. Dhillon, N. K.; Peng, F.; Ransohoff, R. M.; Buch, S. PDGF Synergistically Enhances IFN-Gamma-Induced Expression of CXCL10 in Blood-Derived Macrophages: Implications for HIV Dementia. *J Immunol* **2007**, *179* (5), 2722–2730. https://doi.org/10.4049/jimmunol.179.5.2722.

81. Dickens, A. M.; Yoo, S. W.; Chin, A. C.; Xu, J.; Johnson, T. P.; Trout, A. L.; Hauser, K. F.; Haughey, N. J. Chronic Low-Level Expression of HIV-1 Tat Promotes a Neurodegenerative Phenotype with Aging. *Sci Rep* **2017**, *7* (1), 7748. https://doi.org/10.1038/s41598-017-07570-5.

82. Dong, X.; Wang, Y.; Qin, Z. Molecular Mechanisms of Excitotoxicity and Their Relevance to Pathogenesis of Neurodegenerative Diseases. *Acta Pharmacol Sin* **2009**, *30* (4), 379–387. https://doi.org/10.1038/aps.2009.24.

83. Donovan, A.; Lima, C. A.; Pinkus, J. L.; Pinkus, G. S.; Zon, L. I.; Robine, S.; Andrews, N. C. The Iron Exporter Ferroportin/Slc40a1 Is Essential for Iron Homeostasis. *Cell Metab* **2005**, *1* (3), 191–200. https://doi.org/10.1016/j.cmet.2005.01.003.

84. Dosch, S. F.; Mahajan, S. D.; Collins, A. R. SARS Coronavirus Spike Protein-Induced Innate Immune Response Occurs via Activation of the NF-KappaB Pathway in Human Monocyte Macrophages in Vitro. *Virus Res* **2009**, *142* (1–2), 19–27. https://doi.org/10.1016/j.virusres.2009.01.005.

85. Dowdle, W. E.; Nyfeler, B.; Nagel, J.; Elling, R. A.; Liu, S.; Triantafellow, E.; Menon, S.; Wang, Z.; Honda, A.; Pardee, G.; Cantwell, J.; Luu, C.; Cornella-Taracido, I.; Harrington, E.; Fekkes, P.; Lei, H.; Fang, Q.; Digan, M. E.; Burdick, D.; Powers, A. F.; Helliwell, S. B.; D'Aquin, S.; Bastien, J.; Wang, H.; Wiederschain, D.; Kuerth, J.; Bergman, P.; Schwalb, D.; Thomas, J.; Ugwonali, S.; Harbinski, F.; Tallarico, J.; Wilson, C. J.; Myer, V. E.; Porter, J. A.; Bussiere, D. E.; Finan, P. M.; Labow, M. A.; Mao, X.; Hamann, L. G.; Manning, B. D.; Valdez, R. A.; Nicholson, T.; Schirle, M.; Knapp, M. S.; Keaney, E. P.; Murphy, L. O. Selective VPS34 Inhibitor Blocks Autophagy and Uncovers a Role for NCOA4 in Ferritin Degradation and Iron Homeostasis in Vivo. *Nat Cell Biol* **2014**, *16* (11), 1069–1079. https://doi.org/10.1038/ncb3053.

86. Drago-Serrano, M. E.; Campos-Rodriguez, R.; Carrero, J. C.; de la Garza, M. Lactoferrin and Peptide-Derivatives: Antimicrobial Agents with Potential Use in Nonspecific Immunity

Modulation. *Curr Pharm Des* **2018**, *24* (10), 1067–1078. https://doi.org/10.2174/1381612824666180327155929.

87. Drake, J. W.; Holland, J. J. Mutation Rates among RNA Viruses. *Proc Natl Acad Sci U S A* **1999**, *96* (24), 13910–13913. https://doi.org/10.1073/pnas.96.24.13910.
88. Drakesmith, H.; Schimanski, L. M.; Ormerod, E.; Merryweather-Clarke, A. T.; Viprakasit, V.; Edwards, J. P.; Sweetland, E.; Bastin, J. M.; Cowley, D.; Chinthammitr, Y.; Robson, K. J. H.; Townsend, A. R. M. Resistance to Hepcidin Is Conferred by Hemochromatosis-Associated Mutations of Ferroportin. *Blood* **2005**, *106* (3), 1092–1097. https://doi.org/10.1182/blood-2005-02-0561.
89. Drakesmith, H.; Prentice, A. Viral Infection and Iron Metabolism. *Nat Rev Microbiol* **2008**, *6* (7), 541–552. https://doi.org/10.1038/nrmicro1930.
90. Du, L.; Zhao, Z.; Cui, A.; Zhu, Y.; Zhang, L.; Liu, J.; Shi, S.; Fu, C.; Han, X.; Gao, W.; Song, T.; Xie, L.; Wang, L.; Sun, S.; Guo, R.; Ma, G. Increased Iron Deposition on Brain Quantitative Susceptibility Mapping Correlates with Decreased Cognitive Function in Alzheimer's Disease. ACS Chem Neurosci 2018, 9 (7), 1849–1857. https://doi.org/10.1021/acschemneuro.8b00194.
91. Duck, K. A.; Connor, J. R. Iron Uptake and Transport across Physiological Barriers. *Biometals* **2016**, *29* (4), 573–591. https://doi.org/10.1007/s10534-016-9952-2.
92. Duck, K. A.; Simpson, I. A.; Connor, J. R. Regulatory Mechanisms for Iron Transport across the Blood-Brain Barrier. *Biochem Biophys Res Commun* **2017**, *494* (1–2), 70–75. https://doi.org/10.1016/j.bbrc.2017.10.083.
93. Elass, E.; Masson, M.; Mazurier, J.; Legrand, D. Lactoferrin Inhibits the Lipopolysaccharide-Induced Expression and Proteoglycan-Binding Ability of Interleukin-8 in Human Endothelial Cells. *Infect Immun* **2002**, *70* (4), 1860–1866. https://doi.org/10.1128/IAI.70.4.1860-1866.2002.
94. Elass-Rochard, E.; Roseanu, A.; Legrand, D.; Trif, M.; Salmon, V.; Motas, C.; Montreuil, J.; Spik, G. Lactoferrin-Lipopolysaccharide Interaction: Involvement of the 28-34 Loop Region of Human Lactoferrin in the High-Affinity Binding to Escherichia Coli 055B5 Lipopolysaccharide. *Biochem J* **1995**, *312 (Pt 3)* (Pt 3), 839–845. https://doi.org/10.1042/bj3120839.
95. Elass-Rochard, E.; Legrand, D.; Salmon, V.; Roseanu, A.; Trif, M.; Tobias, P. S.; Mazurier, J.; Spik, G. Lactoferrin Inhibits the Endotoxin Interaction with CD14 by Competition with the Lipopolysaccharide-Binding Protein. *Infect Immun* **1998**, *66* (2), 486–491. https://doi.org/10.1128/IAI.66.2.486-491.1998.

96. Epand, R. M.; Vogel, H. J. Diversity of Antimicrobial Peptides and Their Mechanisms of Action. *Biochim Biophys Acta* **1999**, *1462* (1–2), 11–28. https://doi.org/10.1016/s0005-2736(99)00198-4.

97. Ernst, T.; Jiang, C. S.; Nakama, H.; Buchthal, S.; Chang, L. Lower Brain Glutamate Is Associated with Cognitive Deficits in HIV Patients: A New Mechanism for HIV-Associated Neurocognitive Disorder. *J Magn Reson Imaging* **2010**, *32* (5), 1045–1053. https://doi.org/10.1002/jmri.22366.

98. Fernandes, K. E.; Carter, D. A. The Antifungal Activity of Lactoferrin and Its Derived Peptides: Mechanisms of Action and Synergy with Drugs against Fungal Pathogens. *Front Microbiol* **2017**, *8*, 2. https://doi.org/10.3389/fmicb.2017.00002.

99. Ferrarese, C.; Aliprandi, A.; Tremolizzo, L.; Stanzani, L.; De Micheli, A.; Dolara, A.; Frattola, L. Increased Glutamate in CSF and Plasma of Patients with HIV Dementia. *Neurology* **2001**, *57* (4), 671–675. https://doi.org/10.1212/wnl.57.4.671.

100. Fischer, R.; Debbabi, H.; Blais, A.; Dubarry, M.; Rautureau, M.; Boyaka, PN.; Tome, D. Uptake of ingested bovine lactoferrin and its accumulation in adult mouse tissues. Int Immunopharmacol **2007**, 7:1387–1393. https://doi.org/10.1016/j.intimp.2007.05.019

101. Fogal, B.; Li, J.; Lobner, D.; McCullough, L. D.; Hewett, S. J. System x(c)- Activity and Astrocytes Are Necessary for Interleukin-1 Beta-Mediated Hypoxic Neuronal Injury. *J Neurosci* **2007**, *27* (38), 10094–10105. https://doi.org/10.1523/JNEUROSCI.2459-07.2007.

102. Frazer, D. M.; Anderson, G. J. The Orchestration of Body Iron Intake: How and Where Do Enterocytes Receive Their Cues? *Blood Cells Mol Dis* **2003**, *30* (3), 288–297. https://doi.org/10.1016/s1079-9796(03)00039-1.

103. Frioni, A.; Conte, M. P.; Cutone, A.; Longhi, C.; Musci, G.; di Patti, M. C. B.; Natalizi, T.; Marazzato, M.; Lepanto, M. S.; Puddu, P.; Paesano, R.; Valenti, P.; Berlutti, F. Lactoferrin Differently Modulates the Inflammatory Response in Epithelial Models Mimicking Human Inflammatory and Infectious Diseases. *Biometals* **2014**, *27* (5), 843–856. https://doi.org/10.1007/s10534-014-9740-9.

104. Furmanski, P.; Li, Z. P.; Fortuna, M. B.; Swamy, C. V.; Das, M. R. Multiple Molecular Forms of Human Lactoferrin. Identification of a Class of Lactoferrins That Possess Ribonuclease Activity and Lack Iron-Binding Capacity. *J Exp Med* **1989**, *170* (2), 415–429. https://doi.org/10.1084/jem.170.2.415.

105. Galaris, D.; Barbouti, A.; Pantopoulos, K. Iron Homeostasis and Oxidative Stress: An Intimate Relationship. *Biochim Biophys Acta Mol Cell Res* **2019**, *1866* (12), 118535. https://doi.org/10.1016/j.bbamcr.2019.118535.

106. Ganz, T.; Nemeth, E. Iron Homeostasis in Host Defence and Inflammation. *Nat Rev Immunol* **2015**, *15* (8), 500–510. https://doi.org/10.1038/nri3863.

107. Gao, G.; Li, J.; Zhang, Y.; Chang, Y.-Z. Cellular Iron Metabolism and Regulation. *Adv Exp Med Biol* **2019**, *1173*, 21–32. https://doi.org/10.1007/978-981-13-9589-5_2.

108. Gavioli, R.; Gallerani, E.; Fortini, C.; Fabris, M.; Bottoni, A.; Canella, A.; Bonaccorsi, A.; Marastoni, M.; Micheletti, F.; Cafaro, A.; Rimessi, P.; Caputo, A.; Ensoli, B. HIV-1 Tat Protein Modulates the Generation of Cytotoxic T Cell Epitopes by Modifying Proteasome Composition and Enzymatic Activity. *J Immunol* **2004**, *173* (6), 3838–3843. https://doi.org/10.4049/jimmunol.173.6.3838.

109. Giannetti, A. M.; Snow, P. M.; Zak, O.; Björkman, P. J. Mechanism for Multiple Ligand Recognition by the Human Transferrin Receptor. *PLoS Biol* **2003**, *1* (3), E51. https://doi.org/10.1371/journal.pbio.0000051.

110. Giansanti, F.; Leboffe, L.; Angelucci, F.; Antonini, G. The Nutraceutical Properties of Ovotransferrin and Its Potential Utilization as a Functional Food. *Nutrients* **2015**, *7* (11), 9105–9115. https://doi.org/10.3390/nu7115453.

111. Gifford, J. L.; Hunter, H. N.; Vogel, H. J. Lactoferricin: A Lactoferrin-Derived Peptide with Antimicrobial, Antiviral, Antitumor and Immunological Properties. *Cell Mol Life Sci* **2005**, *62* (22), 2588–2598. https://doi.org/10.1007/s00018-005-5373-z.

112. Ginzburg, Y. Z. Hepcidin-Ferroportin Axis in Health and Disease. *Vitam Horm* **2019**, *110*, 17–45. https://doi.org/10.1016/bs.vh.2019.01.002.

113. Gkogkou, E.; Barnasas, G.; Vougas, K.; Trougakos, I. P. Expression Profiling Meta-Analysis of ACE2 and TMPRSS2, the Putative Anti-Inflammatory Receptor and Priming Protease of SARS-CoV-2 in Human Cells, and Identification of Putative Modulators. *Redox Biol* **2020**, *36*, 101615. https://doi.org/10.1016/j.redox.2020.101615.

114. González-Chávez, S. A.; Arévalo-Gallegos, S.; Rascón-Cruz, Q. Lactoferrin: Structure, Function and Applications. *Int J Antimicrob Agents* **2009**, *33* (4), 301.e1-8. https://doi.org/10.1016/j.ijantimicag.2008.07.020.

115. Gras, G.; Kaul, M. Molecular Mechanisms of Neuroinvasion by Monocytes-Macrophages in HIV-1 Infection. *Retrovirology* **2010**, *7*, 30. https://doi.org/10.1186/1742-4690-7-30.

116. Greenbaum, N. L. How Tat Targets TAR: Structure of the BIV Peptide-RNA Complex. *Structure* **1996**, *4* (1), 5–9. https://doi.org/10.1016/S0969-2126(96)00003-2.

117. Grobbelaar, L.; Venter, C.; Vlok, M.; Ngoepe, M.; Laubscher, G. J.; Lourens, P. J.; Steenkamp, J.; Kell, D.; Pretorius, E. SARS-CoV-2 Spike Protein S1 Induces Fibrin(Ogen) Resistant to Fibrinolysis: Implications for Microclot Formation in COVID-19. *Bioscience Reports* **2021**, *41*. https://doi.org/10.1042/BSR20210611.
118. Groot, F.; Geijtenbeek, T. B. H.; Sanders, R. W.; Baldwin, C. E.; Sanchez-Hernandez, M.; Floris, R.; van Kooyk, Y.; de Jong, E. C.; Berkhout, B. Lactoferrin Prevents Dendritic Cell-Mediated Human Immunodeficiency Virus Type 1 Transmission by Blocking the DC-SIGN--Gp120 Interaction. *J Virol* **2005**, *79* (5), 3009–3015. https://doi.org/10.1128/JVI.79.5.3009-3015.2005.
119. Gupta, S.; Knight, A. G.; Gupta, S.; Knapp, P. E.; Hauser, K. F.; Keller, J. N.; Bruce-Keller, A. J. HIV-Tat Elicits Microglial Glutamate Release: Role of NAPDH Oxidase and the Cystine-Glutamate Antiporter. *Neurosci Lett* **2010**, *485* (3), 233–236. https://doi.org/10.1016/j.neulet.2010.09.019.
120. Guschina, T. A.; Soboleva, S. E.; Nevinsky, G. A. Recognition of Specific and Nonspecific DNA by Human Lactoferrin. *J Mol Recognit* **2013**, *26* (3), 136–148. https://doi.org/10.1002/jmr.2257.
121. Habib, H. M.; Ibrahim, S.; Zaim, A.; Ibrahim, W. H. The Role of Iron in the Pathogenesis of COVID-19 and Possible Treatment with Lactoferrin and Other Iron Chelators. *Biomed Pharmacother* **2021**, *136*, 111228. https://doi.org/10.1016/j.biopha.2021.111228.
122. Harada, N.; Kanayama, M.; Maruyama, A.; Yoshida, A.; Tazumi, K.; Hosoya, T.; Mimura, J.; Toki, T.; Maher, J. M.; Yamamoto, M.; Itoh, K. Nrf2 Regulates Ferroportin 1-Mediated Iron Efflux and Counteracts Lipopolysaccharide-Induced Ferroportin 1 MRNA Suppression in Macrophages. *Arch Biochem Biophys* **2011**, *508* (1), 101–109. https://doi.org/10.1016/j.abb.2011.02.001.
123. Hare, D. J. Hepcidin: A Real-Time Biomarker of Iron Need. *Metallomics* **2017**, *9* (6), 606–618. https://doi.org/10.1039/c7mt00047b.
124. Haridas, M.; Anderson, B. F.; Baker, E. N. Structure of Human Diferric Lactoferrin Refined at 2.2 A Resolution. *Acta Crystallogr D Biol Crystallogr* **1995**, *51* (Pt 5), 629–646. https://doi.org/10.1107/S0907444994013521.
125. Harmsen, M. C.; Swart, P. J.; de Béthune, M. P.; Pauwels, R.; De Clercq, E.; The, T. H.; Meijer, D. K. Antiviral Effects of Plasma and Milk Proteins: Lactoferrin Shows Potent Activity against Both Human Immunodeficiency Virus and Human Cytomegalovirus Replication in Vitro. *J Infect Dis* **1995**, *172* (2), 380–388. https://doi.org/10.1093/infdis/172.2.380.

126. Hasegawa, K.; Motsuchi, W.; Tanaka, S.; Dosako, S. Inhibition with Lactoferrin of in Vitro Infection with Human Herpes Virus. *Jpn J Med Sci Biol* **1994**, *47* (2), 73–85. https://doi.org/10.7883/yoken1952.47.73.

127. Haughey, N. J.; Nath, A.; Mattson, M. P.; Slevin, J. T.; Geiger, J. D. HIV-1 Tat through Phosphorylation of NMDA Receptors Potentiates Glutamate Excitotoxicity. *J Neurochem* **2001**, *78* (3), 457–467. https://doi.org/10.1046/j.1471-4159.2001.00396.x.

128. Håversen, L.; Ohlsson, B. G.; Hahn-Zoric, M.; Hanson, L. A.; Mattsby-Baltzer, I. Lactoferrin Down-Regulates the LPS-Induced Cytokine Production in Monocytic Cells via NF-Kappa B. *Cell Immunol* **2002**, *220* (2), 83–95. https://doi.org/10.1016/s0008-8749(03)00006-6.

129. Hentze, M. W.; Muckenthaler, M. U.; Andrews, N. C. Balancing Acts: Molecular Control of Mammalian Iron Metabolism. *Cell* **2004**, *117* (3), 285–297. https://doi.org/10.1016/s0092-8674(04)00343-5.

130. Hikmet, F.; Méar, L.; Edvinsson, Å.; Micke, P.; Uhlén, M.; Lindskog, C. The Protein Expression Profile of ACE2 in Human Tissues. *Mol Syst Biol* **2020**, *16* (7), e9610. https://doi.org/10.15252/msb.20209610.

131. Hooda, J.; Shah, A.; Zhang, L. Heme, an Essential Nutrient from Dietary Proteins, Critically Impacts Diverse Physiological and Pathological Processes. *Nutrients* **2014**, *6* (3), 1080–1102. https://doi.org/10.3390/nu6031080.

132. Hsu, C. C.; Senussi, N. H.; Fertrin, K. Y.; Kowdley, K. V. Iron Overload Disorders. *Hepatol Commun* **2022**, *6* (8), 1842–1854. https://doi.org/10.1002/hep4.2012.

133. Hu, Y.; Meng, X.; Zhang, F.; Xiang, Y.; Wang, J. The in Vitro Antiviral Activity of Lactoferrin against Common Human Coronaviruses and SARS-CoV-2 Is Mediated by Targeting the Heparan Sulfate Co-Receptor. *Emerg Microbes Infect* **2021**, *10* (1), 317–330. https://doi.org/10.1080/22221751.2021.1888660.

134. Hubert, N.; Hentze, M. W. Previously Uncharacterized Isoforms of Divalent Metal Transporter (DMT)-1: Implications for Regulation and Cellular Function. *Proc Natl Acad Sci U S A* **2002**, *99* (19), 12345–12350. https://doi.org/10.1073/pnas.192423399.

135. Hwang, S.-A.; Wilk, K. M.; Bangale, Y. A.; Kruzel, M. L.; Actor, J. K. Lactoferrin Modulation of IL-12 and IL-10 Response from Activated Murine Leukocytes. *Med Microbiol Immunol* **2007**, *196* (3), 171–180. https://doi.org/10.1007/s00430-007-0041-6.

136. Hyvärinen, T.; Hagman, S.; Ristola, M.; Sukki, L.; Veijula, K.; Kreutzer, J.; Kallio, P.; Narkilahti, S. Co-Stimulation with IL-1β and TNF-α Induces an Inflammatory Reactive Astrocyte Phenotype with Neurosupportive Characteristics in a Human Pluripotent Stem Cell Model System. *Sci Rep* **2019**, *9* (1), 16944. https://doi.org/10.1038/s41598-019-53414-9.

137. Ianiro, G.; Rosa, L.; Bonaccorsi di Patti, M. C.; Valenti, P.; Musci, G.; Cutone, A. Lactoferrin: From the Structure to the Functional Orchestration of Iron Homeostasis. *Biometals* **2022**. https://doi.org/10.1007/s10534-022-00453-x.

138. Ikeda, M.; Nozaki, A.; Sugiyama, K.; Tanaka, T.; Naganuma, A.; Tanaka, K.; Sekihara, H.; Shimotohno, K.; Saito, M.; Kato, N. Characterization of Antiviral Activity of Lactoferrin against Hepatitis C Virus Infection in Human Cultured Cells. *Virus Res* **2000**, *66* (1), 51–63. https://doi.org/10.1016/s0168-1702(99)00121-5.

139. Inubushi, T.; Kawazoe, A.; Miyauchi, M.; Kudo, Y.; Ao, M.; Ishikado, A.; Makino, T.; Takata, T. Molecular Mechanisms of the Inhibitory Effects of Bovine Lactoferrin on Lipopolysaccharide-Mediated Osteoclastogenesis. *J Biol Chem* **2012**, *287* (28), 23527–23536. https://doi.org/10.1074/jbc.M111.324673.

140. Ivanov, A. V.; Valuev-Elliston, V. T.; Ivanova, O. N.; Kochetkov, S. N.; Starodubova, E. S.; Bartosch, B.; Isaguliants, M. G. Oxidative Stress during HIV Infection: Mechanisms and Consequences. *Oxid Med Cell Longev* **2016**, *2016*, 8910396. https://doi.org/10.1155/2016/8910396.

141. Jadhav, S.; Nema, V. HIV-Associated Neurotoxicity: The Interplay of Host and Viral Proteins. *Mediators Inflamm* **2021**, *2021*, 1267041. https://doi.org/10.1155/2021/1267041.

142. Jeong, S. Y.; David, S. Glycosylphosphatidylinositol-Anchored Ceruloplasmin Is Required for Iron Efflux from Cells in the Central Nervous System. *J Biol Chem* **2003**, *278* (29), 27144–27148. https://doi.org/10.1074/jbc.M301988200.

143. Jiang, R.; Lopez, V.; Kelleher, S. L.; Lönnerdal, B. Apo- and Holo-Lactoferrin Are Both Internalized by Lactoferrin Receptor via Clathrin-Mediated Endocytosis but Differentially Affect ERK-Signaling and Cell Proliferation in Caco-2 Cells. *J Cell Physiol* **2011**, *226* (11), 3022–3031. https://doi.org/10.1002/jcp.22650.

144. Jiang, R.; Lönnerdal, B. Apo- and Holo-Lactoferrin Stimulate Proliferation of Mouse Crypt Cells but through Different Cellular Signaling Pathways. *Int J Biochem Cell Biol* **2012**, *44* (1), 91–100. https://doi.org/10.1016/j.biocel.2011.10.002.

145. Jiang, R.; Hua, C.; Wan, Y.; Jiang, B.; Hu, H.; Zheng, J.; Fuqua, B. K.; Dunaief, J. L.; Anderson, G. J.; David, S.; Vulpe, C. D.; Chen, H. Hephaestin and Ceruloplasmin Play Distinct but Interrelated Roles in Iron Homeostasis in Mouse Brain1, 2, 23. *The Journal of Nutrition* **2015**, *145* (5), 1003–1009. https://doi.org/10.3945/jn.114.207316.

146. Jiang, B.; Liu, G.; Zheng, J.; Chen, M.; Maimaitiming, Z.; Chen, M.; Liu, S.; Jiang, R.; Fuqua, B. K.; Dunaief, J. L.; Vulpe, C. D.; Anderson, G. J.; Wang, H.; Chen, H. Hephaestin and

Ceruloplasmin Facilitate Iron Metabolism in the Mouse Kidney. *Sci Rep* **2016**, *6* (1), 39470. https://doi.org/10.1038/srep39470.

147. Johansen-Leete, J.; Ullrich, S.; Fry, S. E.; Frkic, R.; Bedding, M. J.; Aggarwal, A.; Ashhurst, A. S.; Ekanayake, K. B.; Mahawaththa, M. C.; Sasi, V. M.; Luedtke, S.; Ford, D. J.; O'Donoghue, A. J.; Passioura, T.; Larance, M.; Otting, G.; Turville, S.; Jackson, C. J.; Nitsche, C.; Payne, R. J. Antiviral Cyclic Peptides Targeting the Main Protease of SARS-CoV-2. *Chem Sci* **2022**, *13* (13), 3826–3836. https://doi.org/10.1039/d1sc06750h.
148. Johanson, B. Isolation of an Iron-Containing Red Protein from Human Milk. *Acta Chemica Scandinavica* **1960**, *14* (2), 510–512.
149. Katsarou, A.; Pantopoulos, K. Basics and Principles of Cellular and Systemic Iron Homeostasis. *Mol Aspects Med* **2020**, *75*, 100866. https://doi.org/10.1016/j.mam.2020.100866.
150. Kawabata, H.; Tong, X.; Kawanami, T.; Wano, Y.; Hirose, Y.; Sugai, S.; Koeffler, H. P. Analyses for Binding of the Transferrin Family of Proteins to the Transferrin Receptor 2. *Br J Haematol* **2004**, *127* (4), 464–473. https://doi.org/10.1111/j.1365-2141.2004.05224.x.
151. Kawakami, H.; Lönnerdal, B. Isolation and Function of a Receptor for Human Lactoferrin in Human Fetal Intestinal Brush-Border Membranes. *Am J Physiol* **1991**, *261* (5 Pt 1), G841-846. https://doi.org/10.1152/ajpgi.1991.261.5.G841.
152. Kernan, K. F.; Carcillo, J. A. Hyperferritinemia and Inflammation. *Int Immunol* **2017**, *29* (9), 401–409. https://doi.org/10.1093/intimm/dxx031.
153. Kidane, T. Z.; Sauble, E.; Linder, M. C. Release of Iron from Ferritin Requires Lysosomal Activity. *Am J Physiol Cell Physiol* **2006**, *291* (3), C445-455. https://doi.org/10.1152/ajpcell.00505.2005.
154. Kim, S.-H.; Smith, A. J.; Tan, J.; Shytle, R. D.; Giunta, B. MSM Ameliorates HIV-1 Tat Induced Neuronal Oxidative Stress via Rebalance of the Glutathione Cycle. *Am J Transl Res* **2015**, *7* (2), 328–338.
155. Kirtipal, N.; Bharadwaj, S.; Kang, S. G. From SARS to SARS-CoV-2, Insights on Structure, Pathogenicity and Immunity Aspects of Pandemic Human Coronaviruses. *Infect Genet Evol* **2020**, *85*, 104502. https://doi.org/10.1016/j.meegid.2020.104502.
156. Kitagawa, H.; Yoshizawa, Y.; Yokoyama, T.; Takeuchi, T.; Talukder, M. J. R.; Shimizu, H.; Ando, K.; Harada, E. Persorption of Bovine Lactoferrin from the Intestinal Lumen into the Systemic Circulation via the Portal Vein and the Mesenteric Lymphatics in Growing Pigs. *J Vet Med Sci* **2003**, *65* (5), 567–572. https://doi.org/10.1292/jvms.65.567.

157. Kruman, I. I.; Nath, A.; Mattson, M. P. HIV-1 Protein Tat Induces Apoptosis of Hippocampal Neurons by a Mechanism Involving Caspase Activation, Calcium Overload, and Oxidative Stress. *Exp Neurol* **1998**, *154* (2), 276–288. https://doi.org/10.1006/exnr.1998.6958.

158. Kruzel, M. L.; Actor, J. K.; Radak, Z.; Bacsi, A.; Saavedra-Molina, A.; Boldogh, I. Lactoferrin Decreases LPS-Induced Mitochondrial Dysfunction in Cultured Cells and in Animal Endotoxemia Model. *Innate Immun* **2010**, *16* (2), 67–79. https://doi.org/10.1177/1753425909105317.

159. Kruzel, M. L.; Actor, J. K.; Zimecki, M.; Wise, J.; Płoszaj, P.; Mirza, S.; Kruzel, M.; Hwang, S.-A.; Ba, X.; Boldogh, I. Novel Recombinant Human Lactoferrin: Differential Activation of Oxidative Stress Related Gene Expression. *J Biotechnol* **2013**, *168* (4), 666–675. https://doi.org/10.1016/j.jbiotec.2013.09.011.

160. Kruzel, M. L.; Zimecki, M.; Actor, J. K. Lactoferrin in a Context of Inflammation-Induced Pathology. *Front Immunol* **2017**, *8*, 1438. https://doi.org/10.3389/fimmu.2017.01438.

161. Kuba, K.; Imai, Y.; Rao, S.; Gao, H.; Guo, F.; Guan, B.; Huan, Y.; Yang, P.; Zhang, Y.; Deng, W.; Bao, L.; Zhang, B.; Liu, G.; Wang, Z.; Chappell, M.; Liu, Y.; Zheng, D.; Leibbrandt, A.; Wada, T.; Slutsky, A. S.; Liu, D.; Qin, C.; Jiang, C.; Penninger, J. M. A Crucial Role of Angiotensin Converting Enzyme 2 (ACE2) in SARS Coronavirus-Induced Lung Injury. *Nat Med* **2005**, *11* (8), 875–879. https://doi.org/10.1038/nm1267.

162. Kumari, N.; Ammosova, T.; Diaz, S.; Lin, X.; Niu, X.; Ivanov, A.; Jerebtsova, M.; Dhawan, S.; Oneal, P.; Nekhai, S. Increased Iron Export by Ferroportin Induces Restriction of HIV-1 Infection in Sickle Cell Disease. *Blood Adv* **2016**, *1* (3), 170–183. https://doi.org/10.1182/bloodadvances.2016000745.

163. Lambert, L. A.; Perri, H.; Halbrooks, P. J.; Mason, A. B. Evolution of the Transferrin Family: Conservation of Residues Associated with Iron and Anion Binding. *Comp Biochem Physiol B Biochem Mol Biol* **2005**, *142* (2), 129–141. https://doi.org/10.1016/j.cbpb.2005.07.007.

164. Lambert, L. A. Molecular Evolution of the Transferrin Family and Associated Receptors. *Biochim Biophys Acta* **2012**, *1820* (3), 244–255. https://doi.org/10.1016/j.bbagen.2011.06.002.

165. Lang, J.; Yang, N.; Deng, J.; Liu, K.; Yang, P.; Zhang, G.; Jiang, C. Inhibition of SARS Pseudovirus Cell Entry by Lactoferrin Binding to Heparan Sulfate Proteoglycans. *PLoS One* **2011**, *6* (8), e23710. https://doi.org/10.1371/journal.pone.0023710.

166. Lawrence, C. M.; Ray, S.; Babyonyshev, M.; Galluser, R.; Borhani, D. W.; Harrison, S. C. Crystal Structure of the Ectodomain of Human Transferrin Receptor. *Science* **1999**, *286* (5440), 779–782. https://doi.org/10.1126/science.286.5440.779.

167. Le Parc, A.; Dallas, D. C.; Duaut, S.; Leonil, J.; Martin, P.; Barile, D. Characterization of Goat Milk Lactoferrin N-Glycans and Comparison with the N-Glycomes of Human and Bovine Milk. *Electrophoresis* **2014**, *35* (11), 1560–1570. https://doi.org/10.1002/elps.201300619.
168. Lee, C.; Lim, H.-K.; Sakong, J.; Lee, Y.-S.; Kim, J.-R.; Baek, S.-H. Janus Kinase-Signal Transducer and Activator of Transcription Mediates Phosphatidic Acid-Induced Interleukin (IL)-1beta and IL-6 Production. *Mol Pharmacol* **2006**, *69* (3), 1041–1047. https://doi.org/10.1124/mol.105.018481.
169. Legrand, D.; Vigié, K.; Said, E. A.; Elass, E.; Masson, M.; Slomianny, M.-C.; Carpentier, M.; Briand, J.-P.; Mazurier, J.; Hovanessian, A. G. Surface Nucleolin Participates in Both the Binding and Endocytosis of Lactoferrin in Target Cells. *Eur J Biochem* **2004**, *271* (2), 303–317. https://doi.org/10.1046/j.1432-1033.2003.03929.x.
170. Legrand, D. Overview of Lactoferrin as a Natural Immune Modulator. *J Pediatr* **2016**, *173 Suppl*, S10-15. https://doi.org/10.1016/j.jpeds.2016.02.071.
171. Leidgens, S.; Bullough, K. Z.; Shi, H.; Li, F.; Shakoury-Elizeh, M.; Yabe, T.; Subramanian, P.; Hsu, E.; Natarajan, N.; Nandal, A.; Stemmler, T. L.; Philpott, C. C. Each Member of the Poly-r(C)-Binding Protein 1 (PCBP) Family Exhibits Iron Chaperone Activity toward Ferritin. *J Biol Chem* **2013**, *288* (24), 17791–17802. https://doi.org/10.1074/jbc.M113.460253.
172. Lenardo, M. J.; Baltimore, D. NF-Kappa B: A Pleiotropic Mediator of Inducible and Tissue-Specific Gene Control. *Cell* **1989**, *58* (2), 227–229. https://doi.org/10.1016/0092-8674(89)90833-7.
173. Lepanto, M. S.; Rosa, L.; Cutone, A.; Conte, M. P.; Paesano, R.; Valenti, P. Efficacy of Lactoferrin Oral Administration in the Treatment of Anemia and Anemia of Inflammation in Pregnant and Non-Pregnant Women: An Interventional Study. *Front Immunol* **2018**, *9*, 2123. https://doi.org/10.3389/fimmu.2018.02123.
174. Lepanto, M. S.; Rosa, L.; Paesano, R.; Valenti, P.; Cutone, A. Lactoferrin in Aseptic and Septic Inflammation. *Molecules* **2019a**, *24* (7), 1323. https://doi.org/10.3390/molecules24071323.
175. Lepanto, M. S.; Rosa, L.; Cutone, A.; Scotti, M. J.; Conte, A. L.; Marazzato, M.; Zagaglia, C.; Longhi, C.; Berlutti, F.; Musci, G.; Valenti, P.; Conte, M. P. Bovine Lactoferrin Pre-Treatment Induces Intracellular Killing of AIEC LF82 and Reduces Bacteria-Induced DNA Damage in Differentiated Human Enterocytes. *Int J Mol Sci* **2019b**, *20* (22), 5666. https://doi.org/10.3390/ijms20225666.
176. Levay, P. F.; Viljoen, M. Lactoferrin: A General Review. *Haematologica* **1995**, *80* (3), 252–267.
177. Li, L.; Fang, C. J.; Ryan, J. C.; Niemi, E. C.; Lebrón, J. A.; Björkman, P. J.; Arase, H.; Torti, F. M.; Torti, S. V.; Nakamura, M. C.; Seaman, W. E. Binding and Uptake of H-Ferritin Are

Mediated by Human Transferrin Receptor-1. *Proc Natl Acad Sci U S A* **2010**, *107* (8), 3505–3510. https://doi.org/10.1073/pnas.0913192107.

178. Lim, Y. X.; Ng, Y. L.; Tam, J. P.; Liu, D. X. Human Coronaviruses: A Review of Virus-Host Interactions. *Diseases* **2016**, *4* (3), 26. https://doi.org/10.3390/diseases4030026.
179. Lipuma, J. J. The Changing Microbial Epidemiology in Cystic Fibrosis. *Clin Microbiol Rev* **2010**, *23* (2), 299–323. https://doi.org/10.1128/CMR.00068-09.
180. Liu, X.-B.; Nguyen, N.-B. H.; Marquess, K. D.; Yang, F.; Haile, D. J. Regulation of Hepcidin and Ferroportin Expression by Lipopolysaccharide in Splenic Macrophages. *Blood Cells Mol Dis* **2005**, *35* (1), 47–56. https://doi.org/10.1016/j.bcmd.2005.04.006.
181. Liu, C. X.; Hu, Q.; Wang, Y.; Zhang, W.; Ma, Z. Y.; Feng, J. B.; Wang, R.; Wang, X. P.; Dong, B.; Gao, F.; Zhang, M. X.; Zhang, Y. Angiotensin-Converting Enzyme (ACE) 2 Overexpression Ameliorates Glomerular Injury in a Rat Model of Diabetic Nephropathy: A Comparison with ACE Inhibition. *Mol Med* **2011**, *17* (1–2), 59–69. https://doi.org/10.2119/molmed.2010.00111.
182. Liu, F.; Li, L.; Xu, M.; Wu, J.; Luo, D.; Zhu, Y.; Li, B.; Song, X.; Zhou, X. Prognostic Value of Interleukin-6, C-Reactive Protein, and Procalcitonin in Patients with COVID-19. *J Clin Virol* **2020**, *127*, 104370. https://doi.org/10.1016/j.jcv.2020.104370.
183. Lu, L.; Hangoc, G.; Oliff, A.; Chen, L. T.; Shen, R. N.; Broxmeyer, H. E. Protective Influence of Lactoferrin on Mice Infected with the Polycythemia-Inducing Strain of Friend Virus Complex. *Cancer Res* **1987**, *47* (15), 4184–4188.
184. Madrid, R.; Janvier, K.; Hitchin, D.; Day, J.; Coleman, S.; Noviello, C.; Bouchet, J.; Benmerah, A.; Guatelli, J.; Benichou, S. Nef-Induced Alteration of the Early/Recycling Endosomal Compartment Correlates with Enhancement of HIV-1 Infectivity. *J Biol Chem* **2005**, *280* (6), 5032–5044. https://doi.org/10.1074/jbc.M401202200.
185. Malik, I. A.; Naz, N.; Sheikh, N.; Khan, S.; Moriconi, F.; Blaschke, M.; Ramadori, G. Comparison of Changes in Gene Expression of Transferrin Receptor-1 and Other Iron-Regulatory Proteins in Rat Liver and Brain during Acute-Phase Response. *Cell Tissue Res* **2011**, *344* (2), 299–312. https://doi.org/10.1007/s00441-011-1152-3.
186. Mancinelli, R.; Olivero, F.; Carpino, G.; Overi, D.; Rosa, L.; Lepanto, M. S.; Cutone, A.; Franchitto, A.; Alpini, G.; Onori, P.; Valenti, P.; Gaudio, E. Role of Lactoferrin and Its Receptors on Biliary Epithelium. *Biometals* **2018**, *31* (3), 369–379. https://doi.org/10.1007/s10534-018-0094-6.
187. Mancinelli, R.; Rosa, L.; Cutone, A.; Lepanto, M. S.; Franchitto, A.; Onori, P.; Gaudio, E.; Valenti, P. Viral Hepatitis and Iron Dysregulation: Molecular Pathways and the Role of Lactoferrin. *Molecules* **2020**, *25* (8), 1997. https://doi.org/10.3390/molecules25081997.

188. Mangino, G.; Famiglietti, M.; Capone, C.; Veroni, C.; Percario, Z. A.; Leone, S.; Fiorucci, G.; Lülf, S.; Romeo, G.; Agresti, C.; Persichini, T.; Geyer, M.; Affabris, E. HIV-1 Myristoylated Nef Treatment of Murine Microglial Cells Activates Inducible Nitric Oxide Synthase, NO2 Production and Neurotoxic Activity. *PLoS One* **2015**, *10* (6), e0130189. https://doi.org/10.1371/journal.pone.0130189.

189. Marchetti, M.; Pisani, S.; Antonini, G.; Valenti, P.; Seganti, L.; Orsi, N. Metal Complexes of Bovine Lactoferrin Inhibit in Vitro Replication of Herpes Simplex Virus Type 1 and 2. *Biometals* **1998**, *11* (2), 89–94. https://doi.org/10.1023/a:1009217709851.

190. Marchetti, M.; Superti, F.; Ammendolia, M. G.; Rossi, P.; Valenti, P.; Seganti, L. Inhibition of Poliovirus Type 1 Infection by Iron-, Manganese- and Zinc-Saturated Lactoferrin. *Med Microbiol Immunol* **1999**, *187* (4), 199–204. https://doi.org/10.1007/s004300050093.

191. Marino, J.; Maubert, M. E.; Mele, A. R.; Spector, C.; Wigdahl, B.; Nonnemacher, M. R. Functional Impact of HIV-1 Tat on Cells of the CNS and Its Role in HAND. *Cell Mol Life Sci* **2020**, *77* (24), 5079–5099. https://doi.org/10.1007/s00018-020-03561-4.

192. Marnett, L. J. Oxyradicals and DNA Damage. *Carcinogenesis* **2000**, *21* (3), 361–370. https://doi.org/10.1093/carcin/21.3.361.

193. Marques, L.; Auriac, A.; Willemetz, A.; Banha, J.; Silva, B.; Canonne-Hergaux, F.; Costa, L. Immune Cells and Hepatocytes Express Glycosylphosphatidylinositol-Anchored Ceruloplasmin at Their Cell Surface. *Blood Cells Mol Dis* **2012**, *48* (2), 110–120. https://doi.org/10.1016/j.bcmd.2011.11.005.

194. Mastrantonio, R.; Cervelli, M.; Pietropaoli, S.; Mariottini, P.; Colasanti, M.; Persichini, T. HIV-Tat Induces the Nrf2/ARE Pathway through NMDA Receptor-Elicited Spermine Oxidase Activation in Human Neuroblastoma Cells. *PLoS One* **2016**, *11* (2), e0149802. https://doi.org/10.1371/journal.pone.0149802.

195. Mastrantonio, R.; D'Ezio, V.; Colasanti, M.; Persichini, T. Nrf2-Mediated System Xc- Activation in Astroglial Cells Is Involved in HIV-1 Tat-Induced Neurotoxicity. *Mol Neurobiol* **2019**, *56* (5), 3796–3806. https://doi.org/10.1007/s12035-018-1343-y.

196. Mazumder, B.; Mukhopadhyay, C. K.; Prok, A.; Cathcart, M. K.; Fox, P. L. Induction of Ceruloplasmin Synthesis by IFN-Gamma in Human Monocytic Cells. *J Immunol* **1997**, *159* (4), 1938–1944.

197. McCarthy, R. C.; Kosman, D. J. Ferroportin and Exocytoplasmic Ferroxidase Activity Are Required for Brain Microvascular Endothelial Cell Iron Efflux. *J Biol Chem* **2013**, *288* (24), 17932–17940. https://doi.org/10.1074/jbc.M113.455428.

198. Mediouni, S.; Darque, A.; Baillat, G.; Ravaux, I.; Dhiver, C.; Tissot-Dupont, H.; Mokhtari, M.; Moreau, H.; Tamalet, C.; Brunet, C.; Paul, P.; Dignat-George, F.; Stein, A.; Brouqui, P.; Spector, S. A.; Campbell, G. R.; Loret, E. P. Antiretroviral Therapy Does Not Block the Secretion of the Human Immunodeficiency Virus Tat Protein. *Infect Disord Drug Targets* **2012**, *12* (1), 81–86. https://doi.org/10.2174/187152612798994939.

199. Mehta, P.; McAuley, D. F.; Brown, M.; Sanchez, E.; Tattersall, R. S.; Manson, J. J.; HLH Across Speciality Collaboration, UK. COVID-19: Consider Cytokine Storm Syndromes and Immunosuppression. *Lancet* **2020**, *395* (10229), 1033–1034. https://doi.org/10.1016/S0140-6736(20)30628-0.

200. Michels, K.; Nemeth, E.; Ganz, T.; Mehrad, B. Hepcidin and Host Defense against Infectious Diseases. *PLoS Pathog* **2015**, *11* (8), e1004998. https://doi.org/10.1371/journal.ppat.1004998.

201. Mirabelli, C.; Wotring, J. W.; Zhang, C. J.; McCarty, S. M.; Fursmidt, R.; Pretto, C. D.; Qiao, Y.; Zhang, Y.; Frum, T.; Kadambi, N. S.; Amin, A. T.; O'Meara, T. R.; Spence, J. R.; Huang, J.; Alysandratos, K. D.; Kotton, D. N.; Handelman, S. K.; Wobus, C. E.; Weatherwax, K. J.; Mashour, G. A.; O'Meara, M. J.; Chinnaiyan, A. M.; Sexton, J. Z. Morphological Cell Profiling of SARS-CoV-2 Infection Identifies Drug Repurposing Candidates for COVID-19. *Proc Natl Acad Sci U S A* **2021**, *118* (36), e2105815118. https://doi.org/10.1073/pnas.2105815118.

202. Mishra, R.; Singh, S. K. HIV-1 Tat C Modulates Expression of MiRNA-101 to Suppress VE-Cadherin in Human Brain Microvascular Endothelial Cells. *J Neurosci* **2013**, *33* (14), 5992–6000. https://doi.org/10.1523/JNEUROSCI.4796-12.2013.

203. Misonou, H.; Morishima-Kawashima, M.; Ihara, Y. Oxidative Stress Induces Intracellular Accumulation of Amyloid Beta-Protein (Abeta) in Human Neuroblastoma Cells. *Biochemistry* **2000**, *39* (23), 6951–6959. https://doi.org/10.1021/bi000169p.

204. Mohamed, W. A.; Salama, R. M.; Schaalan, M. F. A Pilot Study on the Effect of Lactoferrin on Alzheimer's Disease Pathological Sequelae: Impact of the p-Akt/PTEN Pathway. *Biomed Pharmacother* **2019**, *111*, 714–723. https://doi.org/10.1016/j.biopha.2018.12.118.

205. Mizutani, K.; Mikami, B.; Hirose, M. Domain Closure Mechanism in Transferrins: New Viewpoints about the Hinge Structure and Motion as Deduced from High Resolution Crystal Structures of Ovotransferrin N-Lobe. *J Mol Biol* **2001**, *309* (4), 937–947. https://doi.org/10.1006/jmbi.2001.4719.

206. Montemiglio, L. C.; Testi, C.; Ceci, P.; Falvo, E.; Pitea, M.; Savino, C.; Arcovito, A.; Peruzzi, G.; Baiocco, P.; Mancia, F.; Boffi, A.; des Georges, A.; Vallone, B. Cryo-EM Structure of the Human Ferritin-Transferrin Receptor 1 Complex. *Nat Commun* **2019**, *10* (1), 1121. https://doi.org/10.1038/s41467-019-09098-w.

207. Moore, S. A.; Anderson, B. F.; Groom, C. R.; Haridas, M.; Baker, E. N. Three-Dimensional Structure of Diferric Bovine Lactoferrin at 2.8 A Resolution. *J Mol Biol* **1997**, *274* (2), 222–236. https://doi.org/10.1006/jmbi.1997.1386.

208. Mosley, R. L.; Benner, E. J.; Kadiu, I.; Thomas, M.; Boska, M. D.; Hasan, K.; Laurie, C.; Gendelman, H. E. Neuroinflammation, Oxidative Stress and the Pathogenesis of Parkinson's Disease. *Clin Neurosci Res* **2006**, *6* (5), 261–281. https://doi.org/10.1016/j.cnr.2006.09.006.

209. Mostad, E. J.; Prohaska, J. R. Glycosylphosphatidylinositol-Linked Ceruloplasmin Is Expressed in Multiple Rodent Organs and Is Lower Following Dietary Copper Deficiency. *Exp Biol Med (Maywood)* **2011**, *236* (3), 298–308. https://doi.org/10.1258/ebm.2010.010256.

210. Nai, A.; Lorè, N. I.; Pagani, A.; De Lorenzo, R.; Di Modica, S.; Saliu, F.; Cirillo, D. M.; Rovere-Querini, P.; Manfredi, A. A.; Silvestri, L. Hepcidin Levels Predict Covid-19 Severity and Mortality in a Cohort of Hospitalized Italian Patients. *Am J Hematol* **2021**, *96* (1), E32–E35. https://doi.org/10.1002/ajh.26027.

211. Nath, A.; Psooy, K.; Martin, C.; Knudsen, B.; Magnuson, D. S.; Haughey, N.; Geiger, J. D. Identification of a Human Immunodeficiency Virus Type 1 Tat Epitope That Is Neuroexcitatory and Neurotoxic. *J Virol* **1996**, *70* (3), 1475–1480. https://doi.org/10.1128/JVI.70.3.1475-1480.1996.

212. Nemeth, E.; Valore, E. V.; Territo, M.; Schiller, G.; Lichtenstein, A.; Ganz, T. Hepcidin, a Putative Mediator of Anemia of Inflammation, Is a Type II Acute-Phase Protein. *Blood* **2003**, *101* (7), 2461–2463. https://doi.org/10.1182/blood-2002-10-3235.

213. Nemeth, E.; Tuttle, M. S.; Powelson, J.; Vaughn, M. B.; Donovan, A.; Ward, D. M.; Ganz, T.; Kaplan, J. Hepcidin Regulates Cellular Iron Efflux by Binding to Ferroportin and Inducing Its Internalization. *Science* **2004**, *306* (5704), 2090–2093. https://doi.org/10.1126/science.1104742.

214. Nemeth, E.; Ganz, T. Hepcidin-Ferroportin Interaction Controls Systemic Iron Homeostasis. *Int J Mol Sci* **2021**, *22* (12), 6493. https://doi.org/10.3390/ijms22126493.

215. Nisole, S.; Krust, B.; Callebaut, C.; Guichard, G.; Muller, S.; Briand, J. P.; Hovanessian, A. G. The Anti-HIV Pseudopeptide HB-19 Forms a Complex with the Cell-Surface-Expressed Nucleolin Independent of Heparan Sulfate Proteoglycans. *J Biol Chem* **1999**, *274* (39), 27875–27884. https://doi.org/10.1074/jbc.274.39.27875.

216. Nuovo, G. J.; Gallery, F.; MacConnell, P.; Braun, A. In Situ Detection of Polymerase Chain Reaction-Amplified HIV-1 Nucleic Acids and Tumor Necrosis Factor-Alpha RNA in the Central Nervous System. *Am J Pathol* **1994**, *144* (4), 659–666.

217. Oda, H.; Kolawole, A. O.; Mirabelli, C.; Wakabayashi, H.; Tanaka, M.; Yamauchi, K.; Abe, F.; Wobus, C. E. Antiviral Effects of Bovine Lactoferrin on Human Norovirus. *Biochem Cell Biol* **2021**, *99* (1), 166–172. https://doi.org/10.1139/bcb-2020-0035.

218. Okazaki, Y.; Kono, I.; Kuriki, T.; Funahashi, S.; Fushimi, S.; Iqbal, M.; Okada, S.; Toyokuni, S. Bovine Lactoferrin Ameliorates Ferric Nitrilotriacetate-Induced Renal Oxidative Damage in Rats. *J Clin Biochem Nutr* **2012**, *51* (2), 84–90. https://doi.org/10.3164/jcbn.11-100.

219. Ott, M.; Lovett, J. L.; Mueller, L.; Verdin, E. Superinduction of IL-8 in T Cells by HIV-1 Tat Protein Is Mediated through NF-KappaB Factors. *J Immunol* **1998**, *160* (6), 2872–2880.

220. Pace, G. W.; Leaf, C. D. The Role of Oxidative Stress in HIV Disease. *Free Radic Biol Med* **1995**, *19* (4), 523–528. https://doi.org/10.1016/0891-5849(95)00047-2.

221. Paesano, R.; Torcia, F.; Berlutti, F.; Pacifici, E.; Ebano, V.; Moscarini, M.; Valenti, P. Oral Administration of Lactoferrin Increases Hemoglobin and Total Serum Iron in Pregnant Women. *Biochem Cell Biol* **2006**, *84* (3), 377–380. https://doi.org/10.1139/o06-040.

222. Paesano, R.; Natalizi, T.; Berlutti, F.; Valenti, P. Body Iron Delocalization: The Serious Drawback in Iron Disorders in Both Developing and Developed Countries. *Pathog Glob Health* **2012**, *106* (4), 200–216. https://doi.org/10.1179/2047773212Y.0000000043.

223. Paesano, R.; Pacifici, E.; Benedetti, S.; Berlutti, F.; Frioni, A.; Polimeni, A.; Valenti, P. Safety and Efficacy of Lactoferrin versus Ferrous Sulphate in Curing Iron Deficiency and Iron Deficiency Anaemia in Hereditary Thrombophilia Pregnant Women: An Interventional Study. *Biometals* **2014**, *27* (5), 999–1006. https://doi.org/10.1007/s10534-014-9723-x.

224. Pakdaman, R.; Petitjean, M.; El Hage Chahine, J. M. Transferrins--a Mechanism for Iron Uptake by Lactoferrin. *Eur J Biochem* **1998**, *254* (1), 144–153. https://doi.org/10.1046/j.1432-1327.1998.2540144.x.

225. Palaneeswari M, S.; Ganesh, M.; Karthikeyan, T.; Devi, A. J. M.; Mythili, S. V. Hepcidin-Minireview. *J Clin Diagn Res* **2013**, *7* (8), 1767–1771. https://doi.org/10.7860/JCDR/2013/6420.3273.

226. Pantopoulos, K.; Porwal, S. K.; Tartakoff, A.; Devireddy, L. Mechanisms of Mammalian Iron Homeostasis. *Biochemistry* **2012**, *51* (29), 5705–5724. https://doi.org/10.1021/bi300752r.

227. Paracha, U. Z.; Fatima, K.; Alqahtani, M.; Chaudhary, A.; Abuzenadah, A.; Damanhouri, G.; Qadri, I. Oxidative Stress and Hepatitis C Virus. *Virol J* **2013**, *10*, 251. https://doi.org/10.1186/1743-422X-10-251.

228. Parker, J. S.; Murphy, W. J.; Wang, D.; O'Brien, S. J.; Parrish, C. R. Canine and Feline Parvoviruses Can Use Human or Feline Transferrin Receptors to Bind, Enter, and Infect Cells. *J Virol* **2001**, *75* (8), 3896–3902. https://doi.org/10.1128/JVI.75.8.3896-3902.2001.

229. Pasternak, A. O.; Lukashov, V. V.; Berkhout, B. Cell-Associated HIV RNA: A Dynamic Biomarker of Viral Persistence. *Retrovirology* **2013**, *10*, 41. https://doi.org/10.1186/1742-4690-10-41.

230. Patra, T.; Meyer, K.; Geerling, L.; Isbell, T. S.; Hoft, D. F.; Brien, J.; Pinto, A. K.; Ray, R. B.; Ray, R. SARS-CoV-2 Spike Protein Promotes IL-6 Trans-Signaling by Activation of Angiotensin II Receptor Signaling in Epithelial Cells. *PLoS Pathog* **2020**, *16* (12), e1009128. https://doi.org/10.1371/journal.ppat.1009128.

231. Persichini, T.; Maio, N.; di Patti, M. C. B.; Rizzo, G.; Toscano, S.; Colasanti, M.; Musci, G. Interleukin-1β Induces Ceruloplasmin and Ferroportin-1 Gene Expression via MAP Kinases and C/EBPβ, AP-1, and NF-KB Activation. *Neurosci Lett* **2010**, *484* (2), 133–138. https://doi.org/10.1016/j.neulet.2010.08.034.

232. Persichini, T.; Mastrantonio, R.; Del Matto, S.; Palomba, L.; Cantoni, O.; Colasanti, M. The Role of Arachidonic Acid in the Regulation of Nitric Oxide Synthase Isoforms by HIV Gp120 Protein in Astroglial Cells. *Free Radic Biol Med* **2014**, *74*, 14–20. https://doi.org/10.1016/j.freeradbiomed.2014.06.009.

233. Persichini, T.; Mariotto, S.; Suzuki, H.; Butturini, E.; Mastrantonio, R.; Cantoni, O.; Colasanti, M. Cross-Talk Between NO Synthase Isoforms in Neuro-Inflammation: Possible Implications in HIV-Associated Neurocognitive Disorders. *Curr Med Chem* **2016**, *23* (24), 2706–2714. https://doi.org/10.2174/0929867323666160809100452.

234. Pfefferkorn, M. D.; Boone, J. H.; Nguyen, J. T.; Juliar, B. E.; Davis, M. A.; Parker, K. K. Utility of Fecal Lactoferrin in Identifying Crohn Disease Activity in Children. *J Pediatr Gastroenterol Nutr* **2010**, *51* (4), 425–428. https://doi.org/10.1097/MPG.0b013e3181d67e8f.

235. Phua, J.; Weng, L.; Ling, L.; Egi, M.; Lim, C.-M.; Divatia, J. V.; Shrestha, B. R.; Arabi, Y. M.; Ng, J.; Gomersall, C. D.; Nishimura, M.; Koh, Y.; Du, B.; Asian Critical Care Clinical Trials Group. Intensive Care Management of Coronavirus Disease 2019 (COVID-19): Challenges and Recommendations. *Lancet Respir Med* **2020**, *8* (5), 506–517. https://doi.org/10.1016/S2213-2600(20)30161-2.

236. Piani, D.; Fontana, A. Involvement of the Cystine Transport System Xc- in the Macrophage-Induced Glutamate-Dependent Cytotoxicity to Neurons. *J Immunol* **1994**, *152* (7), 3578–3585.

237. Pietropaoli, S.; Leonetti, A.; Cervetto, C.; Venturini, A.; Mastrantonio, R.; Baroli, G.; Persichini, T.; Colasanti, M.; Maura, G.; Marcoli, M.; Mariottini, P.; Cervelli, M. Glutamate Excitotoxicity Linked to Spermine Oxidase Overexpression. *Mol Neurobiol* **2018**, *55* (9), 7259–7270. https://doi.org/10.1007/s12035-017-0864-0.

238. Pillai, R.; Hayashi, M.; Zavitsanou, A.-M.; Papagiannakopoulos, T. NRF2: KEAPing Tumors Protected. *Cancer Discov* **2022**, *12* (3), 625–643. https://doi.org/10.1158/2159-8290.CD-21-0922.

239. Prell, C.; Koletzko, B. Breastfeeding and Complementary Feeding. *Dtsch Arztebl Int* **2016**, *113* (25), 435–444. https://doi.org/10.3238/arztebl.2016.0435.

240. Probst, S.; Fels, J.; Scharner, B.; Wolff, N. A.; Roussa, E.; van Swelm, R. P. L.; Lee, W.-K.; Thévenod, F. Role of Hepcidin in Oxidative Stress and Cell Death of Cultured Mouse Renal Collecting Duct Cells: Protection against Iron and Sensitization to Cadmium. *Arch Toxicol* **2021**, *95* (8), 2719–2735. https://doi.org/10.1007/s00204-021-03106-z.

241. Puddu, P.; Borghi, P.; Gessani, S.; Valenti, P.; Belardelli, F.; Seganti, L. Antiviral Effect of Bovine Lactoferrin Saturated with Metal Ions on Early Steps of Human Immunodeficiency Virus Type 1 Infection. *Int J Biochem Cell Biol* **1998**, *30* (9), 1055–1062. https://doi.org/10.1016/s1357-2725(98)00066-1.

242. Qiao, B.; Sugianto, P.; Fung, E.; Del-Castillo-Rueda, A.; Moran-Jimenez, M.-J.; Ganz, T.; Nemeth, E. Hepcidin-Induced Endocytosis of Ferroportin Is Dependent on Ferroportin Ubiquitination. *Cell Metab* **2012**, *15* (6), 918–924. https://doi.org/10.1016/j.cmet.2012.03.018.

243. Qin, S.; Colin, C.; Hinners, I.; Gervais, A.; Cheret, C.; Mallat, M. System Xc- and Apolipoprotein E Expressed by Microglia Have Opposite Effects on the Neurotoxicity of Amyloid-Beta Peptide 1-40. *J Neurosci* **2006**, *26* (12), 3345–3356. https://doi.org/10.1523/JNEUROSCI.5186-05.2006.

244. Recalcati, S.; Locati, M.; Marini, A.; Santambrogio, P.; Zaninotto, F.; De Pizzol, M.; Zammataro, L.; Girelli, D.; Cairo, G. Differential Regulation of Iron Homeostasis during Human Macrophage Polarized Activation. *Eur J Immunol* **2010**, *40* (3), 824–835. https://doi.org/10.1002/eji.200939889.

245. Reshi, M. L.; Su, Y.-C.; Hong, J.-R. RNA Viruses: ROS-Mediated Cell Death. *Int J Cell Biol* **2014**, *2014*, 467452. https://doi.org/10.1155/2014/467452.

246. Reyes, R. E.; Manjarrez, H. A.; Drago, M. E. El hierro y la virulencia bacteriana. *Enf Inf Microbiol* **2005**, *25*, 104–107.

247. Roberts, S. K.; Henderson, R. W.; Young, G. P. Modulation of Uptake of Heme by Rat Small Intestinal Mucosa in Iron Deficiency. *Am J Physiol* **1993**, *265* (4 Pt 1), G712-718. https://doi.org/10.1152/ajpgi.1993.265.4.G712.

248. Rochette, L.; Gudjoncik, A.; Guenancia, C.; Zeller, M.; Cottin, Y.; Vergely, C. The Iron-Regulatory Hormone Hepcidin: A Possible Therapeutic Target? *Pharmacol Ther* **2015**, *146*, 35–52. https://doi.org/10.1016/j.pharmthera.2014.09.004.

249. Rojas-Celis, V.; Valiente-Echeverría, F.; Soto-Rifo, R.; Toro-Ascuy, D. New Challenges of HIV-1 Infection: How HIV-1 Attacks and Resides in the Central Nervous System. *Cells* **2019**, *8* (10), 1245. https://doi.org/10.3390/cells8101245.

250. Romeo, A. M.; Christen, L.; Niles, E. G.; Kosman, D. J. Intracellular Chelation of Iron by Bipyridyl Inhibits DNA Virus Replication: Ribonucleotide Reductase Maturation as a Probe of Intracellular Iron Pools. *J Biol Chem* **2001**, *276* (26), 24301–24308. https://doi.org/10.1074/jbc.M010806200.

251. Rosa, L.; Cutone, A.; Lepanto, M. S.; Paesano, R.; Valenti, P. Lactoferrin: A Natural Glycoprotein Involved in Iron and Inflammatory Homeostasis. *Int J Mol Sci* **2017**, *18* (9), 1985. https://doi.org/10.3390/ijms18091985.

252. Rosa, L.; Cutone, A.; Lepanto, M. S.; Scotti, M. J.; Conte, M. P.; Paesano, R.; Valenti, P. Physico-Chemical Properties Influence the Functions and Efficacy of Commercial Bovine Lactoferrins. *Biometals* **2018**, *31* (3), 301–312. https://doi.org/10.1007/s10534-018-0092-8.

253. Rosa, L.; Tripepi, G.; Naldi, E.; Aimati, M.; Santangeli, S.; Venditto, F.; Caldarelli, M.; Valenti, P. Ambulatory COVID-19 Patients Treated with Lactoferrin as a Supplementary Antiviral Agent: A Preliminary Study. *J Clin Med* **2021**, *10* (18), 4276. https://doi.org/10.3390/jcm10184276.

254. Ross, S. L.; Tran, L.; Winters, A.; Lee, K.-J.; Plewa, C.; Foltz, I.; King, C.; Miranda, L. P.; Allen, J.; Beckman, H.; Cooke, K. S.; Moody, G.; Sasu, B. J.; Nemeth, E.; Ganz, T.; Molineux, G.; Arvedson, T. L. Molecular Mechanism of Hepcidin-Mediated Ferroportin Internalization Requires Ferroportin Lysines, Not Tyrosines or JAK-STAT. *Cell Metab* **2012**, *15* (6), 905–917. https://doi.org/10.1016/j.cmet.2012.03.017.

255. Saadi, F.; Pal, D.; Sarma, J. D. Spike Glycoprotein Is Central to Coronavirus Pathogenesis-Parallel Between m-CoV and SARS-CoV-2. *Ann Neurosci* **2021**, *28* (3–4), 201–218. https://doi.org/10.1177/09727531211023755.

256. Sagel, S. D.; Sontag, M. K.; Accurso, F. J. Relationship between Antimicrobial Proteins and Airway Inflammation and Infection in Cystic Fibrosis. *Pediatr Pulmonol* **2009**, *44* (4), 402–409. https://doi.org/10.1002/ppul.21028.

257. Salman, S; Berrula L. Immune modulators of HIV infection: the role of reactive oxygen species. *J Clin Cell Immunol* **2012**, 3-121. doi:10.4172/2155.9899.1000121.

258. Salsgiver, E. L.; Fink, A. K.; Knapp, E. A.; LiPuma, J. J.; Olivier, K. N.; Marshall, B. C.; Saiman, L. Changing Epidemiology of the Respiratory Bacteriology of Patients With Cystic Fibrosis. *Chest* **2016**, *149* (2), 390–400. https://doi.org/10.1378/chest.15-0676.

259. Sargent, P. J.; Farnaud, S.; Evans, R. W. Structure/Function Overview of Proteins Involved in Iron Storage and Transport. *Curr Med Chem* **2005**, *12* (23), 2683–2693. https://doi.org/10.2174/092986705774462969.

260. Saylor, D.; Dickens, A. M.; Sacktor, N.; Haughey, N.; Slusher, B.; Pletnikov, M.; Mankowski, J. L.; Brown, A.; Volsky, D. J.; McArthur, J. C. HIV-Associated Neurocognitive Disorder--Pathogenesis and Prospects for Treatment. *Nat Rev Neurol* **2016**, *12* (4), 234–248. https://doi.org/10.1038/nrneurol.2016.27.

261. Schmidt, S. M. The Role of Iron in Viral Infections. *Front Biosci (Landmark Ed)* **2020**, *25* (5), 893–911. https://doi.org/10.2741/4839.

262. Secchiero, P.; Zella, D.; Capitani, S.; Gallo, R. C.; Zauli, G. Extracellular HIV-1 Tat Protein up-Regulates the Expression of Surface CXC-Chemokine Receptor 4 in Resting CD4+ T Cells. *J Immunol* **1999**, *162* (4), 2427–2431.

263. Selliah, N.; Finkel, T. H. Biochemical Mechanisms of HIV Induced T Cell Apoptosis. *Cell Death Differ* **2001**, *8* (2), 127–136. https://doi.org/10.1038/sj.cdd.4400822.

264. Senapati, S.; Banerjee, P.; Bhagavatula, S.; Kushwaha, P. P.; Kumar, S. Contributions of Human ACE2 and TMPRSS2 in Determining Host-Pathogen Interaction of COVID-19. *J Genet* **2021**, *100* (1), 12. https://doi.org/10.1007/s12041-021-01262-w.

265. Sénécal, V.; Barat, C.; Tremblay, M. J. The Delicate Balance between Neurotoxicity and Neuroprotection in the Context of HIV-1 Infection. *Glia* **2021**, *69* (2), 255–280. https://doi.org/10.1002/glia.23904.

266. Sessa, R.; Di Pietro, M.; Filardo, S.; Bressan, A.; Mastromarino, P.; Biasucci, A. V.; Rosa, L.; Cutone, A.; Berlutti, F.; Paesano, R.; Valenti, P. Lactobacilli-Lactoferrin Interplay in Chlamydia Trachomatis Infection. *Pathog Dis* **2017**, *75* (5). https://doi.org/10.1093/femspd/ftx054.

267. Sessa, R.; Di Pietro, M.; Filardo, S.; Bressan, A.; Rosa, L.; Cutone, A.; Frioni, A.; Berlutti, F.; Paesano, R.; Valenti, P. Effect of Bovine Lactoferrin on Chlamydia Trachomatis Infection and Inflammation. *Biochem Cell Biol* **2017**, *95* (1), 34–40. https://doi.org/10.1139/bcb-2016-0049.

268. Shayeghi, M.; Latunde-Dada, G. O.; Oakhill, J. S.; Laftah, A. H.; Takeuchi, K.; Halliday, N.; Khan, Y.; Warley, A.; McCann, F. E.; Hider, R. C.; Frazer, D. M.; Anderson, G. J.; Vulpe, C. D.; Simpson, R. J.; McKie, A. T. Identification of an Intestinal Heme Transporter. *Cell* **2005**, *122* (5), 789–801. https://doi.org/10.1016/j.cell.2005.06.025.

269. Sheikh, N.; Dudas, J.; Ramadori, G. Changes of Gene Expression of Iron Regulatory Proteins during Turpentine Oil-Induced Acute-Phase Response in the Rat. *Lab Invest* **2007**, *87* (7), 713–725. https://doi.org/10.1038/labinvest.3700553.

270. Shin, K.; Wakabayashi, H.; Yamauchi, K.; Yaeshima, T.; Iwatsuki, K. Recombinant Human Intelectin Binds Bovine Lactoferrin and Its Peptides. *Biol Pharm Bull* **2008**, *31* (8), 1605–1608. https://doi.org/10.1248/bpb.31.1605.

271. Siciliano, R.; Rega, B.; Marchetti, M.; Seganti, L.; Antonini, G.; Valenti, P. Bovine Lactoferrin Peptidic Fragments Involved in Inhibition of Herpes Simplex Virus Type 1 Infection. *Biochem Biophys Res Commun* **1999**, *264* (1), 19–23. https://doi.org/10.1006/bbrc.1999.1318.

272. Sienkiewicz, M.; Jaśkiewicz, A.; Tarasiuk, A.; Fichna, J. Lactoferrin: An Overview of Its Main Functions, Immunomodulatory and Antimicrobial Role, and Clinical Significance. *Crit Rev Food Sci Nutr* **2022**, *62* (22), 6016–6033. https://doi.org/10.1080/10408398.2021.1895063.

273. Simpson, I. A.; Ponnuru, P.; Klinger, M. E.; Myers, R. L.; Devraj, K.; Coe, C. L.; Lubach, G. R.; Carruthers, A.; Connor, J. R. A Novel Model for Brain Iron Uptake: Introducing the Concept of Regulation. *J Cereb Blood Flow Metab* **2015**, *35* (1), 48–57. https://doi.org/10.1038/jcbfm.2014.168.

274. Sokolov, A. V.; Solovyov, K. V.; Kostevich, V. A.; Chekanov, A. V.; Pulina, M. O.; Zakharova, E. T.; Shavlovski, M. M.; Panasenko, O. M.; Vasilyev, V. B. Protection of Ceruloplasmin by Lactoferrin against Hydroxyl Radicals Is PH Dependent. *Biochem Cell Biol* **2012**, *90* (3), 397–404. https://doi.org/10.1139/o2012-004.

275. Sokolov, A. V.; Zakharova, E. T.; Kostevich, V. A.; Samygina, V. R.; Vasilyev, V. B. Lactoferrin, Myeloperoxidase, and Ceruloplasmin: Complementary Gearwheels Cranking Physiological and Pathological Processes. *Biometals* **2014**, *27* (5), 815–828. https://doi.org/10.1007/s10534-014-9755-2.

276. Song, L.; Nath, A.; Geiger, J. D.; Moore, A.; Hochman, S. Human Immunodeficiency Virus Type 1 Tat Protein Directly Activates Neuronal N-Methyl-D-Aspartate Receptors at an Allosteric Zinc-Sensitive Site. *J Neurovirol* **2003**, *9* (3), 399–403. https://doi.org/10.1080/13550280390201704.

277. Sonnweber, T.; Boehm, A.; Sahanic, S.; Pizzini, A.; Aichner, M.; Sonnweber, B.; Kurz, K.; Koppelstätter, S.; Haschka, D.; Petzer, V.; Hilbe, R.; Theurl, M.; Lehner, D.; Nairz, M.; Puchner, B.; Luger, A.; Schwabl, C.; Bellmann-Weiler, R.; Wöll, E.; Widmann, G.; Tancevski, I.; Judith-Löffler-Ragg, null; Weiss, G. Persisting Alterations of Iron Homeostasis in COVID-19 Are Associated with Non-Resolving Lung Pathologies and Poor Patients' Performance: A Prospective Observational Cohort Study. *Respir Res* **2020**, *21* (1), 276. https://doi.org/10.1186/s12931-020-01546-2.

278. Sorensen, M.; Sorensen, S. P. L. The proteins in whey. *Compte rendu des Travaux du Laboratoire de Carlsberg, Ser. Chim.* **1940**, *23* (7), 55–99.

279. Staal, F. J.; Roederer, M.; Herzenberg, L. A.; Herzenberg, L. A. Intracellular Thiols Regulate Activation of Nuclear Factor Kappa B and Transcription of Human Immunodeficiency Virus. *Proc Natl Acad Sci U S A* **1990**, *87* (24), 9943–9947. https://doi.org/10.1073/pnas.87.24.9943.

280. Suhail, S.; Zajac, J.; Fossum, C.; Lowater, H.; McCracken, C.; Severson, N.; Laatsch, B.; Narkiewicz-Jodko, A.; Johnson, B.; Liebau, J.; Bhattacharyya, S.; Hati, S. Role of Oxidative Stress on SARS-CoV (SARS) and SARS-CoV-2 (COVID-19) Infection: A Review. *Protein J* **2020**, *39* (6), 644–656. https://doi.org/10.1007/s10930-020-09935-8.

281. Superti, F.; Ammendolia, M. G.; Valenti, P.; Seganti, L. Antirotaviral Activity of Milk Proteins: Lactoferrin Prevents Rotavirus Infection in the Enterocyte-like Cell Line HT-29. *Med Microbiol Immunol* **1997**, *186* (2–3), 83–91. https://doi.org/10.1007/s004300050049.

282. Superti, F.; Siciliano, R.; Rega, B.; Giansanti, F.; Valenti, P.; Antonini, G. Involvement of Bovine Lactoferrin Metal Saturation, Sialic Acid and Protein Fragments in the Inhibition of Rotavirus Infection. *Biochim Biophys Acta* **2001**, *1528* (2–3), 107–115. https://doi.org/10.1016/s0304-4165(01)00178-7.

283. Suriawinata, E.; Mehta, K. J. Iron and Iron-Related Proteins in COVID-19. *Clin Exp Med* **2022**, 1–23. https://doi.org/10.1007/s10238-022-00851-y.

284. Suryo Rahmanto, Y.; Dunn, L. L.; Richardson, D. R. The Melanoma Tumor Antigen, Melanotransferrin (P97): A 25-Year Hallmark--from Iron Metabolism to Tumorigenesis. *Oncogene* **2007**, *26* (42), 6113–6124. https://doi.org/10.1038/sj.onc.1210442.

285. Suzuki, Y. A.; Lopez, V.; Lönnerdal, B. Mammalian Lactoferrin Receptors: Structure and Function. *Cell Mol Life Sci* **2005**, *62* (22), 2560–2575. https://doi.org/10.1007/s00018-005-5371-1.

286. Swart, P. J.; Kuipers, M. E.; Smit, C.; Pauwels, R.; deBéthune, M. P.; de Clercq, E.; Meijer, D. K.; Huisman, J. G. Antiviral Effects of Milk Proteins: Acylation Results in Polyanionic Compounds with Potent Activity against Human Immunodeficiency Virus Types 1 and 2 in Vitro. *AIDS Res Hum Retroviruses* **1996**, *12* (9), 769–775. https://doi.org/10.1089/aid.1996.12.769.

287. Tacchini, L.; Gammella, E.; De Ponti, C.; Recalcati, S.; Cairo, G. Role of HIF-1 and NF-KappaB Transcription Factors in the Modulation of Transferrin Receptor by Inflammatory and Anti-Inflammatory Signals. *J Biol Chem* **2008**, *283* (30), 20674–20686. https://doi.org/10.1074/jbc.M800365200.

288. Takahashi, K.; Wesselingh, S. L.; Griffin, D. E.; McArthur, J. C.; Johnson, R. T.; Glass, J. D. Localization of HIV-1 in Human Brain Using Polymerase Chain Reaction/in Situ Hybridization

and Immunocytochemistry. *Ann Neurol* **1996**, *39* (6), 705–711. https://doi.org/10.1002/ana.410390606.

289. Takeda, M. Proteolytic Activation of SARS-CoV-2 Spike Protein. *Microbiol Immunol* **2022**, *66* (1), 15–23. https://doi.org/10.1111/1348-0421.12945.
290. Tang, X.; Yang, M.; Duan, Z.; Liao, Z.; Liu, L.; Cheng, R.; Fang, M.; Wang, G.; Liu, H.; Xu, J.; Kamau, P. M.; Zhang, Z.; Yang, L.; Zhao, X.; Peng, X.; Lai, R. Transferrin Receptor Is Another Receptor for SARS-CoV-2 Entry. bioRxiv October 23, **2020**, p 2020.10.23.350348. https://doi.org/10.1101/2020.10.23.350348.
291. Taniguchi, R.; Kato, H. E.; Font, J.; Deshpande, C. N.; Wada, M.; Ito, K.; Ishitani, R.; Jormakka, M.; Nureki, O. Outward- and Inward-Facing Structures of a Putative Bacterial Transition-Metal Transporter with Homology to Ferroportin. *Nat Commun* **2015**, *6*, 8545. https://doi.org/10.1038/ncomms9545.
292. Thomassen, E. A. J.; van Veen, H. A.; van Berkel, P. H. C.; Nuijens, J. H.; Abrahams, J. P. The Protein Structure of Recombinant Human Lactoferrin Produced in the Milk of Transgenic Cows Closely Matches the Structure of Human Milk-Derived Lactoferrin. *Transgenic Res* **2005**, *14* (4), 397–405. https://doi.org/10.1007/s11248-005-3233-0.
293. Tisato, V.; Gallo, S.; Melloni, E.; Celeghini, C.; Passaro, A.; Zauli, G.; Secchiero, P.; Bergamini, C.; Trentini, A.; Bonaccorsi, G.; Valacchi, G.; Zuliani, G.; Cervellati, C. TRAIL and Ceruloplasmin Inverse Correlation as a Representative Crosstalk between Inflammation and Oxidative Stress. *Mediators Inflamm* **2018**, *2018*, 9629537. https://doi.org/10.1155/2018/9629537.
294. Tran, T. N.; Eubanks, S. K.; Schaffer, K. J.; Zhou, C. Y.; Linder, M. C. Secretion of Ferritin by Rat Hepatoma Cells and Its Regulation by Inflammatory Cytokines and Iron. *Blood* **1997**, *90* (12), 4979–4986.
295. Tsuji, Y. Transmembrane Protein Western Blotting: Impact of Sample Preparation on Detection of SLC11A2 (DMT1) and SLC40A1 (Ferroportin). *PLoS One* **2020**, *15* (7), e0235563. https://doi.org/10.1371/journal.pone.0235563.
296. Tumpara, S.; Gründing, A. R.; Sivaraman, K.; Wrenger, S.; Olejnicka, B.; Welte, T.; Wurm, M. J.; Pino, P.; Kiseljak, D.; Wurm, F. M.; Janciauskiene, S. Boosted Pro-Inflammatory Activity in Human PBMCs by Lipopolysaccharide and SARS-CoV-2 Spike Protein Is Regulated by α-1 Antitrypsin. *Int J Mol Sci* **2021**, *22* (15), 7941. https://doi.org/10.3390/ijms22157941.
297. V'kovski, P.; Kratzel, A.; Steiner, S.; Stalder, H.; Thiel, V. Coronavirus Biology and Replication: Implications for SARS-CoV-2. *Nat Rev Microbiol* **2021**, *19* (3), 155–170. https://doi.org/10.1038/s41579-020-00468-6.

298. Valenti, P.; Antonini, G. Lactoferrin: An Important Host Defence against Microbial and Viral Attack. *Cell Mol Life Sci* **2005**, *62* (22), 2576–2587. https://doi.org/10.1007/s00018-005-5372-0.

299. Valenti, P.; Frioni, A.; Rossi, A.; Ranucci, S.; De Fino, I.; Cutone, A.; Rosa, L.; Bragonzi, A.; Berlutti, F. Aerosolized Bovine Lactoferrin Reduces Neutrophils and Pro-Inflammatory Cytokines in Mouse Models of Pseudomonas Aeruginosa Lung Infections. *Biochem Cell Biol* **2017**, *95* (1), 41–47. https://doi.org/10.1139/bcb-2016-0050.

300. van der Kraan, M. I. A.; Groenink, J.; Nazmi, K.; Veerman, E. C. I.; Bolscher, J. G. M.; Nieuw Amerongen, A. V. Lactoferrampin: A Novel Antimicrobial Peptide in the N1-Domain of Bovine Lactoferrin. *Peptides* **2004**, *25* (2), 177–183. https://doi.org/10.1016/j.peptides.2003.12.006.

301. van der Strate, B. W.; Beljaars, L.; Molema, G.; Harmsen, M. C.; Meijer, D. K. Antiviral Activities of Lactoferrin. *Antiviral Res* **2001**, *52* (3), 225–239. https://doi.org/10.1016/s0166-3542(01)00195-4.

302. Verhaeghe, C.; Remouchamps, C.; Hennuy, B.; Vanderplasschen, A.; Chariot, A.; Tabruyn, S. P.; Oury, C.; Bours, V. Role of IKK and ERK Pathways in Intrinsic Inflammation of Cystic Fibrosis Airways. *Biochem Pharmacol* **2007**, *73* (12), 1982–1994. https://doi.org/10.1016/j.bcp.2007.03.019.

303. Viani, R. M.; Gutteberg, T. J.; Lathey, J. L.; Spector, S. A. Lactoferrin Inhibits HIV-1 Replication in Vitro and Exhibits Synergy When Combined with Zidovudine. *AIDS* **1999**, *13* (10), 1273–1274. https://doi.org/10.1097/00002030-199907090-00018.

304. Voss, P.; Horakova, L.; Jakstadt, M.; Kiekebusch, D.; Grune, T. Ferritin Oxidation and Proteasomal Degradation: Protection by Antioxidants. *Free Radic Res* **2006**, *40* (7), 673–683. https://doi.org/10.1080/10715760500419357.

305. Vulpe, C. D.; Kuo, Y. M.; Murphy, T. L.; Cowley, L.; Askwith, C.; Libina, N.; Gitschier, J.; Anderson, G. J. Hephaestin, a Ceruloplasmin Homologue Implicated in Intestinal Iron Transport, Is Defective in the Sla Mouse. *Nat Genet* **1999**, *21* (2), 195–199. https://doi.org/10.1038/5979.

306. Wakabayashi, H.; Oda, H.; Yamauchi, K.; Abe, F. Lactoferrin for Prevention of Common Viral Infections. *J Infect Chemother* **2014**, *20* (11), 666–671. https://doi.org/10.1016/j.jiac.2014.08.003.

307. Walls, A. C.; Park, Y.-J.; Tortorici, M. A.; Wall, A.; McGuire, A. T.; Veesler, D. Structure, Function, and Antigenicity of the SARS-CoV-2 Spike Glycoprotein. *Cell* **2020**, *181* (2), 281-292.e6. https://doi.org/10.1016/j.cell.2020.02.058.

308. Wang, D.; Song, Y.; Li, J.; Wang, C.; Li, F. Structure and Metal Ion Binding of the First Transmembrane Domain of DMT1. *Biochimica et Biophysica Acta (BBA) - Biomembranes* **2011**, *1808* (6), 1639–1644. https://doi.org/10.1016/j.bbamem.2010.11.005.

309. Ward, P. P.; Zhou, X.; Conneely, O. M. Cooperative Interactions between the Amino- and Carboxyl-Terminal Lobes Contribute to the Unique Iron-Binding Stability of Lactoferrin. *J Biol Chem* **1996**, *271* (22), 12790–12794. https://doi.org/10.1074/jbc.271.22.12790.

310. Ward, R. J.; Zucca, F. A.; Duyn, J. H.; Crichton, R. R.; Zecca, L. The Role of Iron in Brain Ageing and Neurodegenerative Disorders. *Lancet Neurol* **2014**, *13* (10), 1045–1060. https://doi.org/10.1016/S1474-4422(14)70117-6.

311. Weiss, S. R.; Leibowitz, J. L. Coronavirus Pathogenesis. *Adv Virus Res* **2011**, *81*, 85–164. https://doi.org/10.1016/B978-0-12-385885-6.00009-2.

312. Weiss, G.; Ganz, T.; Goodnough, L. T. Anemia of Inflammation. *Blood* **2019**, *133* (1), 40–50. https://doi.org/10.1182/blood-2018-06-856500.

313. Wesselius, L. J.; Nelson, M. E.; Skikne, B. S. Increased Release of Ferritin and Iron by Iron-Loaded Alveolar Macrophages in Cigarette Smokers. *Am J Respir Crit Care Med* **1994**, *150* (3), 690–695. https://doi.org/10.1164/ajrccm.150.3.8087339.

314. Wessling-Resnick, M. Iron Homeostasis and the Inflammatory Response. *Annu Rev Nutr* **2010**, *30*, 105–122. https://doi.org/10.1146/annurev.nutr.012809.104804.

315. Wessling-Resnick, M. Crossing the Iron Gate: Why and How Transferrin Receptors Mediate Viral Entry. *Annu Rev Nutr* **2018**, *38*, 431–458. https://doi.org/10.1146/annurev-nutr-082117-051749.

316. Wiesner, J.; Vilcinskas, A. Antimicrobial Peptides: The Ancient Arm of the Human Immune System. *Virulence* **2010**, *1* (5), 440–464. https://doi.org/10.4161/viru.1.5.12983.

317. Willemetz, A.; Beatty, S.; Richer, E.; Rubio, A.; Auriac, A.; Milkereit, R. J.; Thibaudeau, O.; Vaulont, S.; Malo, D.; Canonne-Hergaux, F. Iron- and Hepcidin-Independent Downregulation of the Iron Exporter Ferroportin in Macrophages during Salmonella Infection. *Front Immunol* **2017**, *8*, 498. https://doi.org/10.3389/fimmu.2017.00498.

318. Williams, J.; Grace, S. A.; Williams, J. M. Evolutionary Significance of the Renal Excretion of Transferrin Half-Molecule Fragments. *Biochem J* **1982**, *201* (2), 417–419. https://doi.org/10.1042/bj2010417.

319. Williams, R.; Dhillon, N. K.; Hegde, S. T.; Yao, H.; Peng, F.; Callen, S.; Cheblоune, Y.; Davis, R. L.; Buch, S. J. Proinflammatory Cytokines and HIV-1 Synergistically Enhance CXCL10 Expression in Human Astrocytes. *Glia* **2009**, *57* (7), 734–743. https://doi.org/10.1002/glia.20801.

320. Wotring, J. W.; Fursmidt, R.; Ward, L.; Sexton, J. Z. Evaluating the in Vitro Efficacy of Bovine Lactoferrin Products against SARS-CoV-2 Variants of Concern. *J Dairy Sci* **2022**, *105* (4), 2791–2802. https://doi.org/10.3168/jds.2021-21247.

321. Xiong, S.; She, H.; Takeuchi, H.; Han, B.; Engelhardt, J. F.; Barton, C. H.; Zandi, E.; Giulivi, C.; Tsukamoto, H. Signaling Role of Intracellular Iron in NF-KappaB Activation. *J Biol Chem* **2003**, *278* (20), 17646–17654. https://doi.org/10.1074/jbc.M210905200.

322. Xu, Y.; Zhang, Y.; Zhang, J.-H.; Han, K.; Zhang, X.; Bai, X.; You, L.-H.; Yu, P.; Shi, Z.; Chang, Y.-Z.; Gao, G. Astrocyte Hepcidin Ameliorates Neuronal Loss through Attenuating Brain Iron Deposition and Oxidative Stress in APP/PS1 Mice. *Free Radic Biol Med* **2020**, *158*, 84–95. https://doi.org/10.1016/j.freeradbiomed.2020.07.012.

323. Yu, T.; Guo, C.; Wang, J.; Hao, P.; Sui, S.; Chen, X.; Zhang, R.; Wang, P.; Yu, G.; Zhang, L.; Dai, Y.; Li, N. Comprehensive Characterization of the Site-Specific N-Glycosylation of Wild-Type and Recombinant Human Lactoferrin Expressed in the Milk of Transgenic Cloned Cattle. *Glycobiology* **2011**, *21* (2), 206–224. https://doi.org/10.1093/glycob/cwq151.

324. Yu, P.; Chang, Y.-Z. Brain Iron Metabolism and Regulation. *Adv Exp Med Biol* **2019**, *1173*, 33–44. https://doi.org/10.1007/978-981-13-9589-5_3.

325. Zakharova, E. T.; Shavlovski, M. M.; Bass, M. G.; Gridasova, A. A.; Pulina, M. O.; De Filippis, V.; Beltramini, M.; Di Muro, P.; Salvato, B.; Fontana, A.; Vasilyev, V. B.; Gaitskhoki, V. S. Interaction of Lactoferrin with Ceruloplasmin. *Arch Biochem Biophys* **2000**, *374* (2), 222–228. https://doi.org/10.1006/abbi.1999.1559.

326. Zakharova, E. T.; Sokolov, A. V.; Pavlichenko, N. N.; Kostevich, V. A.; Abdurasulova, I. N.; Chechushkov, A. V.; Voynova, I. V.; Elizarova, A. Y.; Kolmakov, N. N.; Bass, M. G.; Semak, I. V.; Budevich, A. I.; Kozhin, P. M.; Zenkov, N. K.; Klimenko, V. M.; Kirik, O. V.; Korzhevskii, D. E.; Menshchikova, E. B.; Vasilyev, V. B. Erythropoietin and Nrf2: Key Factors in the Neuroprotection Provided by Apo-Lactoferrin. *Biometals* **2018**, *31* (3), 425–443. https://doi.org/10.1007/s10534-018-0111-9.

327. Zhang, G. H.; Mann, D. M.; Tsai, C. M. Neutralization of Endotoxin in Vitro and in Vivo by a Human Lactoferrin-Derived Peptide. *Infect Immun* **1999**, *67* (3), 1353–1358. https://doi.org/10.1128/IAI.67.3.1353-1358.1999.

328. Zhang, Y.; Mikhael, M.; Xu, D.; Li, Y.; Soe-Lin, S.; Ning, B.; Li, W.; Nie, G.; Zhao, Y.; Ponka, P. Lysosomal Proteolysis Is the Primary Degradation Pathway for Cytosolic Ferritin and Cytosolic Ferritin Degradation Is Necessary for Iron Exit. *Antioxid Redox Signal* **2010**, *13* (7), 999–1009. https://doi.org/10.1089/ars.2010.3129.

329. Zhang, Z.; Lu, M.; Chen, C.; Tong, X.; Li, Y.; Yang, K.; Lv, H.; Xu, J.; Qin, L. Holo-Lactoferrin: The Link between Ferroptosis and Radiotherapy in Triple-Negative Breast Cancer. *Theranostics* **2021**, *11* (7), 3167–3182. https://doi.org/10.7150/thno.52028.

330. Zhou, B. Y.; Liu, Y.; Kim, B. oh; Xiao, Y.; He, J. J. Astrocyte Activation and Dysfunction and Neuron Death by HIV-1 Tat Expression in Astrocytes. *Mol Cell Neurosci* **2004**, *27* (3), 296–305. https://doi.org/10.1016/j.mcn.2004.07.003.